ABSTRACT

Title of Dissertation: AN INTEGRATED OPTIMAL CONTROL SYSTEM FOR EMERGENCY EVACUATION

Ying Liu, Doctor of Philosophy, 2007

Directed By: Professor Gang-Len Chang
Department of Civil and Environmental Engineering

How to effectively control evacuation traffic has emerged as one of the critical research issues in transportation community, due to the unusually high demand surge and the often limited network capacity. This dissertation has developed an integrated traffic control system for evacuation operations that may require concurrent implementation of different control options, including traffic routing, contraflow operation, staged evacuation, and intersection signal control.

The system applies a hierarchical control framework to achieve a trade-off between modeling accuracy and operational efficiency for large-scale network applications. The network-level optimization formulations function to assign traffic to different evacuation corridors, select lane reversal configurations for contraflow operations, and identify the evacuation sequence of different demand zones for staged evacuation. With special constraints to approximate flow interactions at intersections, the formulations have introduced two network enhancement approaches with the aim

to capture the real-world operational complexities associated with contraflow operations and staged evacuation.

The corridor-level optimization formulations, taking the network-level decisions as input, function to identify the critical control points and generate the optimal signal timings along the major evacuation corridors. The formulations feature the critical intersection concept to reduce the interference of side-street traffic on arterial evacuation flows. This study has also developed an efficient solution method using the Genetic Algorithm based heuristics along with an embedded macroscopic simulator.

This dissertation has also proposed a revised cell transmission model that aims to capture the complex temporal and spatial interactions of evacuation traffic flows for both levels of optimization formulations. This model can significantly reduce the size of the optimization problem, and yet preserve the ability in effectively modeling network traffic dynamics.

Numerical studies were conducted for each individual control component as well as for the entire integrated control system. The results reveal that the staged evacuation and contraflow strategies generated from the proposed formulations can substantially improve the evacuation efficiency and effectively reduce network congestions. Signal control strategies with the critical intersection concept also outperform the state-of-the-practice evacuation signal plans.

AN INTEGRATED OPTIMAL CONTROL SYSTEM FOR EMERGENCY EVACUATION

By

Ying Liu

Dissertation submitted to the Faculty of the Graduate School of the
University of Maryland, College Park, in partial fulfillment
of the requirements for the degree of
Doctor of Philosophy
2007

Advisory Committee:

Professor Gang-Len Chang, Chair
Professor Martin Dresner
Professor Ali Haghani
Professor Paul Schonfeld
Professor Kelly Clifton

© Copyright by
Ying Liu
2007

Acknowledgements

I give my deepest thanks to my advisor, Professor Gang-Len Chang, for his inspiration, guidance and encouragement throughout my Ph.D. study at the University of Maryland. His support and valuable advice have been the keys to the completeness of this research.

My special thanks go to the members of my doctoral examination committee, Dr. Martin Dresner, Dr. Ali Haghani, Dr. Paul Schonfeld, and Dr. Kelly Clifton, for their constructive comments and suggestions on this work.

I also would like to express my appreciation to the team working on the CAPEVACUATION project, Yue Liu, Zichuan Li and Xiaodong Zhang, for their hard work in converting part of this research to a computer program submitted to the District Department of Transportation. My thanks also go to the project members from Precision Systems Incorporation for providing us the real-world data for Washington D.C.

Finally, I thank my husband and my parents for their encouragement and understanding during my pursuit of higher education. Without their unconditional love and support, I would not have been able to make it through those difficult times.

Table of Contents

List of Tables

List of Figures

Chapter 1: Introduction

1.1. Background

Human society is vulnerable to various emergency events that can cause widespread and severe damages. Most emergency events can be classified as either natural or human-induced type, the latter covering both technological failures and deliberate terrorist attacks. Despite their differences in nature, these unforeseen events often inflict the same negative effects on every sector of the entire society, and may even result in permanent changes to ecosystems and environments. Aiming to reduce such negative effects, the subject of Emergency/Disaster Management has evolved over time as a continuous process of mitigating, preparing for, responding to, and recovering from an emergency situation (McLoughlin, 1985).

As one of the cornerstones in the response phase of Emergency Management, evacuation refers to the movement of populations from a dangerous place to a safe refuge. The process involves various issues, such as physical hazard identification, warning message dissemination, socioeconomic attributes of evacuees, preparedness /response organizations, and expected response patterns (Sorensen et al., 1987). For instance, in responds to an attack in Washington, D.C., responsible agents need to predict the temporal/spatial evolution of hazardous impacts, decide the evacuation area, issue and publicize the evacuation order, estimate evacuation demand as well as evacuee response patterns, guide evacuees to their neighboring evacuation routes, and update traffic signals to efficiently move evacuees out of the hazardous zone.

In view of all such complexities and the often limited capacity of transportation infrastructure, how to effectively control evacuation traffic so as to best utilize available network capacity has emerged as one of the primary research issues in evacuation planning.

1.2. Research Objectives

The primary focus of this dissertation is to develop an efficient evacuation traffic control system that can assist evacuation planners/operators in generating effective network control strategies under various evacuation scenarios. More specifically, the system should have the capability to:

- Design proper control plans to guide evacuees from original nodes to their neighboring evacuation corridors via the local network;
- Select critical roadway segments for implementing contraflow operations, i.e., to temporarily reverse the direction of danger-bound lanes for safety-bound vehicles;
- Determine the most appropriate time for activating evacuation operations for different locations within the potentially hazardous zone; and

- Update intersection control strategies, such as closing some side streets/ramps and changing the timing of signals to facilitate the evacuation operations on main arterials.

To accomplish all above objectives, the proposed evacuation system shall have the following features:

- Inclusion of various network control strategies — which are either borrowed from state of the practice or have been specially designed in this study for evacuation traffic — applicable to various evacuation scenarios;
- Realistic representation of the temporal and spatial interactions among evacuation traffic, especially for the non-stationary network conditions due to time-varying demands and congestions that often incur during an evacuation;
- Proper formulations of real-world operational constraints, such as evacuees' response behaviors to evacuation orders, characteristics of evacuation traffic, and limitations of control hardware;
- Development of sufficiently efficient solution algorithms that can solve the proposed optimization formulations and generate target control strategies for a large-scale network; and
- Identification of proper performance measurements for evaluating the effectiveness of the proposed system in real-world evacuation scenarios.

1.3. Dissertation Organization

Based on the functions and features of the target system, this study has organized the primary research activities into seven chapters. The interrelations among those activities are illustrated in Figure 1.1.

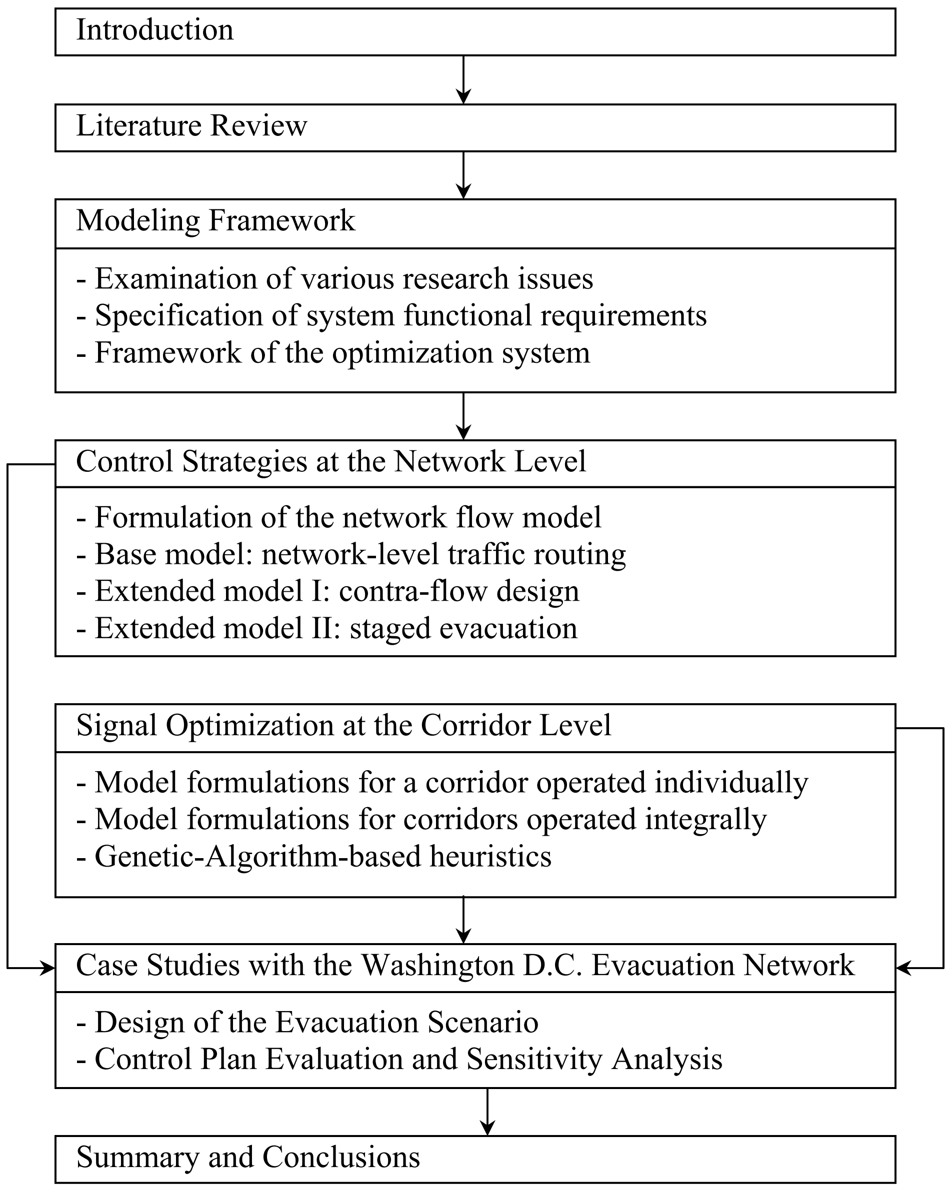

Figure 1.1 Dissertation Organization

The remaining chapters of this dissertation are organized as follows:

- *Literature Review*: Chapter 2 presents a comprehensive literature review of existing studies on the design of various network control strategies for evacuation operations, including both analytical and simulation-based models. The focus of the review is to identify the special characteristics of each control strategy and their effectiveness in moving the evacuation traffic.
- *Modeling Framework*: Chapter 3 illustrates the framework of the proposed optimization system, based on critical technical issues that need to be taken into account in the design of traffic control strategies. It first specifies the required system input and then presents a hierarchical optimization structure, aiming to tackle the operational complexities that may be caused by concurrently implementing multiple strategies for large-scale network evacuations.
- *Control Strategies at the Network Level*: Chapter 4 details the formulations of those optimization models for design of network-level control strategies, which include network-level traffic routing, contraflow design, and staged evacuation decisions. This chapter also proposes a revised cell transmission concept to serve as the basic network flow model in the proposed optimization system.

- *Signal Optimization at the Corridor Level*: Chapter 5 presents two sets of formulations for design of signal control strategies, one for an evacuation corridor operated independently, and the other for several integrally operated corridors. The formulations feature the use of the critical intersection concept, which aims to facilitate the arterial progression on the main evacuation routes. This chapter also includes a genetic-algorithm-based heuristic to solve the proposed formulations.
- *System Applications*: Chapter 6 applies the proposed optimization system in the Washington D.C. evacuation network. This chapter details the two-level control concept and evaluates the generated evacuation plans with different control strategies. Sensitivity analysis is conducted regarding the design of staged evacuation strategies. Findings and recommendations are summarized accordingly based on the case study results.
- *Research Summary*: Chapter 7 summarizes the contributions of this dissertation and the directions for future research. Such directions include multi-mode evacuation including passenger cars, emergency buses and subways, and the development of efficient heuristic algorithms to solve the network-level formulations.

Chapter 2: Literature Review

2.1. Introduction

In view of the large body of literature on various aspects of evacuation operations, this chapter will present a comprehensive review of only those research efforts in design of the control strategies for network evacuation. The purpose is to identify the special characteristics, strengths, and deficiencies of existing studies and thus to define the primary directions for this study.

To facilitate the presentation, this review has divided all related studies on network evacuation controls into the following four categories:

- Traffic Routing Strategies: to utilize the available network capacity more efficiently by guiding route selections of evacuees;
- Contraflow Design: to reverse the normal driving direction of some travel lanes in the evacuation network so as to increase the safety-bound capacity;
- Staged Evacuation: to reduce network congestion by evacuating those evacuation zones with different evacuation time windows in a proper sequence; and
- Arterial Signal Control: to maximize arterial traffic throughput with a set of specially designed signal plans.

The next four sections will review and discuss the available methodologies in the above four categories in sequence. Based on a review of the existing literature, the last section will present further research needs for this critical evacuation subject.

2.2. Traffic Routing Strategies in Emergency Evacuation

While route selection depends upon a number of driver- and situation-specific characteristics, the most important question to be resolved by the modeler is the level of myopia versus preplanning that drivers put into their route selection process (Southworth, 1991). Traffic routing, as one of the main control efforts, aims to identify the potentially best set of routing decisions so as to fully utilize the available capacity of an evacuation network.

Urbanik (2000) described the mechanism of traffic routing as load balancing, with evacuation traffic being diverted from routes of excess demand to those of excess capacity. Such a balancing state is mainly achieved by optimizing some predefined performance measurements for the entire evacuation operation with the approximated network traffic demand. Based on the methodology employed to approximate traffic evolution, this section divides related studies into the following three groups: network flow models, dynamic traffic assignment (DTA) models, and other models. Review of each model will emphasize the performance index for evaluating the evacuation operations, the type of routing decisions generated, and the operational constraints embedded in route generations.

Note that traffic routing is different from those route selection models widely used in most simulation-based software packages, which are for simulating the route selection behavior of drivers, based on the prevailing network conditions. Examples of such studies include NETVAC1 (Sheffi et al., 1982), which allows dynamic route selection in each interval at each intersection, based on traffic conditions directly ahead; MASSVAC (Hobeika, et al., 1994; 1998), that determines routes for evacuees departing from their origins with static traffic assignment algorithms; and CEMPS (Pidd et al., 1996; de Silva and Eglese, 2000), whose route selection mechanism has evolved from an immediate-congestion-based mechanism in its earlier versions to a shortest-path-based mechanism. Such route selection models are myopic in nature and will not be included in the following review.

2.2.1. Network Flow Models

By formulating evacuation routing as a minimal cost flow problem, Dunn (1992) proposed two algorithms to find the set of path flows that minimize the total travel distance through a capacity-constrained network.

Cova et al. (2003) proposed the concept of lane-based routing to reduce intersection delays by temporarily transforming intersections into uninterrupted flow facilities through proper turning restrictions. The output mainly includes the allowable turning movements at each intersection or the mapping between approaching lanes and exiting lanes. As an extension of the minimal cost flow problem, the model minimizes the total travel distance while preventing flow conflicts and restricting merging points at intersections. Network flow is simplified with the flow conservation constraints at each node as shown in Equation 2.1, and the link capacity constraints.

$$\sum_{j \in \Gamma^{-1}(i)} x_{ij} - \sum_{j \in \Gamma(i)} x_{ji} = b_i \tag{2.1}$$

where x_{ij} is the vehicle flow from lane i to lane j; b_i is net flow generated at i; $\Gamma(i)$ denotes the set of predecessor nodes of node i; and $\Gamma^{-1}(i)$ denotes the set of successor nodes of node i.

To represent the evolution of a building evacuation process over time, Chalmet et al. (1982) constructed a dynamic network flow model by expanding the network into a time-space network. The objective is to minimize the time to when the last evacuee exits, which is known as the quickest flow problem. Following the same line of inquiry, Hamacher and Tufekci (1987) extended the quickest flow problem to take into account different priority levels for different parts of the evacuation network. Choi et al. (1988) formulated three dynamic network flow problems for building evacuation (i.e., maximum flow, minimum cost and quickest flow problems), which introduced additional constraints to define link capacity as a function of the incoming flow rate.

Miller-Hooks and Patterson (2004) proposed the time-dependent quickest flow problem in time-varying capacitated evacuation networks, where link travel times and capacities vary with time. Network flow is modeled with flow conservation constraints at each node (Equation 2.2) as well as link capacity constraints (Equation 2.3).

$$\sum_{j\in\Gamma^{-1}(i)} x_{ij}(t) - \sum_{j\in\Gamma(i)} \sum_{t':t'+\tau_{ji}(t')=t} x_{ji}(t') = b_i(t) \tag{2.2}$$

$$0 \le x_{ij}(t) \le u_{ij}(t) \tag{2.3}$$

where $x_{ij}(t)$ is the flow on link (*i*,*j*) that leaves node *i* at *t* and arrives at node *j* after travel time $\tau_{ij}(t)$; $b_i(t)$ is the flow generated at node *i* during time *t*; and $u_{ij}(t)$ is the capacity of link (*i*,*j*) at time *t*.

As an extension of the time-dependent quickest flow problem, Opasanon (2004) addressed the stochastic nature of the evacuation network for a large building and formulated two network flow problems to generate the optimal path flows. The minimal cost problem seeks to minimize the total travel time when both link capacities and travel time are random variables with time-varying probability mass functions. In contrast, the safest escape problem aims to maximize the minimum path probability of successful arrivals at destinations (Equation 2.4) on a network with the deterministic travel time and stochastic time-varying link capacities. Network flows are modeled with the same conservation equations as Equation 2.3 and the modified capacity equations as Equation 2.5.

$$Max \qquad [\min_{\sigma\in\Omega} \prod_{((i,j),t)\in\sigma} P_{ij}^{x_{ij}(t)}(t)] \tag{2.4}$$

$$0 \le x_{ij}(t) \le \max_{z}\{u_{ij}^{z}(t)\} \tag{2.5}$$

where Ω is the set of all possible paths; $P_{ij}^{n}(t)$ denotes the probability that the capacity of link (*i*,*j*) at time *t* is not less than *n*; and $\{u_{ij}^{z}(t)\}$ is the set of possible capacities for link (*i*,*j*) at time *t*.

In summary, these studies formulate the evacuation networks as facilities with limited capacity, where traffic can go through links with known travel times as long as they do not exceed link capacity. These problems typically involve two types of network flow constraints, namely, flow conservation constraints at every node and capacity constraints for each link. However, some traffic phenomena, such as congestion-caused delay and queue formation/dissipation, are not captured in such models.

2.2.2. Dynamic Traffic Assignment Models

Sattayhatewa and Ran (2000) applied an analytical DTA model to minimize the total evacuation time under a nuclear power plant failure. The output includes the optimal inflow rate into and exit flow rate from each link at each time interval. The constraints are the basic network flow constraints, which represent vehicle propagation over the network with link and node flow conservation equations (Equations 2.6 and 2.7) as well as propagation equations (Equation 2.8) with a travel time function $\tau_a(t) = f(u,v,x)$.

$$dx_a^{rs}(t)/dt = u_a^{rs}(t) - v_a^{rs}(t) \tag{2.6}$$

$$\sum_{a\in B(j)} v_a^{rs}(t) = \sum_{a\in A(j)} u_a^{rs}(t) \tag{2.7}$$

$$u_a^{rs}(t) = v_a^{rs}(t + \tau_a(t)) \tag{2.8}$$

where $x_a^{rs}(t)$ is the number of vehicles on link *a* at time *t* traveling from origin *r* to destination *s*; $u_a^{rs}(t)$ is the inflow rate into link *a* at time *t* between OD pair *r* and *s*; $v_a^{rs}(t)$ is the exit flow rate from link *a* at time *t* between OD pair *r* and *s*; and *A(j)* and *B(j)* are, respectively, the set of links whose upstream and downstream node is j.

Liu et al. (2006) also applied the DTA approach in a Model Reference Adaptive Control (MRAC) framework for real-time evacuation traffic management. The DTA model functions to generate the desired traffic states and associated control strategies with a rolling horizon, which will serve as a reference point for the adaptive control. With a discrete time frame, the evacuation traffic flow is captured in two aspects, namely, link dynamics (Equation 2.9) and node dynamics (Equation 2.10).

$$x_{as}(k+1) - x_{as}(k) = u_{as}(k) - v_{as}(k) \tag{2.9}$$

$$\sum_{a\in B(j)} v_{as}(t) = \sum_{a\in A(j)} u_{as}(t) - d^{js}(k) \tag{2.10}$$

where $x_{as}(k)$ is the number of vehicles on link *a* at interval *k* traveling to destination *s*; $u_{as}(k)$ is the inflow rate into link *a* during interval *k* heading to *s*; $v_{as}(k)$ is the exit flow rate from link *a* during interval *k* heading to *s*; and $d^{js}(k)$ is the demand generated at node *j* during interval *k* heading to destination *s*.

Yuan et al. (2006) formulated the evacuation routing problem with the simulation-DTA models embedded in the software package DYNASMART-P. Using mesoscopic simulation to capture vehicle movements over the network, the program can generate two types of routing plans for minimization of total travel cost: 1) static routing that dispatches vehicles to different routes only at their departures, and 2) dynamic routing where vehicles can be assigned to a new route based on the prevailing network conditions.

Some other evacuation studies have also applied DTA models to generate optimal traffic routing schemes concurrently with other control strategies, such as contraflow design (Tuydes and Ziliaskopoulos, 2004, 2006; Tuydes, 2005; Mahmassani and Sbayti, 2005), staged evacuation order (Tuydes and Ziliaskopoulos, 2005), and scheduling of the evacuation demand (Chiu, 2004; Chiu et al., 2006, Sbayti and Mahmassani, 2006). These studies will be reviewed in later sections.

2.2.3. Other Models

Focused mainly on the evacuation network, Campos et al. (2000) presented a heuristic to identify k-optimal independent routes for evacuating the areas surrounding a nuclear power plant. The objective was to maximize the sum of capacity/travel time ratios for those selected routes.

Talebi and Smith (1985) modeled the stochastic evacuation problem with analytical queuing network models. In the extension work, Smith (1991) proposed a state-dependent queuing model for building evacuation. Assuming that evacuees' arrivals follow a Poisson distribution, the model approximates the evacuation process with M/G/C/C state-dependent queues, which capture the nonlinear effects of increased traffic flows on the service rate along emergency evacuation routes with the following exponential function (Equation 2.11):

$$\mu_n = nr_n = n\frac{V_n}{L} = n\frac{A}{L}\exp[-(\frac{n-1}{\beta})^r] \tag{2.11}$$

where μ_n is the state-dependent service rate of the evacuation corridor, n is the number of evacuees using the corridor, r_n is the service rate for each of the n evacuees (actually inverse of the average travel time), V_n is the average speed for n evacuees, A is the free flow speed for n=1, L is the corridor length, and β and r are model parameters.

2.3. Contraflow Design in Emergency Evacuation

Contraflow design, or lane-reversing operation, refers to the shift of normal driving directions of some or all danger-bound lanes for use by safety-bound evacuation traffic. Such control is based on the observation that danger-bound traffic is usually light, whereas evacuation traffic always oversaturates the safety-bound capacity.

Contraflow design can significantly increase the capacity of the evacuation network. In the Southeast U.S. Hurricane Evacuation Traffic Study, PBS&J (2000) examined several alternatives of contraflow operations for a four-lane freeway, including reversing both danger-bound lanes (one-way-out operation) or reversing only one lane. FEMA (2000) estimated that a full reversal would provide an increase in capacity of near 70% over the conventional two-outbound-lane configuration, while the single-inbound-lane reversals are estimated to increase the outbound capacity by about 30%. Several simulation studies have also proved the effectiveness of contraflow operations in improving evacuation efficiency (Zou et al. 2005; Kwon and Pitt, 2005).

Recognizing its effectiveness, responsible agencies in those nine states along the Atlantic and Gulf Coasts have widely applied contraflow design in developing hurricane evacuation plans (Urbina, 2002; Urbina and Wolshon, 2003). For example, Georgia and South Carolina implemented freeway contraflow plans for the 1999 Hurricane Floyd evacuation. Despite a wide acceptance of contraflow operations in practice, limited research has been published regarding which lanes should be reversed for contraflow operations for the maximal effectiveness if under resource limitations.

On this issue, Tuydes and Ziliaskopoulos (2004) proposed link-coupling techniques for contraflow design, which match network segments that can exchange capacity in case of reversing. Assuming the coupled pair of links I and I^* share a total flow capacity Q^t_{I-I*} and storage capacity N^t_{I-I*}, this study formulated a system-optimal DTA problem to obtain the optimal capacity allocation. Network flows are captured with the cell transmission model, which moves vehicles among road segments based on flow conservation law (Equation 2.12) and segment traffic states (Equations 2.13 and 2.14).

$$x_I^t = x_I^{t-1} + \sum_{k \in \Gamma(I)} y_{kI}^{t-1} - \sum_{j \in \Gamma^{-1}(I)} y_{Ij}^{t-1} \tag{2.12}$$

$$y_{Ij}^t = \min\{x_I^t,\ \ r_I Q_{I-I^*}^t,\ \ ,r_j Q_{j-j^*}^t,\ \ ,\delta_j^t (r_j N_{j-j^*}^t - x_j^t\} \tag{2.13}$$

$$r_I + r_{I^*} = 1 \tag{2.14}$$

where x_I^t is the number of vehicles on segment *I* during interval *t*; y_{Ij}^t is the number of vehicles from segment *I* to segment *j* during interval *t*; $\Gamma(I)$ and $\Gamma^{-1}(I)$ denote, respectively, the set of predecessor or successor segments of segment *I*; r_I is the proportion of capacity allocated to segment *I*; and δ_j^t is a traffic flow parameter.

In the extended work, Tuydes (2005) introduced the definitions of lane-based capacity reversibility (LCR) and total-or-no-capacity reversibility (TCR) to replace the continuous variable r_I . Moreover, to cope with the high computational cost associated with the analytical DTA formulations, Tuydes and Ziliaskopoulos (2006) proposed a heuristic algorithm using both simulation-assignment and Tabu Search methods for potential application in real-life large-scale evacuation networks.

With a similar simulation DTA procedure, Mahmassani and Sbayti (2005) proposed an optimization scheme for dynamic capacity reallocation. Using the simulation software package DYNASMART, this study showed how to generate a time-dependent contraflow control policy to be deployed at target links during a major evacuation.

Except for the selection of roadway segments for implementing lane reversals, contraflow design involves various other operational issues. Wolshon (2001, 2002) discussed such issues related to hurricane evacuation and emphasized the rerouting of traffic at the entrance and the end of the reversed segments. With the microscopic simulation program CORSIM, Theodoulou and Wolshon (2004) and Lim and Wolshon (2005) assessed, respectively, the alternative entrance and termination designs of contraflow segments in evaluating the hurricane evacuation plan for the city of New Orleans. Kwon and Pitt (2005) also underscored the critical design of contraflow entry points while using the simulation software DYNASMART-P to test alternative plans for evacuating downtown Minneapolis.

2.4. Staged Evacuation

Staged evacuation, also known as phased evacuation or zoned evacuation, is another widely used control strategy to guide evacuation flows. Without changing the network geometry like contraflow design or enforcing route choice restrictions, staged evacuation aims to achieve more efficient network utilization mainly through a better distribution of evacuation demand over the allowable time window.

In a staged evacuation, the entire area to be evacuated is typically divided into small zones, based on the predicted evolution of emergency impacts and other associated factors. Operators will then issue evacuation orders at an earlier time to those zones with higher levels of urgency (e.g., with a shorter safety time window or with higher concentrations of hazardous chemicals) and start evacuating the low-urgency zones some time later. By restricting unnecessarily early evacuation of low-urgency areas, staged evacuation can effectively limit the surge in evacuation demand, reduce overall network congestion and, more importantly, avoid or at least mitigate potential casualty and stress levels caused by evacuees being blocked in more dangerous areas.

To justify different priorities in the evacuation process, staged evacuation is generally proposed only for those evacuation scenarios during which the impacts of the emergency event will expand progressively before covering the entire network and/or causing different levels of impact severity. For example, staged evacuation strategies have been widely proposed in high-rise building evacuations during fires, where only those floors in the vicinity of the fire source are urged to evacuate immediately (Pauls and Jones, 1980; Teo, 2001; Harrington, 2005). Some other regional evacuations with moving hazards have also considered the use of staged evacuation (Chen and Zhan, 2004; Snyder, 2004; Farrell, 2005).

The critical operational decisions in a staged evacuation plan are when to issue evacuation orders for different evacuation zones. Once an evacuation order is announced, the demand generation process will be determined only by evacuees' responses and is beyond the control of any system operator or enforcement agency. However, effective approaches to obtaining such starting times during a staged evacuation have not been adequately addressed in the literature or in practice. Chen and Zhan (2004) investigated the effectiveness of simultaneous (concurrent) and staged evacuation strategies in three road network structures using the microscopic simulation program PARAMICS, where the staged evacuation times are determined intuitively. Mitchell and Radwan (2006) identified some zonal parameters that might influence the staging decisions, such as population density, roadway exit capacity, distance to safety/shelter, and distance to a major evacuation route. However, the staging strategies tested in their study were also intuitive in nature.

So far, the most relevant study on the optimal design of staged evacuation decisions was conducted by Tuydes and Ziliaskopoulos (2005). They formulated a mixed-integer linear programming model to concurrently optimize destination/route choice and zone scheduling with demand mobilization duration χ^o. Here, χ^o refers to the time period during which all demands generated at origin *o* have to get onto the evacuation network. With network flow constraints similar to Equations 2.12 and 2.13, this study introduced Equations 2.15 to 2.18 to control the demand mobilization process with binary variables $a^{o,t}$ and auxiliary variables $s^{o,t}$.

$$\sum_{(o,j)} \sum_{k=t}^{t+\chi^o} y_{oj}^t + s^{o,t} = d^o \tag{2.15}$$

$$s^{o,t} \le INF \times (1 - a^{o,t}) \tag{2.16}$$

$$1 - a^{o,t} \leq s^{o,t} \tag{2.17}$$

$$\sum_t a^{o,t} = 1 \tag{2.18}$$

where binary variable $a^{o,t}$ equals 1 and auxiliary variable $s^{o,t}$ equals 0 only when demand at origin o is mobilized starting at time t; y_{oj}^{t} is the flow getting out of origin o to its downstream link j during interval t; and d^{o} is the total demand at origin o.

Although the above study provided a starting time for each origin, it did not model the evacuees' actual response behaviors to the evacuation order. The only requirement was that the total demand should enter the evacuation network within a given time window once the evacuation process started at an origin. Further along this direction is the so-called evacuation scheduling problem, where operators are assumed to be able to control the demand generated during each interval (or the evacuation departure time for each evacuee).

Chiu (2004) formulated the evacuation scheduling problem as a mathematical programming model to minimize the total travel time by controlling $r_{i,k}^{t}$, the demand generated during interval t at origin i to travel via path k. The DTA program DYNASMART was used to provide the solution. Chiu et al. (2006) applied the cell transmission model to formulate the optimal evacuation destination-route-flow-staging problem, where similar formulations are used to generate the demand getting out of original points. Trying to minimize the evacuation clearance time, Sbayti and

Mahmassani (2006) proposed an iterative bi-level formulation framework to solve the evacuation scheduling problem, where a dynamic network assignment problem is solved in the upper level to determine the time-dependent route assignments, and a dynamic loading problem is solved with DYNASMART in the lower level to determine the corresponding route travel times.

2.5. Signal Control in Emergency Evacuation

Signal control has been widely accepted as an effective strategy to increase arterial capacity and to mitigate congestion during daily traffic scenarios. For evacuation operations, PBS&J (2000) noted that a good timing plan could increase the capacity of local streets that provide access to/from evacuation routes and prevent bottlenecks at their access points. Various other documents associated with evacuation planning have also proposed to include arterial signal control as an integrated part of the overall evacuation control strategy (ITE, 2004; Ballard and Borchardt, 2005; PBS&J, 2005).

Despite this wide recognition of the critical role of signal control in emergency evacuation, the development of evacuation signal-timing plans has received limited attention in the literature. The current studies in this regard are quite scarce and mostly along the following two lines: 1) to apply simplified controls based on experience, and 2) to apply standard signal optimization practices for normal traffic conditions, but with a high demand.

Among the first group, Chen (2005) applied the microscopic simulation software CORSIM for two evacuation corridors of Washington, D.C., and examined four different signal-timing plans: 1) Red Flash Plan, providing red flash phase to all approaches; 2) Yellow Flash Plan, providing a yellow flash phase to arterials and a red flash phase to side streets; 3) Minimal Green Plan, which uses the longest cycle length the controller allows while offering only minimal green phases to side streets; and 4) Ordinary Peak Hour Plan, which was designed based on normal afternoon peak hour traffic conditions. Although this study offered some insights into the effects of different timing plans, its analysis of plan selection under various evacuation scenarios is mostly qualitative.

Among the second group of practices, Sisiopiku et al. (2004) used the signal optimization software SYNCHRO to establish the optimal signal-timing plans for a small area in Birmingham, Alabama. They then used the CORSIM simulator to test different evacuation plans and evaluated the impacts of signal-timing optimization on the selected measurements of effectiveness. The results suggested that traffic signal optimization could significantly reduce average vehicle delays and improve evacuation time. McHale and Collura (2003) applied another signal optimization program, TRANSYT-7F, to generate the optimal signal-timing plan when assessing the impact of emergency vehicles preemption strategies in a CORSIM simulator.

One area in emergency signal control that has received extensive attention is the preemption of emergency response vehicles. When these vehicles have to use the same roads as evacuees, the emergency vehicle preemption (EVP) function will prioritize the movement of emergency vehicles at intersections and thus may affect evacuation traffic.

In this regard, Bullock et al. (1999) used the CORSIM traffic simulator to model the EVP systems for three intersections on a major commuting corridor in Virginia, and the results showed that EVP has statistically significant negative impacts on other network traffic under given signal-timing plans and preemption strategies. A similar impact analysis of EVP, using the CORSIM simulation model, can be found in McHale and Collura (2003). Among another series of studies to evaluate EVP impacts, Louisell et al. (2003) proposed a conflict point analysis approach to evaluate the potential safety benefits of EVP. Furthermore, Louisell et al. (2004) developed a worksheet method to assess the crash reduction benefits of EVP on a given intersection or corridor during a preemption signal phase. Based on extensive field observations in the Northern Virginia Region, Louisell and Collura (2005) adopted the traditional time-space diagrams to estimate the benefits of EVP in performance improvement for an intersection or an emergency response corridor.

2.6. Closure

In summary, this chapter has provided a comprehensive review of those existing research efforts in the design of various network control strategies for evacuation operations. Those strategies, if properly designed, can effectively improve evacuation efficiency via demand control (e.g., staged evacuation), capacity enhancement (contraflow design and arterial signal control), or a better match of the demand pattern and the available network capacity (e.g., traffic routing).

Although each of these four popular traffic control strategies for evacuation has been reported in the literature or, in some cases, even applied in actual operations, there exist some technical deficiencies that remain to be overcome. For example,

- There lacks an overall operational framework or guidelines that can effectively integrate all four types of control strategies. If implemented concurrently in an evacuation operation, different control strategies will apparently interact with each other and affect traffic flows in the same time-space network. A properly designed staged evacuation may reduce the need for contraflow operations, while an arterial with effective traffic signal-timing plans will certainly better accommodate evacuees assigned by responsible system operators.
- Some critical nature of the evacuation traffic is not fully represented in the analytical formulations. For example, most studies for contraflow design typically treat reversed lanes exactly the same as the normal lanes. In reality, the driving behavior in the reversed and normal lanes may differ

significantly due to the fact that most traffic signs, markings, and safety devices are intended for use only in the designed driving direction (Theodoulou and Wolshon, 2004).

- Some unnecessary or unrealistic assumptions have been employed in the literature for design of optimal evacuation control strategies. For example, models for contraflow design should take into account the geometric features and their discrepancies among different arterial segments so as to avoid creating local bottlenecks. Also, staged evacuation decisions should account for realistic response patterns of evacuees to the evacuation orders, rather than assuming that operators can fully control the departure time of each evacuee.

Chapter 3: Modeling Framework

3.1. Introduction

This chapter presents the framework of the proposed integrated optimal control system and the interrelations between its principle components. Also included are the key research issues and challenges to be addressed in the modeling of each key component. In response to those deficiencies identified in the literature review, the proposed system intends to effectively incorporate different evacuation control strategies under an integrated modeling framework and to generate viable control parameters by realistically capturing the critical nature of evacuation traffic and operations.

The remaining chapter is organized as follows: Section 3.2 presents major research issues to be addressed in the development of integrated evacuation control strategies. Based on the research scope of this study, Section 3.3 specifies the key features of the proposed integrated control system, followed by a description of necessary system input. Section 3.4 briefly describes the functions of each principle control component and their operational interrelations, which provides the foundation for the identification of research tasks for this study.

3.2. Major Research Issues

The integrated control system for evacuation operations aims to improve the efficiency of the entire evacuation process via possible network redesign and/or proper traffic guidance. The optimization for evacuation control operations requires extensive modeling analyses that shall take into account the dynamic interactions between all critical system components. Some major analytical issues encountered in development of the integrated evacuation system are listed below:

- Incident impact prediction, which yields the area potentially affected by the hazard and builds a timeline for evolution of the impacts.
- Evacuation demand estimation, which provides the estimated population to be evacuated, identifies the needs for different evacuation modes, and predicts evacuees' responses to evacuation orders.
- Network traffic projection, which models the movements of evacuees over the evacuation network and captures the spatial and temporal interactions between traffic controls and network flows.
- Traffic control modeling, which identifies the feasible control decisions, control objectives, and operational constraints embedded in implementing each control strategy.
- Optimal control design, which applies some solution algorithms to solve the optimization formulations, and searches for the optimal control parameters.

While the aforementioned issues present different tasks for modeling analysis, they are closely interrelated, and each is indispensable for the design/implementation of an effective evacuation control system. The first two issues involve the estimation of impact areas and populations to be evacuated, while the remaining three issues deal with providing optimal control and guidance to accommodate the estimated evacuation demand. The focus of this research will be on the development of systematic models to contend with the last three critical control issues. Accordingly, the next section will identify the functional requirements to be fulfilled by each proposed system component.

3.3. System Functional Requirements

This study aims to design an optimal control system for emergency evacuation which can efficiently generate effective traffic control strategies for various evacuation scenarios. Such a system can assist those involved in planning evacuation activities, such as emergency management personnel or engineers from responsible agencies. The proposed system should have the following functions:

- *Projecting traffic states over the network to reflect the dynamic nature of evacuation operations*. This function should realistically capture the time-varying evacuation demand, the traffic flow propagation over the evacuation network, and the potential queue formation and dissipation process. Such a function is essential for the proposed system to generate effective control strategies.

- *Integrating applicable control strategies with a proper system architecture*. In general, a system with a higher level of integration needs more sophisticated theoretical models to formulate its complex logic, and it is thus more difficult to solve. Hence, this function is designed to achieve a trade-off between the two fundamental aspects, i.e., modeling accuracy and operational efficiency, with proper hierarchical control architecture.
- *Pursuing optimal control strategies within the operational constraints*. The formulations of the control model should take into account realistic operational constraints as well as the special characteristics of evacuation traffic. The objectives should fit into the evacuation needs.
- *Generating desirable control parameters with an efficient algorithm*. The scope of the evacuation network and the type of employed control strategies will affect the size of the formulations and thus determine the required computing efforts. Hence, some heuristic techniques may be necessary for obtaining suboptimal, but efficient and implementable control solutions within a tolerable time window even for large-size networks.
- *Generating desirable measurements of effectiveness for evaluating the control strategies*. Given a control plan, system operators may need to know the effectiveness of the implemented evacuation plans additional to those control objectives. This function will generate all the measurements of effectiveness for an overall system evaluation.

Required System Input

Section 3.2 identified two analytical issues, incident impact prediction and evacuation demand estimation, which are beyond our research scope but are necessary components for implementation of the proposed integrated control system for evacuation.

More specifically, the incident impact model must be capable of predicting the progression of potential hazardous impacts under identified factors (e.g., incident nature and surrounding environments). In this regard, a large body of hazard-related literature and commercial software packages exist, which can be expected to generate the following three types of input for the proposed optimal evacuation control system.

- The target area to be evacuated. Note that its boundaries depend not only on the progression of incident impacts but also on other factors. Such information is essential for evacuation planning and for communicating proper guidance to evacuees during the operations (USACE, 1986, 1994, 1995; Wilmot and Meduri, 2004; Dotson et al., 2005).
- Maximal level of hazardous impacts at different network locations. For instance, the hazardous impact generally refers to the storm surge (elevation of water surface) in a hurricane evacuation, whereas, for a HAZMAT-caused evacuation, it usually refers to the concentration of the hazardous material.

- Safety time windows for different network locations. This type of information depends on the temporal and spatial evolution of the incident impact, and it is critical for the design of evacuation strategies.

Evacuation demand estimation has also been studied and reported extensively in the literature. The related input for the proposed system consists of the following three types of information:

- The total evacuation demand at each origin, which should cover permanent residents, transients and special facility populations. The total demand depends on a variety of factors, such as the land-use pattern, time of day and the evacuation type (i.e., mandatory, recommended, or voluntary). The estimation methods include standard planning approaches (Southworth, 1991; Alam and Goulias, 1999; Urbinak, 2000; Dotson et al., 2005) and regression-based methods (Mei, 2002).
- Evacuees' responses to the evacuation instructions, which may yield the temporal profile for the total evacuation demand to load onto the network. It has been defined in the following three ways in the literature: dynamic loading curve (Sheffi, 1985; Tweedie et al., 1986; USACE, 2000), response time distribution (Cova and Johnson, 2002), and regression models of decision-making behaviors (Fu and Wilmot, 2004).
- Choice of transportation modes. This is mainly determined by the socioeconomic attributes of evacuees, as reported in the studies by Rontiris and Crous (2000) and Cova and Johnson (2002).

3.4. System Framework

Figure 3.1 depicts the framework of the proposed optimal control system for emergency evacuation, highlighting interrelations between principal system components.

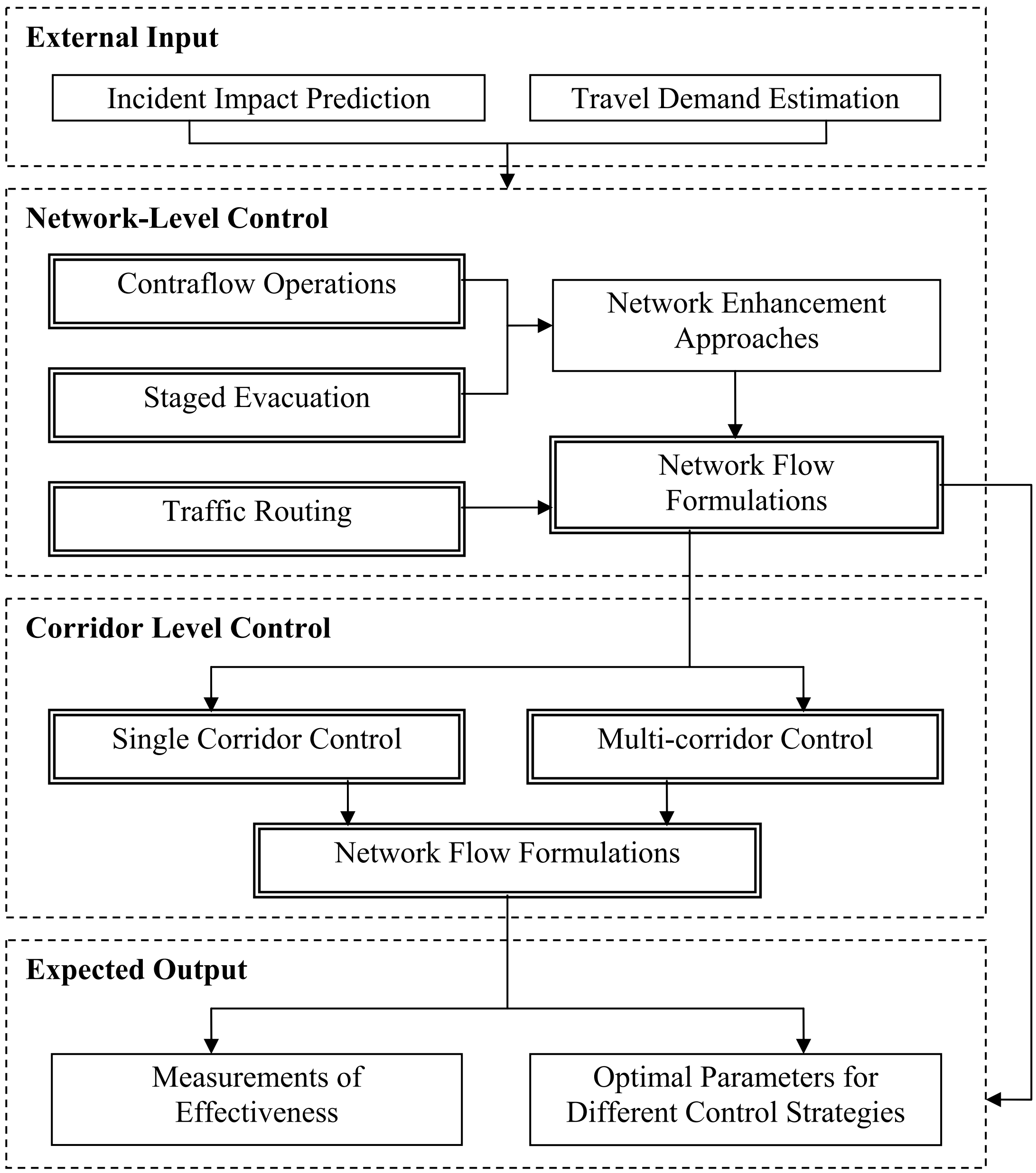

Figure 3.1 Modeling Framework of the Proposed System

This framework applies a two-level control structure: the high-level control focuses on balancing the network traffic by assigning evacuation demand over different time windows and evacuation routes, and the low-level control centers on optimizing signal timings at the corridor level. Such a bi-level structure aims to achieve a trade-off between modeling accuracy and operational efficiency, as a fully integrated control model may involve too many control decisions and constraints to be solved effectively within an acceptable time interval, especially for large-scale network evacuations. This concept of hierarchical control has been widely discussed in other transportation areas, such as traffic signal networks (Sadek and Chowdhury, 2003). It is also consistent with standard evacuation practices, where system operators typically identify major evacuation corridors and urge evacuees to escape via these corridors. A brief description of each key system component is presented below:

- *Network flow formulations*. This component uses mathematical equations to represent traffic dynamics over the evacuation network. As an essential part of the entire optimal control system, these formulations should be able to accommodate the time-varying evacuation demand, to represent the time-varying network capacity, to realistically model traffic flow propagation along the evacuation routes, and to capture potential queue formation and dissipation. Section 4.1 will discuss the detailed formulations for this component with the revised cell transmission concept, which is proposed to reduce the number of variables, thereby improving computing efficiency but preserving the capability of the original cell transmission concept to capture the network dynamics.

- *Traffic routing*. This component functions to determine the best set of routing strategies to efficiently utilize the given evacuation network under the estimated evacuation demands. The set of formulations for this component should capture flow propagation along the evacuation routes as well as flow interactions at intersections/interchanges. Assuming the full compliance of evacuees, Section 4.2 will present the base model for traffic routing with the revised cell transmission concept. The output includes the diverging rates from each origin to its downstream links and the turning fractions at each intersection/interchange.
- *Contraflow design*. This component deals with the selection of lanes/road segments to implement lane-reversing operations under resource limitations. The set of formulations in this component should take into account the different driving behaviors in the normal lanes and reversed lanes, which result from drivers' unfamiliarity with the contraflow operations. Section 4.3 will present an enhanced network modeling approach to tackle related problems. The proposed approach uses dummy segments to conveniently address the potential differences in driving behaviors and also combines the lane-based design concept to capture the nonlinear capacity in contraflow operations.
- *Staged evacuation*. This component functions to determine the most proper time to issue an evacuation order to a target origin (or a target set of adjacent origins) under given safety time windows. The set of formulations in this component should take into account the responses of

potential evacuees to the evacuation orders. In other words, once an evacuation order is activated, the evacuation demand generated in subsequent intervals will depend on the dissemination of the evacuation order as well as on the preparation time of evacuees, which is beyond the control of any system operator. Section 4.4 will present an extended network modeling approach using dummy links at the origins to model the evacuees' response patterns.

- *Individual corridor signal control*. This component functions to generate signal control strategies for a corridor operated independently, i.e., the main arterial in the corridor receives demands directly from origins and sends them in turn to the safety destination without interacting with its neighboring corridors. The formulations should account for the necessary designs to facilitate traffic progression and the impact of signal timings on traffic flows. Section 5.2 will present the detailed formulations with the proposed critical intersection concept, i.e., only key intersections will provide protective phases for turning movements onto the main arterial.
- *Multi-corridor signal control*. This component functions to generate signal control strategies for concurrent evacuation via multiple corridors, during which each corridor may receive traffic from, or send traffic to its neighboring corridors via local streets. The formulations should accommodate various operational complexities caused by the interactions between corridors. Section 5.3 will present the detailed formulations similarly with the critical intersection concept.

3.5. Closure

Based on the analysis of major research issues and the identification of essential functional requirements, this chapter has presented a modeling framework for the proposed integrated optimal control system for emergency evacuation. The proposed modeling framework, consisting of all principal control components, features a two-level control structure for contending with the potential computational issues in large-scale evacuation operations. This hierarchical control structure is consistent with current practice, where system operators tend to identify major evacuation corridors and then implement traffic controls on a corridor basis.

Grounded on the proposed modeling framework, this study will devote the remaining chapters to the following tasks.

- Task 1: Develop effective network flow models;
- Task 2: Develop formulations for network-level controls, including traffic routing strategies, contraflow design, and staged evacuation;
- Task 3: Develop formulations for signal control along an individual corridor, including signal timings and related routing strategies;
- Task 4: Develop formulations for signal control along multiple corridors that may interact with each other, including signal timings and routing strategies;
- Task 5: Develop measurements of effectiveness and evaluate the proposed optimal control system in real-world evacuation scenarios.

Chapter 4: Control Strategies at the Network Level

4.1. Introduction

Chapter 4 presents the formulations for design of evacuation control strategies at the network level, which includes traffic routing, contraflow design and staged evacuation. The objective is to determine the time to issue an evacuation order for each origin, the segments to implement contraflow operations under limited budget, and the guidance of evacuation traffic to different evacuation corridors. Note that as mainly for the planning purpose, the following formulations for optimal control strategies are based on the assumption that evacuees will comply with the instructions issued by the operation center.

The remaining sections are organized as follows. To ensure that the proposed formulations for network flow relations can realistically capture the temporal/spatial interactions of evacuation traffic over the network, Section 4.2 introduces a revised cell transmission concept. The revised modeling concept preserves the capability of the original methodology in capturing traffic dynamics, but allowing the use of cells of different sizes to improve the computing efficiency. This chapter will present the application of this concept in formulating all three network control strategies, which are traffic routing, contraflow design and staged evacuation.

Section 4.3 discusses the modeling issues regarding the design of traffic routing strategies. The proposed basic model is based on the following two assumptions: 1) the evacuation network is predetermined, although it can be either constant or time-varying during the evacuation operations; and 2) the time for activating an evacuation order is predetermined for each origin, i.e., the evacuation demand generated during each interval is known. With these assumptions, presentations of the proposed base model will emphasize the selection of objective functions and the modeling of network traffic interactions.

Section 4.4 discusses the modeling issues regarding the contraflow design. As an extension of the base model, the proposed model will relax the assumption regarding the network conditions, and intend to reallocate capacities by reversing some travel lanes. This extended model features a network enhancement that expands the network with dummy segments and modifies the objective functions and network traffic formulations shown in Section 4.3.

Section 4.5 discusses another extension of the base model, which targets the design of staged evacuation. The extended model aims to determine the time for activating an evacuation order for each origin, given the projected responses of evacuees. This model also features its use of a series of dummy links at the origins to capture the impacts of different evacuation activation times.

The last section summarizes research efforts that have been completed in this chapter. Figure 4.1 has demonstrated the logical relations between different sections in this Chapter.

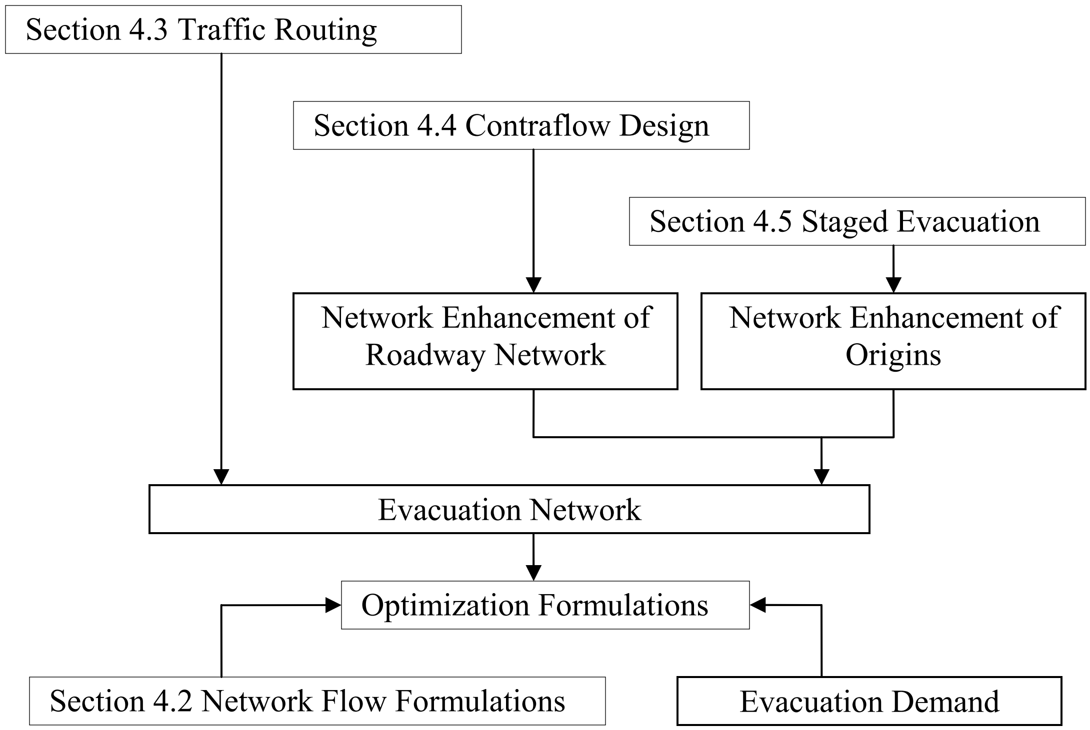

Figure 4.1 Logical Relations of Chapter 4

4.2. Network Flow Formulations

To ensure the effectiveness of the proposed optimization models, one has to choose an approach to mathematically represent traffic flow evolution in an evacuation network. To accommodate the complexity associated with large-scale network applications and to improve the computational efficiency, this study proposes a revised cell transmission formulation for use as the underlying network flow model.

The basic idea of the cell transmission concept proposed by Daganzo (1994; 1995) is to convert roadway links into equal-sized segments, or called cells, that could be traversed in a unit time interval at the free-flow speed. Then, the movements of vehicles among these cells are defined with two types of relations, namely, flow propagation relations to decide flows between two cells based on upstream/ downstream traffic conditions and flow conservation equations to depict the evolution of the cell status (i.e., the number of vehicles in each cell) over time.

To reduce the size of formulations in large-scale network applications, Ziliaskopoulos and Lee (1996) have proposed the use of cells of an adjustable size. Their idea is to update those longer cells with a lower frequency, and use the averaged parameters for those intermediate intervals. Such a formulation requires the size of a long cell to be an integral multiple of its connected short cells, and may cause the propagated flows deviated from those homogenous cells.

To offer the flexibility and also to improve the accuracy in large-scale network applications, the revised cell transmission formulation proposed in this study will allow cells of different sizes to be connected as needed. Its core concept is presented below.

4.2.1. Network Conversion

To successfully apply the revised cell transmission formulation, one needs to convert the road network into a set of connected cells, based on the following principal steps:

- *Identify homogenous road segments*: homogeneity is defined by the same free flow speed, same number of lanes, same jam density, same saturation flow rate, and no ramps within a segment.
- *Define unit time interval*: the maximal unit interval τ is constrained by the shortest time to traverse a homogenous segment, as in Equation 4.1. Other unit intervals can also be used, provided τ is the integral multiple of it.

$$\tau = \min\{\frac{length \quad of \quad a \quad segment}{corresponding \quad free \quad flow \quad speed}\} \tag{4.1}$$

- *Convert road segments to cells*: basically, every homogenous segment is converted to a cell, and the cell size l is defined by Equation 4.2.

$$l = INT\{\frac{length \quad of \quad segment}{corresponding \quad free \quad flow \quad speed \times unit \quad interval \quad length} + 0.5\} \tag{4.2}$$

- *Define connectors between cells*: A connector is defined to indicate the potential traffic flows between two connected segments.

4.2.2. Flow Conservation Formulations

Flow conservation equations depict the evolution of the cell status (i.e., the number of vehicles in each cell) over time. With the revised cell transmission formulation, all cells will be updated at every unit time interval τ, regardless of their size. As illustrated in Figure 4.2, Equation 4.3 and Equation 4.4 define the flow conservation relations for different types of cells.

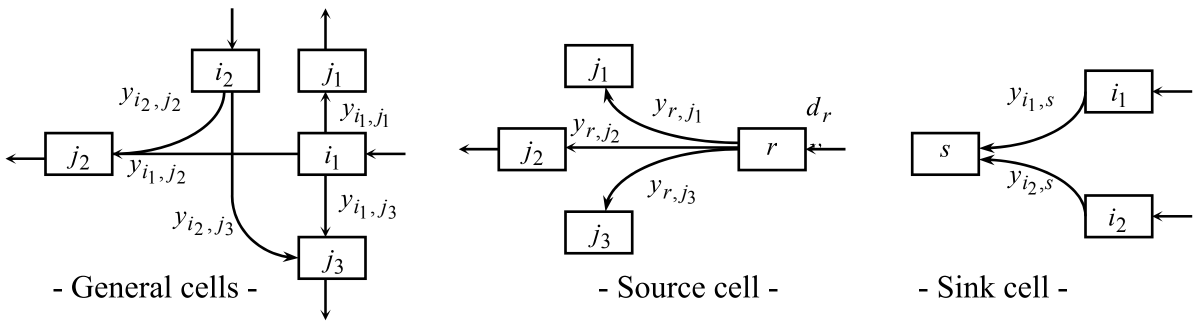

Figure 4.2 Graphical Illustration of Cell Connections

- For general cells (actual highway segments) and sink cells (destinations),

$$x_i^{t+1} = x_i^t + \sum_{k \in \Gamma(i)} y_{ki}^t - \sum_{j \in \Gamma^{-1}(i)} y_{ij}^t \tag{4.3}$$

- For source cells (origins),

$$x_r^{t+1} = x_r^t + d_r^t - \sum_{j \in \Gamma^{-1}(r)} y_{rj}^t \tag{4.4}$$

where x_i^t is the number of vehicles in cell i at the beginning of interval t; y_{ij}^t is connector flows from cell i to cell j during t; d_r^t is evacuation demand from origin r during interval t, which is also called dynamic loading pattern and defined with response curves in practice; $\Gamma^{-1}(i)$ is the set of downstream cells to cell i; $\Gamma(i)$ is the set of upstream cells to cell i; The subscript r is the index of source cells; and i, j, k is the index of other cells.

4.2.3. Revised Flow Propagation Formulations

The flow propagation relations decide the connecting flows between cells during each time interval, which are presented with the following expressions:

$$\sum_{k \in \Gamma(i)} y_{ki}^t \leq R_i^t \tag{4.5}$$

$$\sum_{j \in \Gamma^{-1}(i)} y_{ij}^t \leq S_i^t \tag{4.6}$$

Equation 4.5 is to model flow propagation relations considering the traffic conditions in a downstream cell, whereas Equation 4.6 is for the traffic conditions in an upstream cell. R_i^t is the receiving capacity of downstream cell i during interval t (veh), and S_i^t is the sending capability of upstream cell i during interval t (veh);

Equation 4.7 defines the receiving capacity of cell i, which is proposed after considering the initial cell status x_i^t as well as its potential *internal* evolution during interval t.

$$R_i^t = \min\{Q_i^t, N_i^t / l_i, N_i^t - x_i^t\} \tag{4.7}$$

where Q_i^t is the number of vehicles that can flow into/out of cell i during t; N_i^t is the number of vehicles that can be accommodated in cell i during t; and l_i is the size of cell i. Note that if the cell length l_i is equal to 1, Equation 4.7 will converge to the equation for equal-sized cells in the classic cell transmission formulation. The mathematical proof of Equation 4.7 is shown in Appendix A.

Equation 4.8 defines the sending capacity of cell i. Note that if l_i is equal to 1, Equation 4.8 is also equivalent to the equation for equal-sized cells (Daganzo 1994).

$$S_i^t = \min\{Q_i^t,\ \ N_i^t / l_i,\ \ x_i^{t-l_i+1} - \sum_{j\in\Gamma^{-1}(i)} \sum_{m=t-l_i+1}^{t-1} y_{ij}^m\} \tag{4.8}$$

Here the first two terms are direct presentation of the maximal flow that can leave cell i during a unit time interval. The third term can be explained as follows: according to the definition of cell size, l_i unit intervals are required to traverse cell i at the free-flow speed. Thus, the total flows that should have left cell i are $\sum_{k\in\Gamma(i)} \sum_{m=1}^{t-li} y_{ki}^m$, while the total flows that have actually left cell i are $\sum_{j\in\Gamma^{-1}(i)} \sum_{m=1}^{t-1} y_{ij}^m$. The sending capacity cannot exceed their difference, i.e.,

$$S_i^t \le \sum_{k\in\Gamma(i)} \sum_{m=1}^{t-li} y_{ki}^m - \sum_{j\in\Gamma^{-1}(i)} \sum_{m=1}^{t-1} y_{ij}^m$$

$$= x_i^{t-li+1} - \sum_{j\in\Gamma^{-1}(i)} \sum_{m=t-li+1}^{t-1} y_{ij}^m \tag{4.9}$$

A numerical test is given in Appendix B to demonstrate the effectiveness of the revised cell transmission formulation.

4.3. Base Model: Traffic Routing in Concurrent Evacuation

Applying the revised cell transmission concept as the underlying network flow model, this section will detail the formulations of the base model, which addresses the design of traffic routing strategies under the operation of concurrent evacuation without contraflow options. The optimized control plan mainly includes two types of information, namely, 1) the percentage of demand to be diverted to links immediately downstream of the origins, and 2) the target turning fractions to be controlled at each diverging point during each time interval.

4.3.1. Objective Functions

In response to the unique operational constraints during emergency evacuation, the proposed formulation features a two-level optimization scheme.

The high-level optimization aims to maximize the total throughput within the specified evacuation duration T. Since the throughput can be represented with the total number of vehicles entering all destinations over the study period, one can formulate the objective function as follows:

$$\max \qquad \sum_{i \in S_s} \sum_{k \in \Gamma(i)} \sum_{t=1}^{T} y_{ki}^{t} = \sum_{i \in S_s} x_i^{T+1} \tag{4.10}$$

where S_s is the set of sink cells (destinations); and $\Gamma(i)$ is the set of upstream cells to cell i.

The low-level optimization model intends to minimize the total trip time (including the waiting time in origins) if the specified duration T is sufficient for evacuating all demands. The special structure of the underlying network flow model implies that a vehicle in a cell will either wait for one interval without move or take one interval to reach the downstream cell. Thus, the objective function has the following expression:

$$\min \qquad \sum_{i \in S \cup S_r} \sum_{t=1}^{T} x_i^{t} \tag{4.11}$$

where S is the set of general cells (roadway segments); and S_r is the set of source cells (origins).

4.3.2. Operational Constraints

4.3.2.1. Network Flow Constraints

Although Cell Transmission concept was originally proposed for simulation-based operations, it has later been transformed and utilized in various optimization contexts. Some early studies (Li, et al. 1999; Ziliaskopoulos, 2000) have applied Cell Transmission concept to formulate dynamic traffic assignment as an LP model, which uses a set of less-than constraints to relax the minimal-value in flow propagation relations and thus allow vehicle holding (i.e., traffic will not necessarily exit a cell even if it can do so under the prevailing network situation). Note that vehicle holding may be undesirable since no individual driver would wait when perceives the sufficient capacity ahead. However, holding vehicles in evacuation implies that responsible agencies can improve the overall operation efficiency by delaying certain groups of travelers.

Thus, this study will follow these practices when applying the revised cell transmission concept to formulate the underlying network flow constraints. Note that these constraints, as shown in Equations 4.12-4.19, are the same for both levels of optimization formulations.

$$x_i^{t+1} = x_i^t + \sum_{k \in \Gamma(i)} y_{ki}^t - \sum_{j \in \Gamma^{-1}(i)} y_{ij}^t, \qquad i \in S \cup S_s \tag{4.12}$$

$$x_r^{t+1} = x_r^t + d_r^t - \sum_{j \in \Gamma^{-1}(r)} y_{rj}^t, \qquad r \in S_r \tag{4.13}$$

$$\sum_{k \in \Gamma(i)} y_{ki}^t \le Q_i^t, \qquad i \in S \cup S_s \tag{4.14}$$

$$\sum_{k \in \Gamma(i)} y_{ki}^t \le N_i^t / l_i, \qquad i \in S \cup S_s \tag{4.15}$$

$$\sum_{k \in \Gamma(i)} y_{ki}^t \le N_i^t - x_i^t, \qquad i \in S \cup S_s \tag{4.16}$$

$$\sum_{j \in \Gamma^{-1}(i)} y_{ij}^t \le Q_i^t, \qquad i \in S \cup S_r \tag{4.17}$$

$$\sum_{j \in \Gamma^{-1}(i)} y_{ij}^t \le N_i^t / l_i, \qquad i \in S \cup S_r \tag{4.18}$$

$$\sum_{j \in \Gamma^{-1}(i)} y_{ij}^t \le x_i^{t-l_i+1} - \sum_{j \in \Gamma^{-1}(i)} \sum_{m=t-l_i+1}^{t-1} y_{ij}^m, \; i \in S \cup S_r \tag{4.19}$$

$$y_{ij}^t \le Q_{ij}^t \tag{4.20}$$

Among the above network flow constraints, Equation 4.12 is the flow conservation equation for both general cells and sink cells; Equation 4.13 is the flow conservation equation for source cells; Equations 4.14-4.16 present the relaxed flow propagation constraints related to the receiving capacity of any downstream cells; Equations 4.17-4.19 present the relaxed flow propagation constraints related to the sending capacity of any upstream cells; and Equation 4.20 presents the flow capacity constraints for connectors, which can model the reduced capacity of ramps or the right/left turning movements at the intersections.

Note that Equation 4.20) only defines the restriction on a single connector flow. The modeling for intersections is more complex because different connector flows may conflict with each other and need to share the intersection capacity. Since signal design is not the focus of the network level control, a set of simplified relations as shown in Equation 4.21 is employed here. The equation implies that if one selects a movement arbitrarily from each conflicting phase at an intersection, the sum of the v/c ratios on these movements will not exceed one (i.e., the intersection capacity is satisfied during each interval).

$$\sum_{p \in Ph_I} \{ y_{ij}^t / Q_{ij}^t : \ ij \in p \} \leq 1 \tag{4.21}$$

where I is the index of intersections; Ph_I is the set of conflict phases at intersection I; and p is the index of each conflict phase at intersection I, $p \in ph_I$.

4.3.2.2. Demand Related Constraints

The high level optimization enforces no additional constraints on the evacuation demand. For the low level optimization, since evacuation flows are counted in the objective function only before they have arrived at their destinations, the model tends to push vehicles as many as possible at the fastest pace. Thus, one can expect that all evacuation demands can reach their destinations at the end of the evacuation period. Equation 4.22 is proposed to guarantee such a relation: the left-side term is the total number of vehicles that have arrived at destinations after evacuation duration T and the right-side term denotes the total demand.

$$\sum_{i \in S_s} x_i^{T+1} = \sum_{r \in S_r} D_r \tag{4.22}$$

where $x_i^{T+1}, i \in S_s$ is the number of vehicles that has arrived at the destination i after the evacuation time window T; and $D_r, r \in S_r$ is the total evacuation demand generated at origin r.

4.3.2.3. Other General Constraints

The general constraints include nonnegative constraints, initial value of cell state variables x_i^1, and initial value of connector flows y_{ij}^0. In most cases, x_i^1 (excluding source cells) and y_{ij}^0 are set to zero, although x_i^1 can be other values to simulate the background traffic prior to the evacuation. Note that x_i^1 can also be used to reflect the actual network condition preceding the onset of an accident during the evacuation, and this enables the model users to adjust the evacuation plans as needed.

Another class of general constraints is for the capacity of destinations. Storage capacity $N_i^t, i \in S_S$ can be restricted if the safety shelter has the space limitation. Flow capacity $Q_i^t, i \in S_S$ may be restricted if the entrance capacity of the safety shelter is lower than the capacity of the upstream routes, or if the destination is not the safety shelter but a dummy node to indicate safe area. In the later case, $Q_i^t, i \in S_S$ is set as the capacity of downstream routes to prevent the queue spillback. As the important evacuation control strategies, both diverging proportions and merging proportions are directly estimable from the optimization results.

4.3.3. Numerical Test of the Base Model

This numerical test aims to demonstrate the applicability of the proposed Base Model for traffic routing with the Ocean City hurricane evacuation network. Ocean City is a famous tour destination located on a narrow peninsula on Maryland Eastern Shore. The population in the summer peak season can reach 150,000 ~ 300,000 people, compared with 7,000 to 25,000 people during the off-peak season. This large size of population in the summer season renders the city especially vulnerable to the threat of hurricanes, which demands the state to design its hurricane evacuation plans.

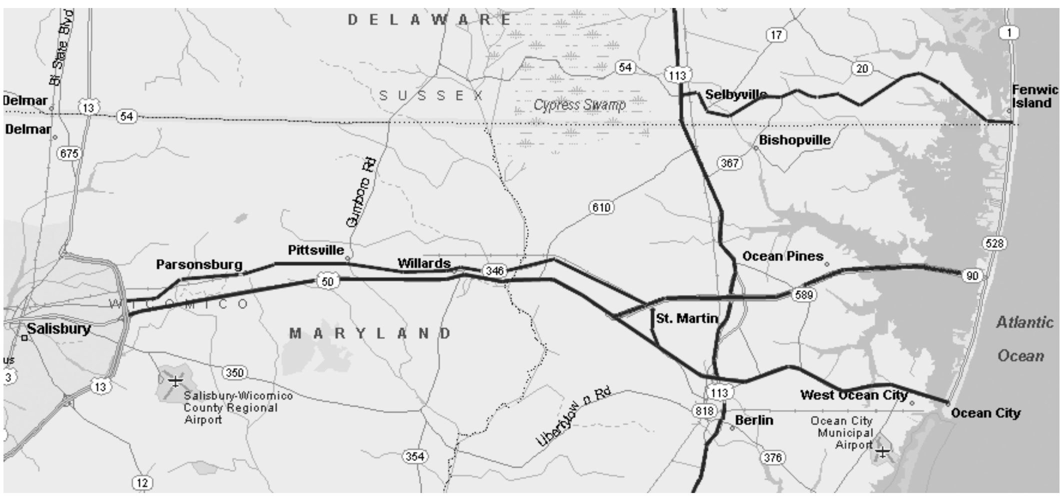

Figure 4.3 Major Evacuation Network for Ocean City

Figure 4.3 presents the major evacuation network for Ocean City. The sole origin is set to be the entire city. Thus, one can divide the city into a number of evacuation zones, based on the optimized demand distribution to the three primary evacuation routes. Among these routes, US50 is an arterial street with two lanes in each direction, MD90 is a freeway with one lane in each direction, and DE20 is an arterial street with one lane in each direction. There are three destinations for evacuation flows. The city of Salisbury is a destination without capacity limit, while US113 north and US113 south are two dummy destinations with a flow capacity of 1800 vehicle per lane per hour.

Following the network conversion procedures in Section 4.2, this numerical test first defines the homogenous segments. Note that all interchanges are modeled with connectors, not cells, to indicate the existence of ramps. The jam density for all cells is set to be 93 vehicles per kilometer per lane, whereas the saturation flow rate is set to be 2160 vehicles per lane per hour for the freeway segment of MD90, and 1800 vehicles per lane per hour for other segments. Based on the actual network geometric data, the length of a unit interval is set to be 20 seconds, which is sufficiently small for evacuation operations. Then, one can convert the network to a cell-connection diagram as illustrated in Figure 4.4. Note that the number in each parenthesis indicates the size of the cell.

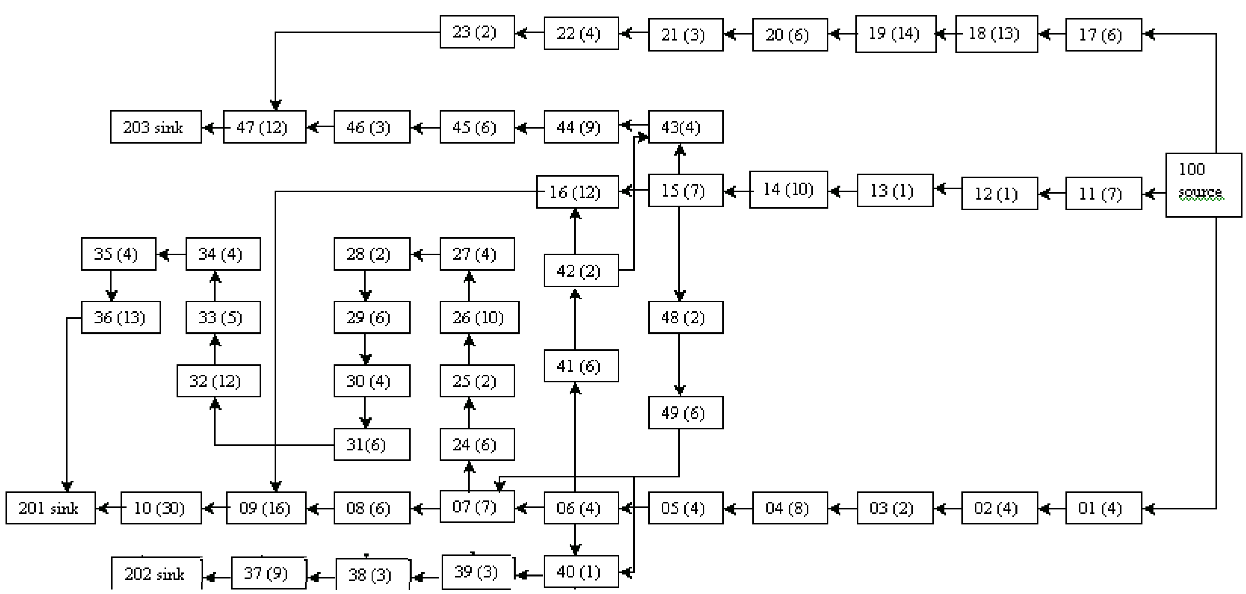

Figure 4.4 Cell Connection Diagram for Ocean City Hurricane Evacuation Network

Note that as indicated in the widely adopted evacuation response curves (Alsnih and Stopher, 2003), the evacuation demand from origin *r* in time interval *t*, d_r^t, tends to greatly exceed the evacuation capacity after the inception of evacuation. This surge in evacuation demand may be more apparent for potential hurricane evacuation of Ocean City, since the major evacuation population will be tourists who have limited personal belongings to collect and few local properties to protect. Thus, this numerical test assumes that all traffic demand enters their corresponding source cell at the beginning of the evacuation process.

For the evacuation scenario specified above, the resultant LP formulations contain 720 time intervals, 79,809 variables, and 250,509 constraints. A computer program was created to generate the standard input file for the professional software LINGO 8.0. The global optimal solution for the maximal throughput over 4 hours amounts to 27,268 vehicles to all three destinations. Figure 4.5 presents the cumulative arriving curve for each destination, where most vehicles are directed to Salisbury.

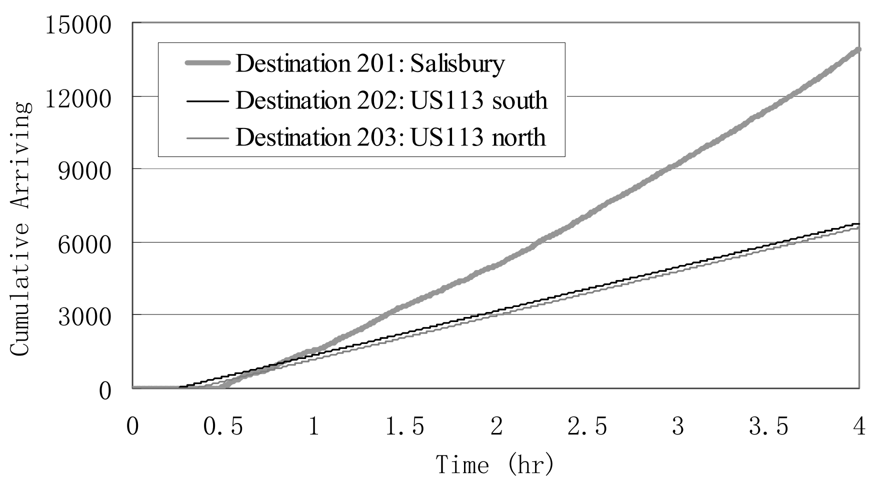

Figure 4 5 Cumulative Arriving Curves for the High-Level Optimization

The numerical test then applies the proposed low-level optimization model to obtain the optimal evacuation patterns to minimize the total travel time and waiting time if the allowed time window is sufficiently long for completing the evacuation. The total evacuation demand is set to be 25,000 vehicles in 4 hours. The new LP formulations with the second level optimization contain 80,528 variables and 251,228 constraints for 720 time intervals. Figure 4.6 presents the cumulative arriving curve of each destination based on the global optimal solution.

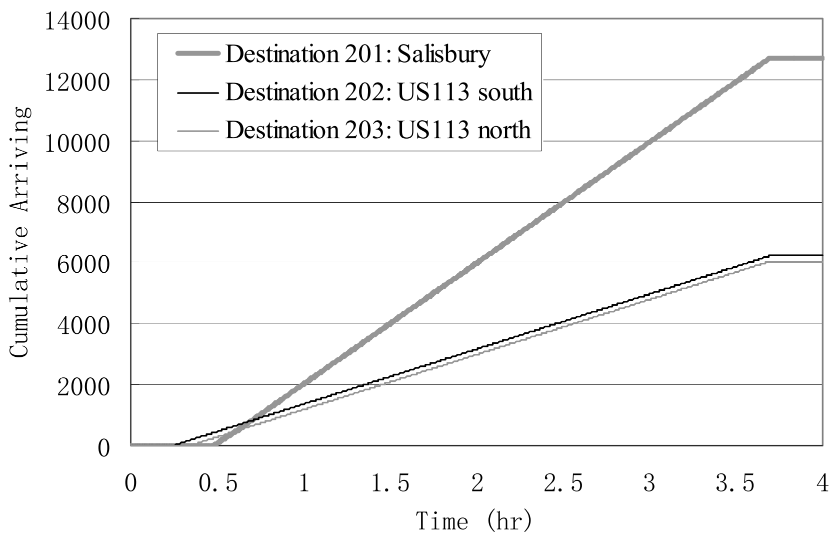

Figure 4.6 Cumulative Arriving Curves for the Low-Level Optimization

The preliminary results from the low-level model indicate that there is no flow in the south direction of US113 between US50 and MD90, and the capacity usage of the north direction of US113 from US50 to DE54 is very low. Thus, one can exclude these road segments from the major evacuation network in practice. Note that after excluding those low-usage routes, only two diverging cells remain in the network and their diverging patterns are relatively stable (except during the dissipation phase) in the optimal solution.

Thus, the last part of the numerical test will input these diverging rates as the target turning fractions in a CORSIM simulator of the Ocean City hurricane evacuation network, with the objective of evaluating the reliability of the proposed formulations. For this purpose, Figure 4.7 compares the cumulative arriving curve at each destination generated from the model with the same curves generated from the microscopic simulator. The comparison indicates that the time-varying network traffic conditions with two approaches are quite similar, which thus demonstrates the potential of the proposed model in accurately formulating traffic flows for large-scale networks and in efficiently generating the optimal set of evacuation strategies.

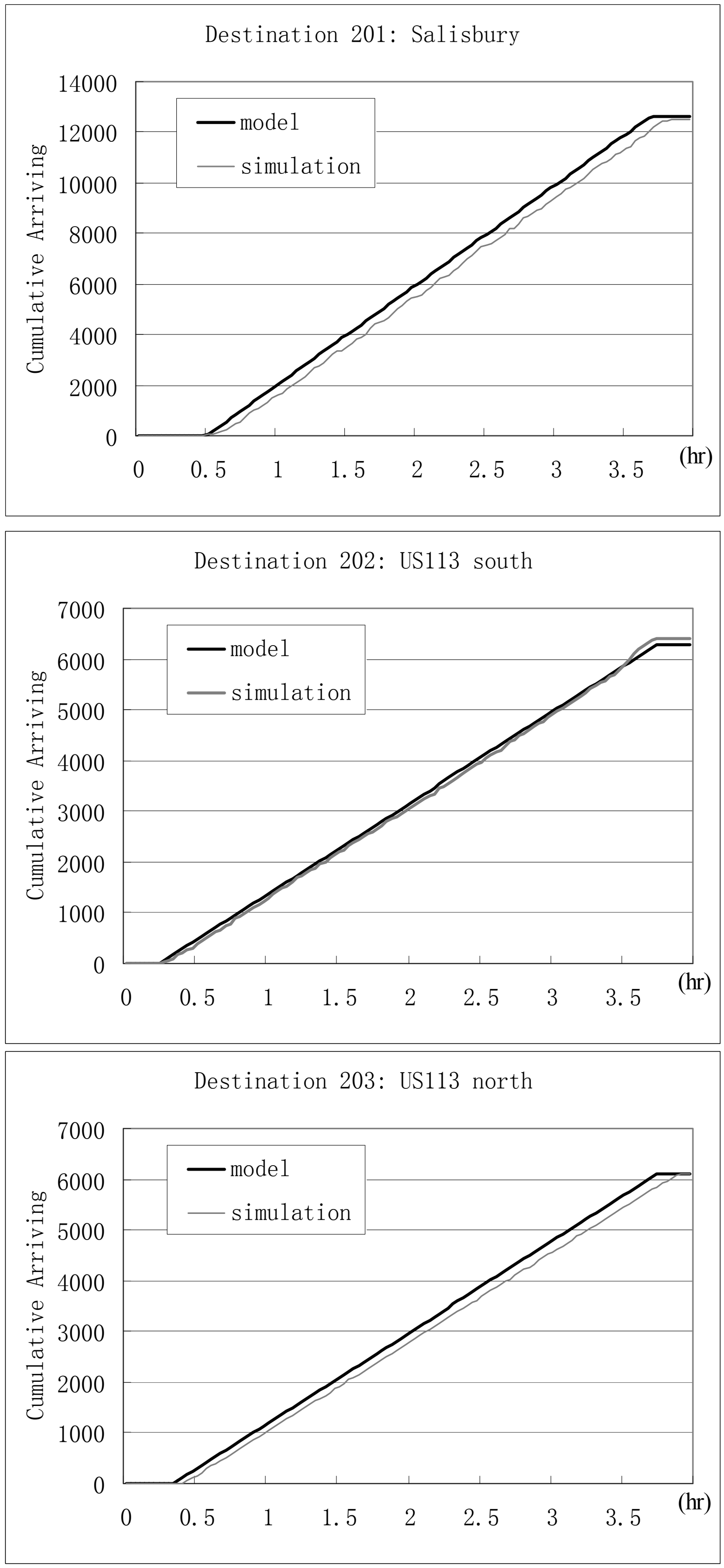

Figure 4.7 Comparison of Cumulative Arriving Curves: Model vs Simulator

4.4. Extended Model-I: Contraflow Design

The extended model-I aims to incorporate the contraflow decisions into the base model for a concurrent evacuation. The optimized control plan mainly includes three types of information, namely: 1) the segments to implement lane reversal operations under the budget limit; 2) the percentage of demand to be diverted to the links immediately downstream of the origin; and 3) the target turning fractions to be controlled at each diverging point during each time interval. This model is especially essential under the following situations.

- With limited resources. Since contraflow operations requires a large amount of manpower and materials such as barricades or cones, system operators have to decide the reversing priority of candidate segments and assign the available resources to the most critical locations.
- With a complex evacuation network. For example, when there are many parallel roads connecting the major evacuation corridors, system operators may face the difficulty in deciding whether to reverse some parallel roads and where to enact the reverse-lane operations.

4.4.1. Operational Concerns for Contraflow Design

As discussed in the literature review chapter, the key concept of contraflow design is to temporarily reverse some travel lanes for the safety-bound traffic so as to increase the available capacity toward the target evacuation destinations. Although some studies have explored the design of contraflow strategies with optimization models, the following critical modeling issues remain to be investigated.

- Traffic streams on the reversed lanes differ significantly from those on the normal lanes. As noted in some studies, such differences are reflected in the reduced capacity and speed observed on the reversed lanes. Thus, it seems inappropriate to model the reversed and normal lanes on the same segment as one cell or with the identical formulation.
- The reversed lane capacity will not be available at the beginning of the evacuation process, as it needs the law enforcement agency to clear all traffic on the target lanes for reverse-lane operations.
- An increase in the flow capacity due to reverse-lane operations has a non-linear relationship with the number of reversed lanes. For a freeway segment with two lanes in each direction, the data in Table 4.1 clearly indicate this non-linearity nature [Wolshon, 2001].

Table 4.1 Evacuation Traffic Flow Rates

Contraflow Strategies	Safety-bound Capacity (vph)
Normal Two Way Operation (no contraflow)	3,000
Three Lane (one contraflow lane)	3,900
One-Way (two contraflow lanes)	5,000

In response to the aforementioned operational concerns, this study proposes the Extended Model-I for contraflow design as the extension of the Base Model. This extended model uses the same two-level optimization objectives as in Equations 4.10 and 4.11. The network flow models are also similar as those in Equations 4.12-4.21, but with a more elaborated network and additional constraints to capture the effects of contraflow decisions on network traffic pattern.

4.4.2. Key Features of the Elaborated Network for Extended Model-I

The key features of the elaborated network for applying the extended model for contraflow operations are summarized below.

- To reflect the difference in normal lanes and reversed lanes, the model represents each homogenous road segment *i* (one direction) with two cells (i^+, i^-), one in its designed direction and the other in its reversed direction. The length of these two cells may not be equal due to the potential speed differences.
- To reflect the non-linearity in lane capacity the model assigns a binary variable δ_{ln} to each lane, ln, on a segment for indicating its direction. In addition, each lane will have two flow capacity indices ($Q^+_{\text{ln}}(t)$, $Q^-_{\text{ln}}(t)$), one for each direction. Thus, the flow capacity for each cell ($Q^t_{i^+}$, $Q^t_{i^-}$) will depend on the reversing decisions of each lane on the target segment i.

Fig. 4.8 illustrates application of the above concept on a highway of two lanes in each direction. There are two segments for use in operations, one for each direction. Such two segments are named as a pair of segments, and operators will not reverse them concurrently. Note that there are five possible operational plans in this case:

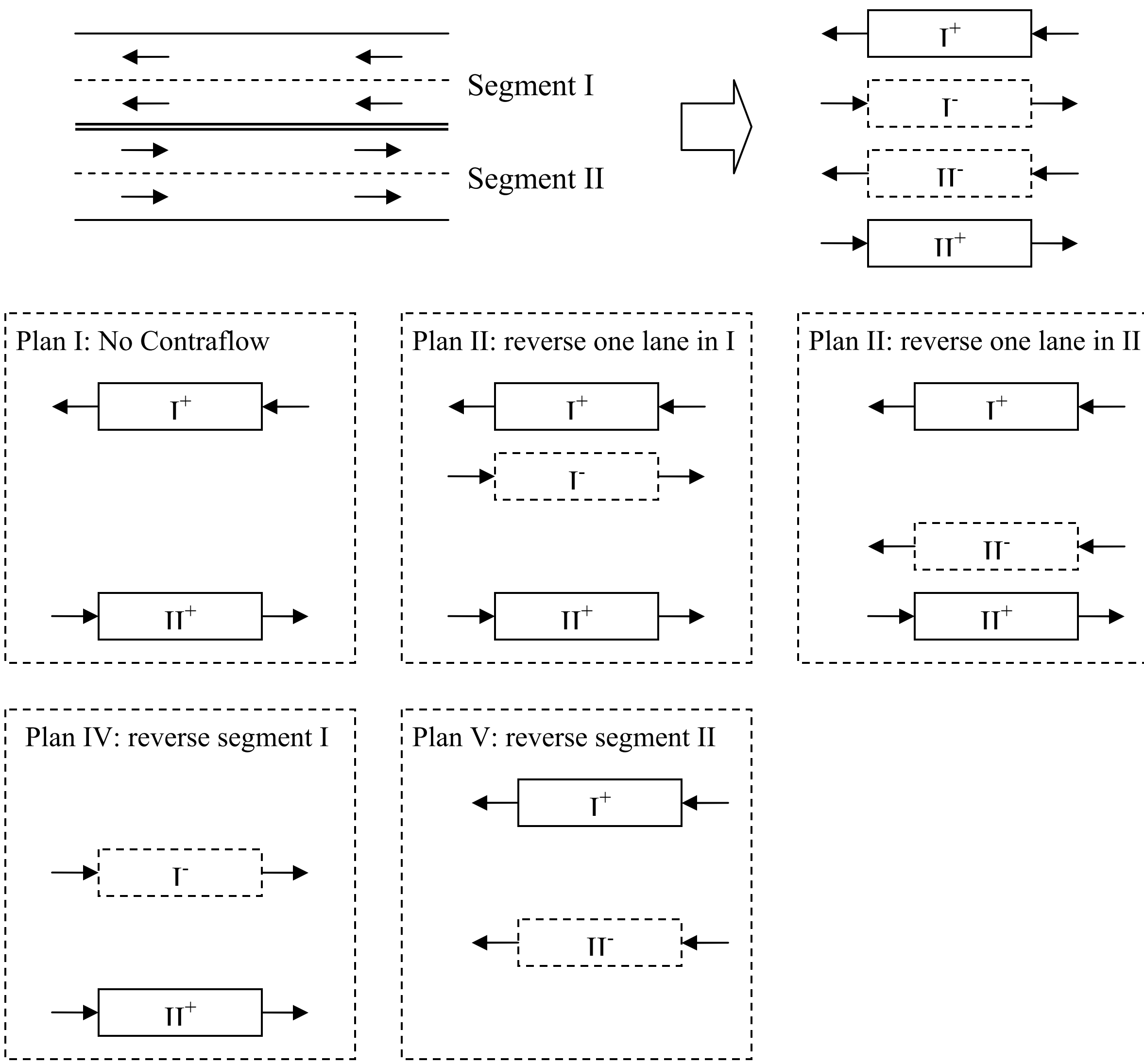

Figure 4.8 Illustration of the Network Transformation in the Extended Model-I

- No lanes are reversed, and thus both reversed cells will have a zero capacity.
- One lane in Segment I (or II) is reversed, and thus both normal cells and the corresponding reversed cell will have a positive capacity.
- Both lanes in Segment I (or II) are reversed, and thus only one normal cell and one reversed cell will have a positive capacity.

When applying the extended model-I to design contraflow strategies in emergency evacuation scenarios, system users can easily exclude some of the above five alternatives and thus reduce the size of the elaborated network. For example, safe-bound lanes on those major evacuation corridors will not be reversed.

4.4.3. Additional Constraints in the Extended Model-I

Based on the illustration in Figure 4.8, one can formulate the flow capacity of each cell in the Extended Model-I with Equations 4.23-4.24. The storage capacity of each cell can be formulated in a similar manner. These capacity parameters will be substituted into the network flow constraints 4.13-4.19 of the Base Model, instead of those fixed capacities.

$$Q^t_{i^+} = \sum_{\mathrm{ln} \in LN(i)} Q^+_{\mathrm{ln}}(t) \cdot (1 - \delta_{\mathrm{ln}}) \tag{4.23}$$

$$Q^t_{i^-} = \sum_{\mathrm{ln} \in LN(i)} Q^-_{\mathrm{ln}}(t) \cdot \delta_{\mathrm{ln}} \tag{4.24}$$

where i^+, i^- are index of the normal and reversed cell for segment i; $Q^t_{i^+}$, $Q^t_{i^-}$ are flow capacity (the number of vehicles that can flow in/out) of cell i^+, i^- during time interval t; $Q_{\ln}^{+}(t)$, $Q_{\ln}^{-}(t)$ are capacity of lane *ln* at time t if the lane is in normal direction or reversed; $\ln : \ln \in LN(i)$ is the index of lanes on segment i (ranked from the left most lane); $\delta_{\ln}$ is a binary variable, which equals one if lane *ln* is reversed and equals zero otherwise.

In addition, Equations 4.25 and 4.26 defines two types of logical relations for lane-reversal decisions.

$$\delta_{\ln} \geq \delta_{\ln'} : \quad \ln \leq \ln', \quad \ln, \ln' \in LN(i) \tag{4.25}$$

$$\delta_{\ln} + \delta_{\ln'} \leq 1 : \quad \ln = 1 \in LN(i), \quad \ln' = 1 \in LN(j) \tag{4.26}$$

where Equation 4.25 defines the logical relations for reversing different lanes in the same segment. In other words, if a segment has multiple lanes traveling in the same direction, operators always have to reverse those lanes on the left first. This equation requires the index of lanes on a segment starting with 1 from the leftmost lane. Equation 4.26 defines the logical relations for reversing lanes in the paired segments i and j, i.e., paired segments cannot be reversed concurrently.

Note that if system operators have specified the time CI_i for clearing a reversed segment i, the model will change the reversed lane capacity $Q_{\ln}^{-}(t)$ to zero before interval CI_i for any lane on the segment. The model can also include additional constraints on the contraflow plans such as keeping certain lanes in the danger-bound direction, which is essential for some traffic to get back to the evacuation zone if needed (e.g., for public transit vehicles to pick up non-motorized populations or for emergency response personnel to enforce the operations).

4.4.4. Numerical Test of the Extended Model-I

The numerical test in this section is designed mainly for two purposes: 1) to demonstrate the applicability of Extended Model-I for identifying appropriate contraflow strategies in a real-world evacuation network, and 2) to evaluate the effectiveness of the optimization model by comparing the optimal control plan with current plans developed by the responsible agency.

The study network is also the Ocean City hurricane evacuation network as given in Section 4.3. In design of the contraflow strategy, the right lane on US50 eastbound has to remain in its normal direction for potential traffic heading to Ocean City for some justifiable reasons. As mainly for illustration, the results for this numerical test are grounded on the following assumptions.

- It takes 30 minutes to clear the normal traffic on travel lanes before they could be reversed for evacuation flows. Thus, the capacity of reversed lanes is set as zero within 30 minutes of the evacuation start time.
- Resource limit is represented with constraints on the total length of reversed segments.
- Vehicle speed under free flow conditions is equal to the speed limit on reversed lanes.

For the constraints of different reversed lengths, Table 4.2 shows the contraflow plan, the maximal throughput over a 4-hour period generated from the high-level optimization process (without demand constraints), and the clearance time for a total demand of 25,000 vehicles from the low-level optimization results.

Table 4.2 Contraflow Plans under Both Levels of Optimization

Total length of reversed segments allowed (km)	Reversed segments	High Level: Maximal throughput over 4 hours	Low Level: Evacuation clearance time for 25,000 vehicles
0	-	27,268	3.70
32	MD90 until US50	31,436	3.29
40	MD90 until US113; US50 between US113 and MD346; US50 after MD90	33,672	3.11
48	MD90 until US50; US50 after MD90	33,780	3.10
52	MD90 until US50; US50 before US113; US50 after MD90;	36,900	2.90

Note that extending the currently reversed lane may not always be the best alternative for the entire operations if the resources for such operations have been increased. Instead, one shall redesign the location and length for reverse-lane operations under the available resources so as to maximize its incremental benefits. For example, if the resources allow the length of reversed segments to be 40km instead of 32km, the previously selected segment between US113 and US50 for reverse-lane operation shall be replaced with two other segments (US50 between US113 and MD346, and US50 after MD90) in the new contraflow plan.

The numerical test then compares the following two evacuation control plans with a microscopic CORSIM simulator. The major control strategies of each plan are listed in Tables 4.3 and 4.4, whereas the performance measurements are shown in Table 4.5.

- Plan 1: the final evacuation plan generated with Extended Model-I where MD90 eastbound lane has been reversed
- Plan 2: the evacuation plan from a previous simulation-based project where MD90 eastbound lane has been reversed

Table 4.3 Diverging Rate for Contraflow Plans 1 and 2

Candidate Evacuation Routes		Plan 1	Plan 2
Ocean City	To DE54	17.22 %	16.5%
	To MD90	47.10 %	41.8%
	To US50	35.67 %	41.7%

Table 4.4 Turning Fractions for Contraflow Plans 1 and 2

Critical Control Points		Plan 1	Plan 2
From MD90	To US113N	0.05 (0-180min) 0 (181-240min)	0.075
	To US113S	0.20 (0-60min) 0.15 (61-180min) 1 (181-240min)	0.425
From US50	To US113N	0	0.1
	To US113S	0.50 (first 180min) 1 (last 60min)	0.2
	To MD346	0.65	0.2
From US113N	To MD90	0	0
From US113S	To US50	0.6	0.1

Table 4.5 Performance Measures for Contraflow Plans 1 and 2

	Plan 1			Plan 2		
Throughput over Time (vehicles)	To Salisbury	To US113 N	To US113 S	To Salisbury	To US113 N	To US113 S
By 0.5 hr	19	139	394	13	166	330
By 1 hr	1800	1122	1586	1722	1359	1434
By 1.5 hr	4653	2191	2823	4074	2652	2542
By 2 hr	7536	3117	3880	6450	3875	3614
By 2.5 hr	10393	4111	5036	8846	5070	4685
By 3 hr	13287	4890	5182	11197	5909	5550
By 3.5 hr	14860	4923	5216	13482	5916	5550
Clearance Time	3.50 hr			3.53 hr		
Average Speed	59.2 km/hr			53.6 km/hr		

Comparison of these two plans with the same contraflow designs indicates that the plan generated with the Extended Model-I outperforms the simulation-based plan, which are designed by the collectal efforts of local experts through a large number of try-and-error experimental simulation runs. Hence, the proposed model can substantially reduce the required knowledge and efforts at the planning stage.

4.5. Extended Model-II: Staged Evacuation

Focused on the design of staged evacuation strategies, the extended model-II aims to generate three types of information, namely: 1) the time to issue an evacuation order to each origin or a set of origins with the similar time window and the same hazardous impact level; 2) the percentage of demand to be diverted to links immediately downstream of each origin, and 3) the target turning fractions to be controlled at each diverging point during each time interval.

Compared with the Evacuation Scheduling problem that optimizes the demand to be generated in each interval, the proposed Extended Model-II features its capability to explicitly determine the time to issue an evacuation order and to capture evacuees' response behavior after the evacuation order has been activated. This problem, although more realistic in nature, has not been adequately addressed yet in the literature. Note that the following formulation will only focus on the low level optimization, which means that the evacuation operation can be completed within the given time window.

4.5.1. Model Assumptions

To ensure that the proposed formulations for the staged evacuation are trackable and also to realistically reflect the real-world constraints, this study has employed the following two assumptions in the model development.

The first assumption is that the available time window for each evacuation zone is predetermined. More specifically, this study assumes that the study network can be divided into different evacuation zones based on the estimated impact area and its expansion rate. Besides, the knowledge of the following two parameters is assumed available as they define the available time window for each evacuation zone and thus reflect the differences in the urgency level among all target evacuation zones.

- The maximal tolerable delay from the onset of an emergency event to the activation of an evacuation order for each evacuation zone;
- The acceptable latest time to evacuate all populations for each evacuation zone.

The second assumption is that the total demand and its dynamic loading pattern at each origin is known once an evacuation order is issued. The dynamic loading pattern refers to the profile of evacuees generated in each time interval after the activation of an evacuation order. This study aims to develop a generic approach for modeling the staged evacuation operations for various demand patterns. Thus, for convenience of model illustration, this study employs the following assumptions on evacuation demand generation:

- Evacuees will depart from some pre-selected origin nodes on the network and the total evacuation demand from each origin has been estimated in advance.
- Each origin node, once receiving an evacuation order, will load its demand onto the evacuation network in accordance with a fixed pattern.

4.5.2. Objective Function

The primary objective of the Extended Model-II is to improve the efficiency of the entire evacuation process while minimizing the total potential emergency impacts, or in other words, to minimize the sum of the following two time-related indices:

- The weighted sum of the times for all evacuees to exit an evacuation zone, which reflects the estimated emergency impacts and congestion level on the evacuation network. The special structure of the underlying network flow model implies that a vehicle in a cell will either wait for one interval or take one interval to reach the downstream cell. Thus, the weighted total time can be represented as follows.

$$\sum_z \{w_z \sum_t [\sum_{i \in S_z} x_i^t + \sum_{r \in S_z^r} (x_r^t + \sum_{i \in S_r^a \cup cw_r} x_i^t)]\} \tag{4.27}$$

- The weighted waiting time of those vehicles ready to load on the actual network but are delayed due to congestion. This is to reflect the congestion at those entry points to the evacuation network. Since all vehicles from an origin r enter the actual network through the waiting cell cw_r, one can compute this index as the total delay in cw_r.

$$\sum_z w_z [\sum_{r \in S_z^r} \sum_t (x_{cw_r}^t - \sum_{j \in \Gamma^{-1}(cw_r)} y_{cw_r,j}^t)] \tag{4.28}$$

Here z is the index of each evacuation zone; w_z is the weighting factor to reflect the level of urgency in zone z; S_z is the set of roadway segments (general cells) in evacuation zone z; S_z^r is the set of origin nodes (source cells) in evacuation zone z; S_r^a is the set of pseudo segments (auxiliary cells) for modeling the delay in ordering evacuation for origin r; cw_r is the pseudo segment (waiting cell) to model the waiting of vehicles from origin r before they can enter the actual network.

The network flow constraints for the evacuation roadway network are the same as Equations 4.12-4.20. By the same token, the completeness of the evacuation process is guaranteed with Equation 4.22. The general constraints are also similar. However, to capture the complex operational relations involved in the staged evacuation process, the proposed Extended Model-II introduced the following additional constraints.

4.5.3. Additional Operational Constraints

4.5.3.1. Additional Constraints Type I: Simulating Staged Evacuation Operations at Each Origin

In the staged evacuation planning, an origin is assumed to release its demand according to predetermined dynamic loading patterns as soon as an evacuation order is issued. In other words, the demand generation process is controlled with a trigger mechanism. However, the time to issue an evacuation order for each evacuation zone is a decision variable to be determined via the proposed optimization model. Thus, without knowing its evacuation starting time (note: time zero in the model formulation refers to the emergency occurrence time) the demand at each origin cannot be loaded onto the network in a straightforward way.

To cope with this problem, this study proposes a Network Enhancement Approach to convert the combined temporal/spatial optimization problem into a pure spatial network optimization formulation. For each origin r in evacuation zone z, the proposed approach employs the following three types of cells to model the trip generation process, which are shown in Figure 4.9.

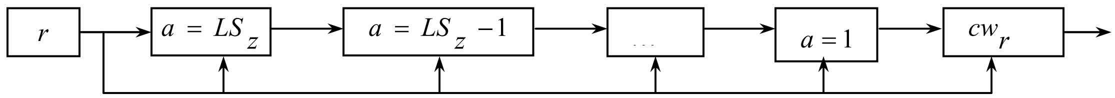

Figure 4.9 Network Enhancement for Origins

- One source cell r with $x_i^0 = D_r$, $N_r^t = \infty$, $Q_r^t = d_r^t$, $t = 0,1,\ldots,T$
- Set of auxiliary cells $a : a = 1,2,...,LS_z$ with $x_a^0 = 0$, $N_a^t = \infty$, $Q_a^t = \infty$, $t = 0,1,\ldots,T$. Here LS_z is the latest time to initiate an evacuation order for evacuation zone z after the emergency occurrence (unit: intervals)
- One waiting cell cw_r with $x_{cwr}^0 = 0$, $N_{cwr}^t = \infty$, $Q_{cwr}^t = \infty$, $t = 0,1,\ldots,T$

Then, a set of binary variables $\delta_z^t : t = 0,1,\ldots,LS_z$ is used in the following flow propagation equations 4.29-4.34 to restrict the flows between the source cell r and the auxiliary cells and the waiting cell.

$$\sum_{t=0}^{LSz} \delta_z^t = 1 \tag{4.29}$$

$$y_{ra}^t = \delta_z^a \cdot d_r^t \quad : a = 1,2,\ldots,LS_z, \ \ r \in S_z^r, \ t = 0,1,\ldots,T \tag{4.30}$$

$$y_{r,cw_r}^t = \delta_z^0 \cdot d_r^t \quad : t = 0,1,\ldots,T, \ \ r \in S_z^r \tag{4.31}$$

$$y_{a+1,a}^t = x_{a+1}^t \quad : a = 1,2,\ldots,LS_z - 1 \tag{4.32}$$

$$y^t_{a=1,cw_r} = x^t_{a=1} \tag{4.33}$$

$$\sum\nolimits_{j \in \Gamma^{-1}(cw_r)} y^t_{cw_r,j} \le x^t_{cw_r} \tag{4.34}$$

By definition, $\delta^t_z = 1$ if evacuation order is activated at the beginning of interval t for evacuation zone z. Equation 4.29 guarantees that for each evacuation zone, the evacuation order is initiated once and only once before the pre-specified latest time LS_z. Equations 4.30 and 4.31 indicate that there will be no flow directly between the origin and an auxiliary/waiting cell if the evacuation order is not at the corresponding interval. Otherwise, evacuation demand will flow from the origin to the auxiliary/waiting cell according to the fixed loading pattern d^t_r. Equations 4.32 and 4.33 guarantee the arrival of evacuees at the waiting cell following the same loading pattern. Equation 4.34 requires that the traffic flowing out a waiting cell during each interval cannot exceed the number of vehicles in the waiting cell.

Then, the flow conservation equations for this enhanced network at origins can be stated as follows.

$$x^{t+1}_r = x^t_r - \sum\nolimits_{a=1}^{LSz} y^t_{ra} - y^t_{r,cwr} \tag{4.35}$$

$$x^{t+1}_a = x^t_a + y^t_{ra} - y^t_{a,a-1} : \quad a = LS_z \tag{4.36}$$

$$x^{t+1}_a = x^t_a + y^t_{ra} + y^t_{a+1,a} - y^t_{a,a-1} : \quad a = 2, \ldots, LS_z - 1 \tag{4.37}$$

$$x^{t+1}_a = x^t_a + y^t_{ra} + y^t_{a+1,a} - y^t_{a,cw_r} : \quad a = 1 \tag{4.38}$$

$$x^{t+1}_{cw_r} = x^t_{cw_r} + y^t_{r,cw_r} + y^t_{a=1,cw_r} - \sum\nolimits_{j \in \Gamma^{-1}(cw_r)} y^t_{cw_r,j} \tag{4.39}$$

The above Equations 4.29-4.39 model the demand generation in a staged evacuation planning for each origin node, $r \in S_z^r$. For example, if the evacuation order is given at interval $k (k \le LS_z)$, the demand will go directly to the auxiliary cell $a = k$ from interval $t = 0$ according to the loading pattern. Since traveling through the chain of downstream auxiliary cells requires k intervals, the demand will arrive at the waiting cell from interval $t = k$, equal to the time when the evacuation order is activated.

4.5.3.2. Additional Constraints Type 2: Clearance of Evacuation Zones

This set of constraints is related to LC_z, the latest time to clear all populations from an evacuation zone z so as to avoid the hazard impacts. Note that the assumption of a progressively expanded impact area in this study implies a higher-urgency zone being surrounded by a lower-urgency zone. Thus, the approach is to control the flow in/out of evacuation zone z by time LC_z, as in Equation 4.40, where z' indicates the inner zone of zone z with higher urgency level and z'' indicates the outer zone with lower urgency level.

$$\sum_{z'} \sum_{t=0}^{LCz} \{y_{ij}^t : \; i \in z, j \in z'\}$$

$$= \sum_{r \in S_z^r} D_r + \sum_{z''} \sum_{t=0}^{LCz''} \{y_{ij}^t : \; i \in z'', j \in z\} \tag{4.40}$$

4.5.4. Numerical Test for the Extended Model-II

To illustrate the staged evacuation strategy and the applicability of the proposed model, this study uses a small network in Figure 4.10 for numerical tests.

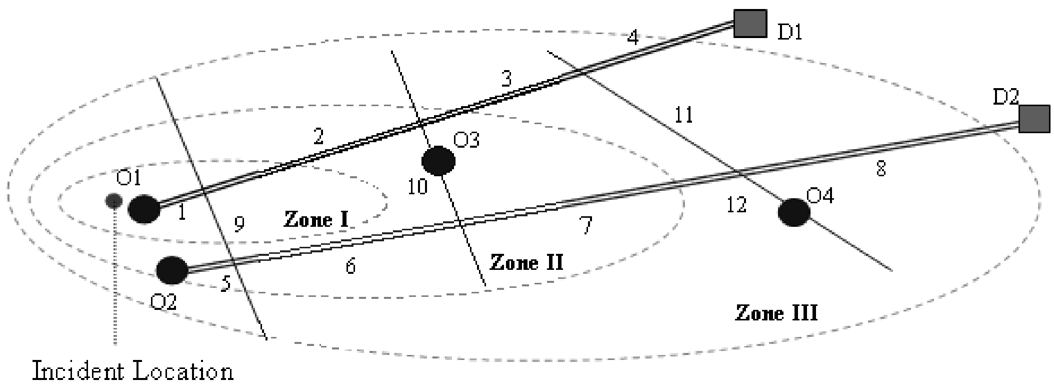

Figure 4.10 Example Network for Numerical Test of Extended Model-II

Surrounding the incident location, there are three evacuation zones indicated with dashed ovals. Table 4.6 shows the pre-determined properties of each evacuation zone.

Table 4.6 Property of Evacuation Zones in the Staged Evacuation Test

Index		Zone I	Zone II	Zone III
Latest Time for Evacuation Order Initiation LS_z (min)	Staged Evacuation	0	60	90
	Concurrent Evacuation	0	0	0
Latest Time for Evacuation Zone Clearance LC_z (min)		40	80	120
Weighting Factor w_z		3	2	1

There are four origin points on the study network, indicated with small black cycles. Among those, origin 1 is in zone I, origin 2 and 3 are in zone II, while origin 4 is in zone III. To test the proposed optimization model under different demand patterns, this study designed five demand scenarios as shown in Table 4.7. The total demand for each origin will be loaded onto the network in accordance with the S-shaped logit function shown in Equation 4.41 (Sheffi, 1985).

$$P(t) = \frac{1}{1 + \exp[-a(t - t_h)]} \tag{4.41}$$

where $P(t)$ is the percentage of loaded demand by time t; t_h is the half-loading time as in Table 4.7; and a is the behavior parameter with the value of 0.5.

Table 4.7 Five Different Demand Scenarios in the Staged Evacuation Test

Origin		Origin 1	Origin 2	Origin 3	Origin 4
Half loading time (min)		5	5	8	10
Total demand (veh)	Scenario 1	3000	4000	0	4000
	Scenario 2	3000	1000	3000	4000
	Scenario 3	3000	1000	3000	2000
	Scenario 4	2000	2000	3000	4000
	Scenario 5	3000	3000	3000	3000

There are two destinations immediately outside of zone III, indicated with grey rectangles. The road network includes two freeway corridors shown with double solid line and three arterials shown with single solid line. Table 4.8 lists the traffic characteristics of different road types.

Table 4.8 Roadway Characteristics in the Stage Evacuation Test

Index	Free-flow speed (mph)	Saturated flow rate (vphpl)	Jam density (vpmpl)
Freeway	60	2160	150
Arterial	30	1800	150

Based on these traffic characteristics and segment length, the actual road network can be converted into a cell-connected diagram as shown in Figure 4.11, with a unit time interval of 1 minute. Figure 4.12 presents the enhanced network formulation at each origin. Note that for illustration purpose, this section assumes that evacuation orders can only be initiated at an interval of 5 minutes after the onset of an incident (i.e., 0 min, 5 min, 10 min…). Thus, the demand from each origin cell can only enter the auxiliary cells that correspond to these time points.

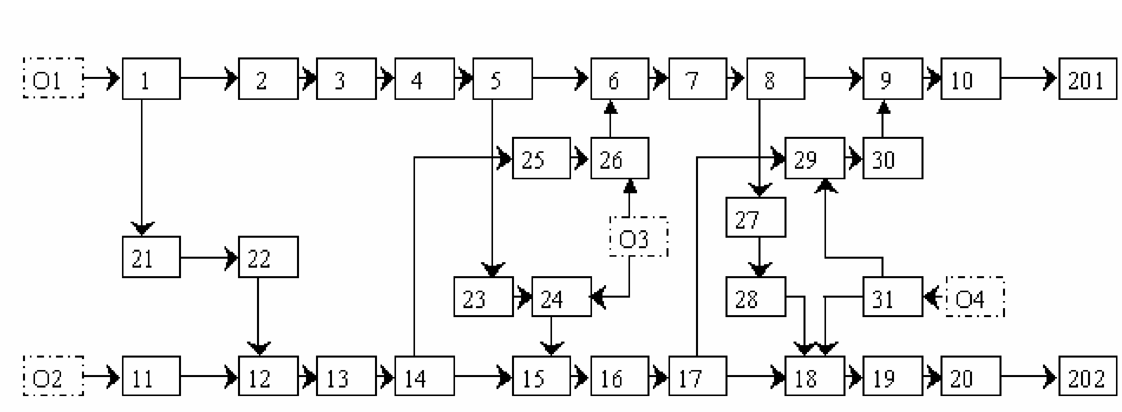

Figure 4.11 Cell Connection Diagram for the Example Network of Extended Model- II

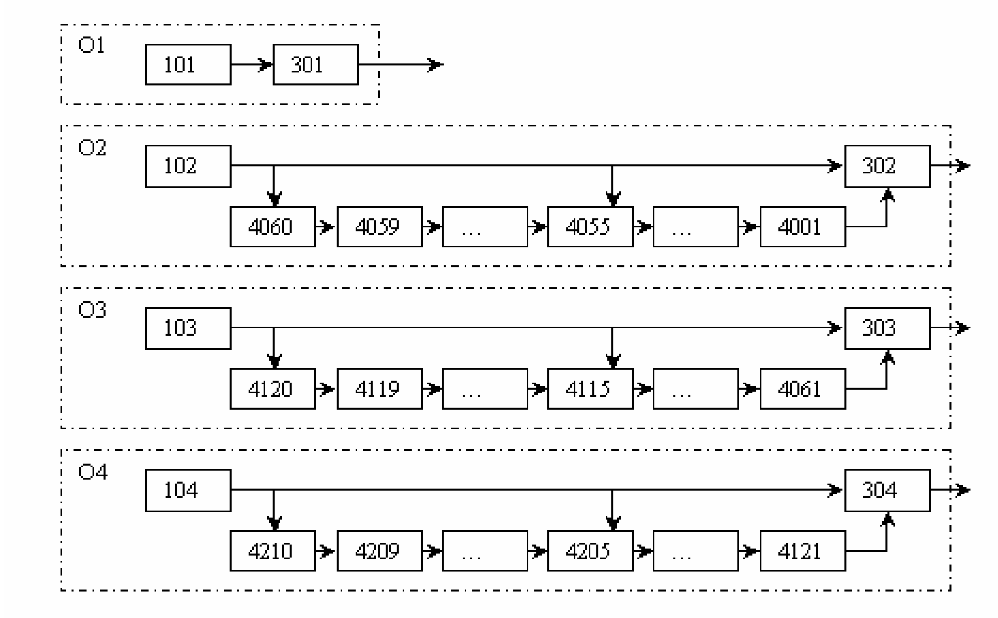

Figure 4.12 Enhanced Cell Connection Diagram at Origins for the Example Network of Extended Model- II

Table 4.9 shows the optimization results for both staged evacuation and concurrent evacuation under different demand patterns defined in Table 4.7. The following five parameters are used to characterize different strategies for each evacuation zone.

- Evacuation order time: the time to initiate an evacuation order for an evacuation zone;
- Zone clearance time: the time for all evacuees to exit an evacuation zone;
- Evacuation time span: the difference between the above two parameters;
- Average travel time: the total travel time spent on the actual network within an evacuation zone divided by the total demand going through this zone;

- Average waiting time at origins: the total time spent in waiting after vehicles have been generated divided by the total demand generated from this evacuation zone.

Table 4.9 Summary of Staged Evacuation Results for Different Demand Scenarios

- For Demand Scenario 1 -

Total Demand at Origins (veh)	O1:3000, O2:4000, O3: 0, O4:4000					
Evacuation Strategy	Staged Evacuation			Concurrent Evacuation		
Evacuation Zone	I	II	III	I	II	III
Evacuation Order Time (min)	0	10	0	0	0	0
Zone Clearance Time (min)	37	78	88	39	75	87
Time Span (min)	37	68	88	39	75	87
Average Travel Time (min)	5.15	8.74	10.22	7.15	10.18	10.68
Average Waiting Time at origins (min)	8.40	24.78	27.63	8.96	26.87	28.98

- For Demand Scenario 2 -

Total Demand at Origins (veh)	O1:3000, O2:1000, O3:3000, O4:4000					
Evacuation Strategy	Staged Evacuation			Concurrent Evacuation		
Evacuation Zone	I	II	III	I	II	III
Evacuation Order Time (min)	0	0	20	0	0	0
Zone Clearance Time (min)	39	64	96	39	73	86
Time Span (min)	39	64	76	39	73	86
Average Travel Time (min)	8.46	13.86	8.02	8.46	17.39	10.54
Average Waiting Time at origins (min)	8.10	8.20	27.63	8.10	8.20	29.40

- For Demand Scenario 3 -

Total Demand at Origins (veh)	O1:3000, O2:1000, O3:3000, O4:2000					
Evacuation Strategy	Staged Evacuation			Concurrent Evacuation		
Evacuation Zone	I	II	III	I	II	III
Evacuation Order Time (min)	0	0	30	0	0	0
Zone Clearance Time (min)	39	57	74	39	60	73
Time Span (min)	39	57	44	39	60	73
Average Travel Time (min)	8.46	13.01	6.33	8.49	13.71	10.19
Average Waiting Time at origins (min)	8.10	8.20	11.79	8.10	8.20	16.63

- For Demand Scenario 4 -

Total Demand at Origins (veh)	O1:2000, O2:2000, O3:3000, O4:4000					
Evacuation Strategy	Staged Evacuation			Concurrent Evacuation		
Evacuation Zone	I	II	III	I	II	III
Evacuation Order Time (min)	0	0	20	0	0	0
Zone Clearance Time (min)	39	64	96	39	74	86
Time Span (min)	39	64	76	39	74	86
Average Travel Time (min)	10.18	13.80	8.02	10.24	17.32	10.54
Average Waiting Time at Origins (min)	4.73	10.61	27.63	4.73	10.61	29.41

- For Demand Scenario 5 -

Total Demand at Origins (veh)	O1:3000, O2:3000, O3:3000, O4:3000					
Evacuation Strategy	Staged Evacuation			Concurrent Evacuation		
Evacuation Zone	I	II	III	I	II	III
Evacuation Order Time (min)	0	20	0	0	0	0
Zone Clearance Time (min)	33	79	95	39	79	93
Time Span (min)	33	59	95	39	79	93
Average Travel Time (min)	4.0	9.94	10.32	8.59	14.70	10.73
Average Waiting Time at Origins (min)	8.04	14.03	31.40	8.18	19.42	33.67

Based on these preliminary numerical results, one can reach the following conclusions by comparing the performance measures of staged evacuation and concurrent evacuation strategies under different demand scenarios.

- The optimized staged evacuation strategy can effectively mitigate network congestion under various demand patterns, which is reflected in a shorter average travel time for evacuees to go through the evacuation network;
- The optimized staged evacuation strategy can effectively mitigate the congestion at the entry points to the evacuation network under various demand patterns, which is evidenced by the lower average waiting time at all origins (i.e., in waiting cells). Note that the proposed formulation may force vehicles to be held temporarily at the entry points so as to facilitate the flow of evacuees from the high urgency level. This kind of enforced traffic control strategies may induce stress or even noncompliance. Thus, a lower waiting time will indicate less stress and consequently less manpower for enforcement.
- Staged evacuation strategy is decided not only by the level of urgency in the evacuation zone, but also by the evacuation demand patterns at different origins in each evacuation zone.

Note that for Demand Scenarios 1 and 5, zone III has a higher clearance time and time span under the staged evacuation than those under concurrent evacuation, but with a lower average travel time and waiting time. This is due to the fact that there does not exist a direct relation between these time indices. Average travel time and waiting time are computed with the total trips of all evacuees in the entire evacuation process, while evacuation clearance time and time span are defined only from the latest evacuee(s). Thus, a lower average travel time and waiting time do not necessarily lead to lower clearance time or time span. The demand distribution across origins, the time to issue evacuation order in each zone and the resultant difference in the routing plan will all affect these MOEs.

4.6. Closure

Chapter 4 has presented the formulations for design of evacuation control strategies at the network level, which include traffic routing, contraflow design, and staged evacuation. A brief summary of research efforts presented in each section is reported below:

- Section 4.2 has proposed a revised cell transmission concept to serve as the underlying network flow model. Compared with the original model, the proposed concept allows cells of different sizes when converting the network, which can significantly reduce the number of state variables and flow constraints. The numerical test conducted in this study has demonstrated the capability of the proposed concept in capturing network traffic dynamics, especially under congestion.

- Section 4.3 has proposed the Base Model for design of traffic routing strategies under concurrent evacuations without contraflow options. With the proposed revised cell transmission concept, the formulations have captured the propagation of evacuation traffic over the evacuation network and other operational constraints. The numerical test has demonstrated the applicability of the proposed Base Model for traffic routing with the Ocean City hurricane evacuation network.
- Section 4.4 has proposed the Extended Model-I, which incorporates the contraflow decisions in the Base Model. With a proper network enhancement approach, the extended model features its lane-based structure to capture the differences in driving behaviors between normal lanes and reversed lanes, and to reflect the non-linearity in the lane capacity for different contraflow designs. The numerical test with the Ocean City hurricane evacuation network has demonstrated the applicability of the Extended Model-I in identifying the contraflow segments under limited resource budget.
- Section 4.5 has proposed the Extended Model-II to address the staged evacuation problem. The proposed Extended Model-II features its capability to explicitly determine the time to issue an evacuation order and to capture evacuees' response behavior after the activation of evacuation orders. The numerical test has demonstrated the effectiveness of the Extended Model-II in a hypothetical network.

Note that for the sake of clarity, this chapter has presented the modeling efforts for traffic routing, contraflow design, and staged evacuation in different sections. In the planning practice, however, one may concurrently employ all these three network level control strategies. Chapter 6 will present a complete case study to demonstrate the effectiveness of the proposed formulations, with the network and the demand distributions in the Washington D.C. metropolitan area.

Chapter 5: Signal Optimization at the Corridor Level

5.1. Introduction

This chapter presents the formulations for design of signal control strategies for designated evacuation corridors. As identified in Chapter 2, existing studies on this regard are quite limited and mostly along the following two lines: a simplified preset control system regardless of the actual demand, or a standardized signal practice with a pre-specified high demand to represent the actual evacuation volumes. Unfortunately, neither approach can adequately address the various operational complexities associated with emergency evacuations. For instance,

- Arterial evacuation operations usually aim at maximizing the throughput, which justifies the use of a limited number of access points to reduce the disturbance of side street traffic to the arterial progression.
- The selected access points should provide a protected green phase to the minor street traffic so as to avoid gap-acceptance based turnings, which is especially dangerous under the oversaturated and stressful evacuation scenarios.
- Since vehicles from minor streets are supposed to enter arterials at selected access points, it is imperative to provide effective routing strategies to guide evacuees from each evacuation origin to those access points via proper local streets.

In response to the aforementioned challenges during emergency evacuations, this chapter proposes two sets of formulations for design of signal control strategies. The base model, presented in Section 5.2, is for an individually operated corridor that typically consists of one major arterial along the evacuation direction. Such an arterial receives evacuation traffic directly from nearby original nodes via local networks, while vehicles after moving onto the arterial will proceed along the arterial until reaching the safe zone. Section 5.3, as an extension, presents the model for more complex situations with several corridors operated integrally. These corridors, as major arterials heading to safe destinations, may exchange traffic flows via connectors so as to avoid local bottlenecks. Note that the grouping of corridors is available from the traffic routing plan at the network level.

Both signal optimization models proposed in this chapter features the use of critical intersection concept, that is, only key intersections will offer protective phases for vehicles from minor streets to turn onto arterials. The proposed core concept intends to reduce the disturbance of side street traffic to the arterial flow progression. With an effective signal control system, the main evacuation arterial should be capable of progressively moving its assigned traffic flows without incurring excessive delay on those waiting at minor streets for joining the evacuation.

Both Sections 5.2 and 5.3 will start with a presentation of model formulations in detail with emphases on the selection of control objectives and identification of various operational constraints, followed by a numerical study to demonstrate the overall effectiveness. The last section summarizes the research efforts in this chapter.

5.2. Signal Optimization for a Corridor Operated Individually

This section proposes a signal optimization model for individual corridor evacuation using the concept of critical intersections. Such a corridor is typically one major arterial along the evacuation direction, with its side streets connecting to some original nodes. Vehicles, after traveling from their origins to the accessible side street(s) at critical intersections, will turn onto the arterial and proceed until reaching the safe zone. The proposed model is expected to help users concurrently perform the following tasks:

- Select a set of critical intersections;
- Assign demand to critical intersections based on the network topology; and
- Design signal timing plans at critical intersections.

5.2.1. Model Formulations

To facilitate the presentation of model formulations, Table 5.1 summarizes the notations of major parameters and decision variables used in this section.

Table 5.1 Notations of Parameters and Decision Variables for Signal Optimization on an Individually Operated Corridor

Parameters	
Δt	Update interval of system status
T	Time horizon of the study (unit: no. of Δt)
CT	Evacuation clearance time (unit: no. of Δt)

s	The evacuation destination at the end of the evacuation corridor
S_r	Set of origins
S_I , S_w	Set of arterial links and set of side streets
S_m	Set of intersections
$d_r^t, r \in S_r$	Demand generated at origin r during interval t
$S_w^r, r \in S_r$	Set of side streets for traffic from origin r to enter the major arterial
$\Omega_r, r \in S_r$	Max no. of alternative side streets evacuees from origin r can choose
$l_i, i \in S_I$	Length of link i, l=physical length/speed (unit: no. of Δt);
$N_i, i \in S_I$	Storage capacity of link i, N=jam density $\times$ no. of lanes $\times$ physical length (unit: veh);
$Q_i, i \in S_I \cup S_w$	Flow capacity of link i, Q=saturation flow rate $\times$ no. of lanes $\times$ Δt (unit: veh)
$AD_{rw}, w \in S_w^r$	Delay for traveling from origin r to side street w (unit: no. of Δt);
$ST_m, m \in S_m$	Set of side streets at intersection m
$u_m, m \in S_m$	Index of the upstream arterial link of intersection m ;
$g_m^{\min}, m \in S_m$	Preset minimal green time for arterial green phase at intersection m
$\hat{g}_m^{\min}, m \in S_m$	Preset minimal green time for side street green phase at intersection m if it is a critical intersection
$rd_m, m \in S_m$	Preset all-red time for intersection m if it is a critical intersection
$\gamma_m^t, m \in S_m$	Binary variable. $\gamma_m^t = 1$ if interval t is arterial green phase at intersection m;
$\hat{\gamma}_m^t, m \in S_m$	Binary variable. $\hat{\gamma}_m^t = 1$ if interval t is side street green phase at intersection m
∞	A large positive number
x_i^t	No. of vehicles on link i at the beginning of interval t;
y_{ij}^t	No. of vehicles traveling from link i to link j during interval t;
Decision Variables	
$\delta_m, m \in S_m$	Binary variables. $\delta_m = 1$ if intersection m is critical intersection
C	Cycle length on the major arterial (unit: no. of Δt);
$g_m, m \in S_m$	Arterial green time of intersection m (unit: no. of Δt).
$\Delta_m, m \in S_m$	Offset of intersection m (Unit: no. of Δt);
$\theta_{rw}, w \in S_w^r$	Binary variable. $\theta_{rw} = 1$ if some demand from origin r go to side street w.

5.2.1.1. Objective Functions

Given the time window T during an emergency evacuation, the primary objective of traffic operators shall be to maximize the total throughput, i.e., the total number of evacuees that can get out of the hazardous area via the evacuation arterial. Since this throughput is equal to the total number of vehicles entering the target destination, it can be formulated as Equation 5.1.

$$\max \qquad x_s^{T+1} = \sum_{t=1}^{T} y_{\Gamma(s),s}^{t} \tag{5.1}$$

Where $\Gamma(s)$ is the upstream link of the destination s.

However, if the evacuation time window T is sufficiently long for all evacuees to get out of the hazardous area, control objective shall be set to minimize the evacuation clearance time, and be formulated as follows.

$$\begin{aligned} &\min \qquad CT \\ &s.t. \qquad x_s^{CT+1} = \sum_{r \in S_r} \sum_{t=1}^{T} d_r(t), \qquad CT \le T \end{aligned} \tag{5.2}$$

Note that as reported in the literature, maximizing throughput on the main evacuation arterial can cause long queue and delay for side street traffic, and thus may result in some evacuees' inobservance of the intersection control. In view of such a concern, the proposed model consists of a supplemental objective, which is to optimally control the difference in the service level among different locations in the evacuation network.

At the most upstream intersection, one can simply compare the average delay on all approaching links. For each of the other critical intersection m, this section proposes to compare the average delay for side street(s) at intersection m with the average delay for all traffic from its upstream intersections. This intends to capture the fact that upstream intersections are closer to the incident site and thus evacuees are likely more panic and thus have lower tolerance to a long delay. Accordingly, one can formulate the supplemental objective as Equation 5.3.

$$\min \quad \sum_{m=1} \delta_m \sum_{w,w' \in ST_m} \left[\frac{\sum_{t=1}^{T} (x_w^t - \sum_{r \in S_r} y_{rw}^t t)}{\sum_{t=1}^{T} \sum_{r \in S_r} y_{rw}^t} - \frac{\sum_{t=1}^{T} (x_{w'}^t - \sum_{r \in S_r} y_{rw'}^t t)}{\sum_{t=1}^{T} \sum_{r \in S_r} y_{rw'}^t} \right]^2$$
$$+ \sum_{m=2}^{M} \delta_m \left[\frac{\sum_{w \in ST_m} \sum_{t=1}^{T} (x_w^t - \sum_{r \in S_r} y_{rw}^t t)}{\sum_{w \in ST_m} \sum_{t=1}^{T} \sum_{r \in S_r} y_{rw}^t} \right.$$
$$\left. - \frac{\sum_{m'=1}^{m-1} \sum_{w \in ST_{m'}} \sum_{t=1}^{T} (x_w^t - \sum_{r \in S_r} y_{rw}^t t) + \sum_{i=1}^{u_m} \sum_{t=1}^{T} x_i^t}{\sum_{m'=1}^{m-1} \sum_{w \in ST_{m'}} \sum_{t=1}^{T} \sum_{r \in S_r} y_{rw}^t} \right]^2 \tag{5.3}$$

where the first term indicates the sum of difference in average delays between each pair of side streets at the most upstream intersection if it is a critical intersection. The second term sums over all other critical intersections the difference in average delays for traffic from side streets and from the arterial to traverse each intersection.

To efficiently contend with the proposed multiple objectives for optimizing arterial control, this study employs the popular Hierarchical Optimization Method (HOM) that allows users to rank the selected objectives in a descending order of importance. Each objective function is then minimized sequentially subject to a constraint that does not allow the minimum for the new function to exceed a prescribed fraction of the minimum of the previous function (Eschenauer et al., 1986; Homburg, 1998).

5.2.1.2. Network Flow Constraints

The network flow constraints define the temporal and spatial interactions among vehicle flows, including the following dynamic processes.

- Vehicles are generated from and sent out of evacuation origins;
- Vehicles travel via local streets to side streets at critical intersections, and then to downstream evacuation arterial; and
- Vehicles traverse the evacuation arterial to target safety destinations.

This study applies the revised cell transmission concept proposed in Chapter 4 to represent these three processes with three sets of formulations.

- Network flow constraints at origins. Equations 5.4-5.9 summarize the constraints to realistically represent the evacuation flows at all possible origins.

$$\sum\nolimits_{w\in S_w^r} \theta_{rw} \geq 1, \qquad r \in S_r \tag{5.4}$$

$$\sum\nolimits_{w\in S_w^r} \theta_{rw} \leq \Omega_r, \qquad r \in S_r \tag{5.5}$$

$$y_{rw}^t \leq \theta_{rw} \times \infty, \qquad w \in S_w^r, \; r \in S_r, \; t = 1,\ldots,T \tag{5.6}$$

$$\theta_{rw} / \infty \le \sum_t y_{rw}^t, \qquad w \in S_w^r, \;\; r \in S_r, \;\; t = 1,...,T \tag{5.7}$$

$$\sum_{w \in S_w^r} y_{rw}^t \le x_r^t, \qquad r \in S_r, \;\; t = 1,...,T \tag{5.8}$$

$$x_r^{t+1} = x_r^t + d_r^t - \sum_{w \in S_w^r} y_{rw}^t, \qquad r \in S_r, \;\; t = 1,...,T \tag{5.9}$$

Here Equations 5.4 and 5.5 indicate that each origin should connect to at least one and at most Ω_r of its neighboring side streets for dissipating its demand, where the latter constraint is often desirable so as to make the evacuation plan convenient to follow. Equations 5.6-5.8 restrict that there exist some flows between origin r and side street w only if they are connected, and the total outflow from origin r cannot exceed the number of vehicles currently in the origin. Finally, Equation 5.9 defines the flow conservation law at origin r, namely, the number of vehicles at the beginning of interval $t+1$ should be equal to the number of vehicles at the beginning of interval t plus demand generated during t and minus the total outgoing flows during t.

- Network flow constraints at side streets. Equations 5.10-5.13 summarize the constraints to realistically model the arrivals of vehicles from origins and their departures to downstream links, based on the side street traffic conditions.

$$x_w^{t+1} = x_w^t - \sum_{j \in \Gamma^{-1}(w)} y_{wj}^t, \qquad w \in S_w, \;\; t = 1,..., AD_{rw} \tag{5.10}$$

$$x_w^{t+1} = x_w^t + \sum_{r: w \in S_w^r} y_{rw}^{t-AD_{rw}} - \sum_{j \in \Gamma^{-1}(w)} y_{wj}^t, \qquad w \in S_w, \;\; t = AD_{rw}+1,...,T \tag{5.11}$$

$$\sum_{r:w\in S_w^r} y_{rw}^t \le Q_w, \qquad w\in S_w,\ \ t=1,...,T \tag{5.12}$$

$$\sum_{j\in\Gamma^{-1}(w)} y_{wj}^t \le \min\{Q_w \hat{\gamma}_{m:w\in ST_m}^t, x_w^t\}, \qquad w\in S_w, t=1,...,T \tag{5.13}$$

Here the flow conservation equations 5.10-5.11 introduce preset delay AD_{rw} to represent the duration for vehicles to travel from an origin *r* to its neighboring side street $w: w\in S_w^r$. Equation 5.12 states that the total number of vehicles that can enter a side street during each interval cannot exceed flow capacity of the side street. Note that this study enforces no storage capacity constraints at the side streets so as to model the potentially long queue. Equation 5.13 describes the restriction of side street traffic conditions on the departure of vehicles from a side street to its downstream links, i.e., the total number of vehicles exiting a side street cannot exceed its flow capacity or the number of vehicles currently on the side street.

- Network flow constraints at arterial links as in Equations 5.14-5.16, which intend to capture the movement of vehicles along the arterial links.

$$x_i^{t+1} = x_i^t + \sum_{k\in\Gamma(i)} y_{ki}^t - \sum_{j\in\Gamma^{-1}(i)} y_{ij}^t,\ i\in S_I, t=1,...,T \tag{5.14}$$

$$\sum_{k\in\Gamma(i)} y_{ki}^t \le \min\{Q_i, N_i / l_i, N_i - x_i^t\},\ i\in S_I, t=1,...,T \tag{5.15}$$

$$\sum_{j\in\Gamma^{-1}(i)} y_{ij}^t \le \min\{Q_i \gamma_m^t, N_i / l_i, x_i^{t-l_i+1} - \sum_{j\in\Gamma^{-1}(i)} \sum_{k=t-l_i+1}^{t-1} y_{ij}^k\},$$

$$i\in S_I, t=1,...,T \tag{5.16}$$

Here Equation 5.14 represents the flow conservation law, whereas Equations 5.15-5.16 define the number of vehicles that can enter or exit a link based on its traffic conditions. Note that this study views evacuation destinations as a special type of links on evacuation corridors, which has no outgoing links and has a length of one unit. Thus, Equations 5.14-5.16 can also apply to formulate those vehicles moving into the destination.

5.2.1.3. Routing to Critical Intersections

This category of constraints defines the sufficient and necessary conditions for an intersection to be defined as a critical intersection. More specifically,

- As the sufficient conditions, Equation 5.17 states that an intersection m is critical ($\delta_m = 1$) if some evacuation traffic has used any side street at the intersection ($\exists w \in ST_m : \theta_{rw} = 1$).

$$\delta_m \geq \theta_{rw: w \in ST_m}, \qquad m \in S_m \tag{5.17}$$

- As the necessary condition, Equation 5.18 requires any critical intersection $m: \delta_m = 1$ to have at least one side street that has been used by evacuation traffic.

$$\sum\nolimits_{w \in ST_m} \sum\nolimits_{r: w \in S_w^r} \theta_{rw} \geq \delta_m, \qquad m \in S_m \tag{5.18}$$

5.2.1.4. Interrelations between Traffic Control Parameters

Constraints 5.19-5.21 define the following relations between signal timing and control type at each intersection: for a non-critical intersection $m: \delta_m = 0$, its arterial green time g_m will equal the cycle length C, whereas the green time for a critical intersection $m: \delta_m = 1$ shall always lie between the preset minimal green time $g_m^{\min}$ and the cycle length.

$$g_m \geq g_m^{\min}, \qquad m \in S_m \tag{5.19}$$

$$g_m \geq C - \infty \times \delta_m, \qquad m \in S_m \tag{5.20}$$

$$g_m \leq C - (\hat{g}_m^{\min} + 2 \times rd_m)\delta_m, \qquad m \in S_m \tag{5.21}$$

Besides, Equation 5.22 constrains any offset value to be between zero and the cycle length.

$$\Delta_m \geq 0, \quad \Delta_m < C, \qquad m \in S_m \tag{5.22}$$

5.2.1.5. Signal Status at Intersection m

This set of constraints intends to capture the signal status of intersection m during time interval t, which shall include the following relations corresponding to Equations 5.23-5.32:

- The non-critical intersections $m\!:\delta_m = 0$ will always have arterial green phase, or in other words, the binary variable γ_m^t will always equal 1 and $\hat{\gamma}_m^t$ will always equal 0.
- For critical intersections $m\!:\delta_m = 1$, the value of γ_m^t and $\hat{\gamma}_m^t$ depends on the cycle time C, green time g_m, offset Δ_m, and all-red time rd_m.

$$\gamma_m^t \geq 1 - \delta_m, \qquad m \in S_m \tag{5.23}$$

$$\hat{\gamma}_m^t \leq \delta_m, \qquad m \in S_m \tag{5.24}$$

$$\infty \times \gamma_m^t \geq g_m - \operatorname{mod}(t - \Delta_m - 1, C), \qquad m \in S_m \tag{5.25}$$

$$-\infty \times (1 - \gamma_m^t) < g_m - \operatorname{mod}(t - \Delta_m - 1, C), \qquad m \in S_m \tag{5.26}$$

$$\infty \times \beta_m^t > \operatorname{mod}(t - \Delta_m - 1, C) - g_m - rd_m, \qquad m \in S_m \tag{5.27}$$

$$-\infty \times (1 - \beta_m^t) \leq \operatorname{mod}(t - \Delta_m - 1, C) - g_m - rd_m, \qquad m \in S_m \tag{5.28}$$

$$\infty \times \hat{\beta}_m^t \geq C - rd_m - \operatorname{mod}(t - \Delta_m - 1, C), \qquad m \in S_m \tag{5.29}$$

$$-\infty \times (1 - \hat{\beta}_m^t) < C - rd_m - \operatorname{mod}(t - \Delta_m - 1, C), \qquad m \in S_m \tag{5.30}$$

$$\hat{\gamma}_m^t > \beta_m^t + \hat{\beta}_m^t - 2, \qquad m \in S_m \tag{5.31}$$

$$-\infty \times (1 - \hat{\gamma}_m^t) \leq \beta_m^t + \hat{\beta}_m^t - 2, \qquad m \in S_m \tag{5.32}$$

Note that there are two all-red periods in one cycle. One is between arterial green phase and side street green phase, and the other lies after the side street green phase. Thus this study uses two auxiliary binary variables in Equations 5.27-5.32, where $\beta_m^t = 1$ if interval t is after the first all red time and intersection m is a critical intersection, and $\hat{\beta}_m^t = 1$ if interval t is before the second all red time. Besides, the above formulations use the function $\mathrm{mod}(a, b)$ to return the remainder after dividing a with b, which can be replaced with a set of additional constraints.

5.2.1.6. Other Constraints

To provide a realistic range for the optimized solution, the proposed model also includes nonnegative constraints, initial value of link state variables x_i^1, and initial value of flows between links y_{ij}^0. In most cases, x_i^1 and y_{ij}^0 are set to zero for all arterial links and side street links, although x_i^1 can be other values to represent the background traffic prior to the evacuation.

5.2.2. The Solution Algorithm

The proposed optimization model consists of complex formulations, including binary decision variables as well as nonlinear system constraints. It will generally take a long time to find the global optimal solution. Due to the emergency nature, this study employs a Genetic Algorithm-based heuristic to yield efficient solutions in a relatively short time window for selection of critical intersections and their signal settings.

Note that Genetic Algorithm is a search technique widely used to find near optimal solutions to a variety of real-world large-scale optimization issues. Inspired by evolutionary biology, Genetic Algorithms are typically implemented as a computer simulation in which a population of abstract representations (chromosomes) of candidate solutions (individuals) to an optimization problem evolves toward better solutions. The evolution starts from a population of completely random individuals and proceeds in iterations (generations). In each generation, the fitness of the whole population is evaluated, while multiple individuals are stochastically selected from the current population based on their fitness and modified with mutation or crossover to form a new population for the next generation. (Goldberg, 1988; Ladd, 1996)

Based on the GA method, this study has developed the solution algorithm with Visual C++ language, and encoded the solutions to the proposed MIP model with binary strings of 0s and 1s to capture the selection of critical intersections, demand routing, and signal timing parameters. A step-by-step description of the solution procedures is presented below:

Step 1. Network Data Initialization:

Read the following data from a GIS database: 1) timing varying demand for each origin, 2) cell and connector information that defines link properties and the network topology, and 3) intersection information that defines the allowed movements and preset signal control parameters for each signal phase.

Step 2. Initial Solution Generation:

Set the iteration index as 1 and then randomly generate the first population of candidate solutions with binary representations (chromosomes). To improve the computation efficiency, this study has always preset the minimal green plan as one of the initial solutions

Step 3. Fitness Function Evaluation (for each candidate solution)

Step 3-1. Chromosome Decoding: decode the corresponding chromosome to obtain the real-valued control parameters. The model proposed in this section consists of the following four types of controls: 1) selection of critical intersections and traffic routing decisions from each origin to side streets at critical intersections; 2) the cycle length for intersections along the arterial; 3) arterial green time at each intersection, and 4) offset at each intersection.

It is noticeable that these four control strategies have a special hierarchical relation. The selection of critical intersections affects the signal timings at intersections, i.e., the non-critical intersections always give the green phase to arterial traffic. Thus, the program introduces a gene-activation mechanism in the decoding procedure, which decodes all the high-level controls first and then only decodes those low-level strategies that get activated by the corresponding high-level strategies. Note that all those inactive controls will remain in the chromosome structure and are carried invisibly to the subsequent generations.

Step 3-2. Fitness Computation: execute a macroscopic simulator based on the revised cell transmission relations after obtaining the real-valued control parameters. During each time interval,

- The simulator will first update each cell status with the connector flows from the previous interval, based on the flow conservation law.
- Based on the updated cell status, the simulator will compute the flows that can move out of each cell.
- The final connector flows between cells are then obtained by taking into account the preset diverging/merging behaviors, the congestion in downstream cells, and the signal phase at intersections.

Note that the fitness function for each candidate solution is first set to maximize the total throughput. Once the algorithm detects the throughput of the solution is equal to the total evacuation demand, the fitness function will automatically change to the minimization of evacuation clearance time. After the optimized throughput or clearance time is found, users can specify the percentage of acceptable loss in these system measurements in order to minimize the difference in the service levels between different locations in the evacuation network. Then, the algorithm will proceed to minimize the third objective function with this additional constraint on the system measurement.

Step 4. Stop Criteria Testing

Exit the algorithm if the number of iterations has reached the preset maximal value, or the best objective function remains unchanged for a preset number of iterations. Otherwise, the algorithm will increase the iteration index by 1 and go to Step 5.

Step 5. Genetic Operators

Run the general genetic operators (selection, crossover and mutation) to generate a new population of candidate solutions based on solutions from the old population. Then the algorithm will turn to Step 3.

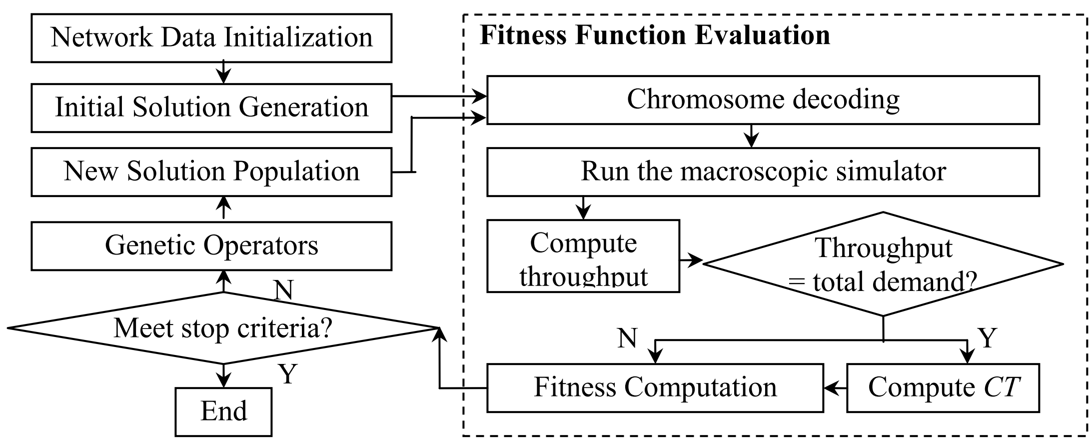

Figure 5.1 Flowchart of the Solution Algorithm for Signal Optimization at the Corridor Level

5.2.3. Case Study

5.2.3.1. Experimental Design

Figure 5.2 presents a target area for numerical experiments, which covers the entire Connecticut Avenue from Washington D.C. to the Capital Beltway. The entire evacuation route starts from the intersection at K Street and ends at the intersection at Chevy Chase Cir. The length of the evacuation corridor is 8km (5 miles), containing a total of 90 origin nodes, 38 signalized intersections, and 24 intersections with stop/yield sign.

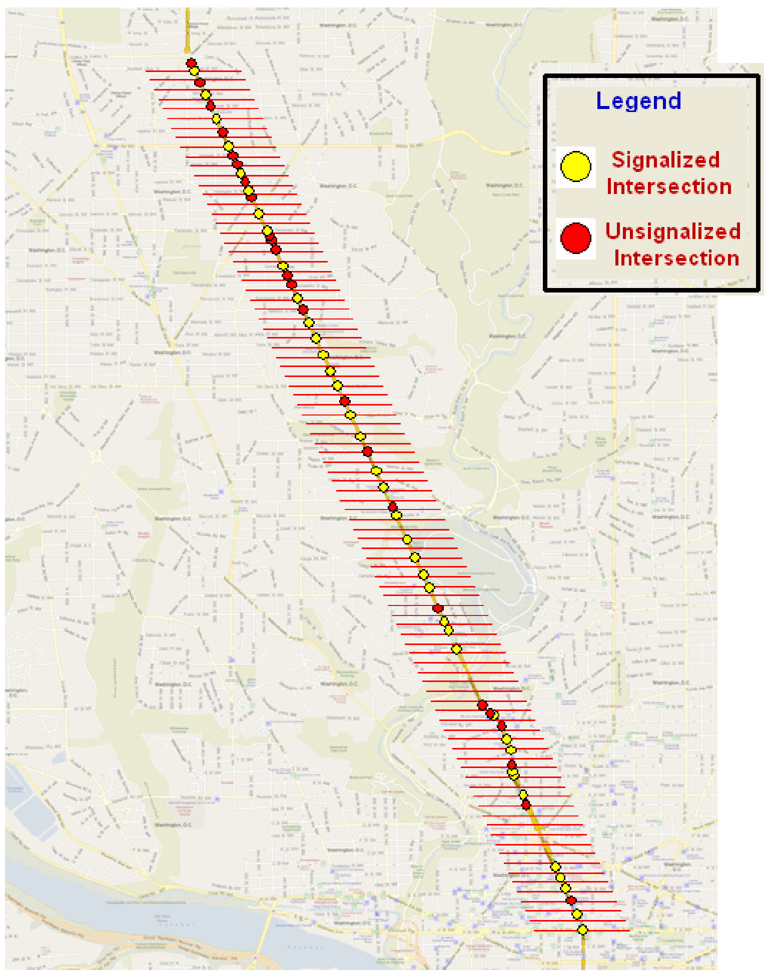

Figure 5.2 Example Evacuation Corridor – Connecticut Avenue in Washington, D.C.

To reflect the operational constraints, the application of the signal optimization model is subjected to the following constraints:

- Non-signalized intersections cannot be critical intersections.
- Cycle time will be within a range of 60 to 300 seconds
- Evacuation demand can be directed to any of its downstream critical intersections.

To test the effectiveness of the proposed model with respect to total throughput and the evacuation clearance time, this study has designed different demand scenarios for experimental analysis.

- Scenarios I-1 and I-2 intend to represent the relatively heavy demand condition under which population cannot be evacuated within the period of 2 hours, where Scenario I-1 has more demand concentrated at the arterial upstream than Scenario I-2.
- Scenarios II-1 and II-2 present those arterials with moderate evacuation demand, which can be cleared within 2 hours of operations. Similarly, Scenario II-1 has more demand concentrated at the arterial upstream than Scenario II-2.

5.2.3.2. Experimental Results

To show the effectiveness of the proposed model in design of arterial control strategies during emergency evacuations, this paper employs a pre-calibrated

CORSIM simulator to compare the control strategies generated from the model with two state-of-art traffic signal plans for evacuation, which are:

- Yellow-Flash Plan: All signalized intersections will give the arterial traffic a yellow-flash phase and the side streets a red-flash phase.
- Minimal-Green Plan: All signalized intersections will have a cycle time of 300 seconds while side street traffic only receive the minimal green time of 10 seconds.

The evaluation results with simulation experiments are organized as follows, where all the indices for comparison are directly extracted from the CORSIM simulation output files:

- Comparing the throughput and/or evacuation clearance time of Yellow Flash Plan and Minimal Green Plan with those of the optimized control strategy that does not restrict the difference in the service level (i.e. have no delay balance considerations) under each demand scenario;
- Presenting throughput and/or evacuation clearance time of the optimized control strategy that intends to restrict the difference in the service level for balanced delay under each demand scenario;
- Comparing the average delay and maximal delay of the Yellow-Flash Plan and Minimal-Green Plan with those two different optimized control strategies.

Table 5.2 and Table 5.3 show the comparison results under Demand Scenarios I and II, whereas the optimized control strategy does not account for the delay balance consideration. These tables have clearly indicated that the optimized arterial control plans outperform those two widely used signal plans in all demand scenarios, and the effectiveness varies with the demand distribution

Table 5.2 Throughput Comparison under Demand Scenario I Without the Secondary Objective of Delay Balance

Throughput (no. of Vehicles)	Yellow Flash Plan	Min-Green Plan	Optimized Plan
Demand Scenario I-1	9102	9494	9624
Demand Scenario I-2	8618	9304	10624

Table 5.3 Throughput Comparison under Demand Scenario II Without the Secondary Objective of Delay Balance

Clearance Time (min)	Yellow Flash Plan	Min-Green Plan	Optimized Plan
Demand Scenario I-1	120	100	94
Demand Scenario I-2	133	120	100

Table 5.4 presents the simulated throughput and/or evacuation clearance time for the optimized control strategy that takes into account Objective 5.3 with a ten percent of acceptable loss in the optimized throughput or clearance time (as in Table 5.2 and Table 5.3) under the two different demand scenarios.

Table 5.4 Simulated Throughput of the Optimized Plan With the Secondary Objective of Delay Balance

Demand Scenario	Scenario I-1	Scenario II-1
Throughput in 2hr (no. of Vehicles)	9378	8880
Clearance Time (min)	N/A	98

Comparing Table 5.4 with Table 5.2 and Table 5.3, one can identify that the optimized plan with delay balance consideration may lead to a lower throughput or a longer clearance time. However, the power of these optimized plans is clearly indicated in Table 5.5 and Table 5.6. Table 5.5 presents the averaged delay of the four control plans under Demand Scenario II, whereas Table 5.6 presents the maximal delay among all side streets at critical intersections for those two optimized control plans with or without delay balance consideration under both demand scenarios.

Table 5.5 Average Delay under Demand Scenario II-1

Control Plan	Yell Flash Plan	Min-Green Plan	Optimized without the Secondary Objective of Delay Balance	Optimized with the Secondary Objective of Delay Balance
Average Delay (min)	20.8	19.0	17.0	14.2

Table 5.6 Maximal Delay at Side Streets (Unit: min)

Control Plan	Demand Scenario I-1	Demand Scenario II-2
Optimized without Secondary Objective of Delay Balance	61.6	40.9
Optimized with Secondary Objective of Delay Balance	49.2	36.0
Improvement with Secondary Objective of Delay Balance	20.1%	12.0%

Table 5.5 and Table 5.6 have indicated that the optimized control plans with delay balance consideration did help the side street traffic but at the price of reduced system throughput or increased evacuation clearance time.

5.3. Signal Optimization for Corridors Operated as an Integrated Network

As an extension of Section 5.2, this section proposes a signal optimization model for more complex evacuation networks with multiple corridors operated as an integrated network. Such networks typically contain the following four types of roads: 1) major arterials as the evacuation corridors heading to the safe destinations; 2) connectors that link neighboring corridors; 3) side streets that receive evacuation traffic from original nodes and send them to corridors/connectors; and 4) local streets connecting the original nodes and the side streets. The proposed model is expected to help users concurrently perform the following tasks:

- Select a set of critical intersections;
- Assign demand to critical intersections based on the network topology;
- Design the signal timing plans at critical intersections; and
- Route traffic between corridors via connectors, if necessary, to balance traffic volumes between different corridors.

5.3.1. Model Formulations

To facilitate the presentation of model formulations, Table 5.7 summarizes the notations of major parameters and decision variables used in this section.

Table 5.7 Notations of Parameters and Decision Variables: Signal Optimization for Corridors Operated Integrally

Δt	Update interval of system status
T	Time horizon of the study (unit: no. of Δt)
CT	Evacuation clearance time (unit: no. of Δt)
S_r, S_s	Set of original nodes and evacuation destinations
S_a	Set of corridors/connection streets
S_m	Set of intersections
$S_m^a, a \in S_a$	Set of intersections on corridor/ connector *a.* The sets are mutually exclusive, and an intersection where connectors meet corridors is defined belong to the corridor.
S_I	Set of links on corridors/connectors
S_w	Set of side streets
$S_w^r, r \in S_r$	Set of side streets for traffic from origin *r* to enter a corridor or a connector
$d_r^t, r \in S_r$	Demand generated at origin *r* during interval *t*
$\Omega_r, r \in S_r$	The maximal no. of alternative side streets that evacuees from origin *r* can choose
$U_m, m \in S_m$	Set of upstream links on major roads at intersection *m*
$UT_m, m \in S_m$	Set of side streets and/or upstream links on minor roads at intersection *m*
$g_m^{\min}, m \in S_m$	Preset minimal green time for major-road green phase at intersection *m*
$\hat{g}_m^{\min}, m \in S_m$	Preset minimal green time for minor-road green phase at intersection *m* if the intersection is a critical intersection
$rd_m, m \in S_m$	Preset all-red time for intersection *m* if the intersection is a critical intersection
$\gamma_m^t, m \in S_m$	Binary variable. $\gamma_m^t = 1$ if interval *t* is major-road green phase at intersection *m*
$\hat{\gamma}_m^t, m \in S_m$	Binary variable. $\hat{\gamma}_m^t = 1$ if interval *t* is minor-road green phase at intersection *m*
$l_i, i \in S_I$	Length of link *i*, *l*=physical length/speed (unit: no. of Δt);
$N_i, i \in S_I$	Storage capacity of link *i*, *N*=jam density $\times$ no. of lanes $\times$ physical length (unit: vehicles);
$Q_i, i \in S_I \cup S_w$	Flow capacity of link *i*, *Q*=saturation flow rate $\times$ no. of lanes $\times$ Δt (unit: vehicles)
$\eta_i, i \in S_I \cup S_w$	Binary variable. $\eta_i = 1$ if link *i* has been used by any evacuation traffic
$AD_{rw}, w \in S_w^r$	Delay for traveling from origin *r* to side street *w* (unit: no. of Δt);

∞	A very large positive number
x_i^t	No. of vehicles on link *i* at the beginning of interval *t*;
y_{ij}^t	No. of vehicles traveling from link *i* to link *j* during interval *t*;
Decision Variables	
$\delta_m, m \in S_m$	Binary variables. $\delta_m = 1$ if intersection *m* is critical intersection
$C_a, a \in S_a$	Cycle length on corridor/connector *a* (unit: no. of Δt);
$g_m, m \in S_m$	Main-road green time of intersection *m* (unit: no. of Δt).
$\Delta_m, m \in S_m$	Offset of intersection *m* (Unit: no. of Δt);
$\theta_{rw}, w \in S_w^r$	Binary variable. $\theta_{rw} = 1$ if some demand from origin *r* is diverted to side street *w*.

Note that this section assumes the use of a two-phase signal control at critical intersections, which include a green phase for major road and a green phase for minor road. Here major road and minor road are defined as below:

- At an intersection where an evacuation corridor meets connectors and/or side streets, main road refers to the evacuation corridor and minor road refers to connectors and/or side streets
- At an intersection where a connector meets side streets, main road refers to the connector and minor road refers to side streets.

5.3.1.1. Objective Functions

This study is focused mainly on improving the efficiency of the entire evacuation process, which may vary with the selected control objectives such as maximization of throughput, minimization of clearance time, minimization of average trip time, and minimization of fatality. The proposed model in this section suggests the use of the clearance time minimization or throughput maximization as the control objective, depending on the length of the safety time window. More specifically,

- If the time window is sufficiently long for all evacuees to reach the safety destinations, the control objective shall be to minimize the evacuation clearance time, CT , as in Equation 5.33.

$$\begin{aligned} &\min \quad CT \\ &s.t. \quad \sum_{i \in S_s} x_i^{CT+1} = \sum_{r \in S_r} \sum_{t=1}^{T} d_r^t, \qquad CT \le T \end{aligned} \tag{5.33}$$

- If the evacuation process cannot be completed within the given time window, the control objective would be to maximize the total throughput $\sum_{i \in S_s} x_i^{T+1}$, where $x_i^{T+1}, i \in S_s$ is the total number of evacuees that have arrived at destination i by time T.

$$\max \quad \sum_{i \in S_s} x_i^{T+1} \tag{5.34}$$

To realistically capture the complex interrelations among network flows so as to design critical intersections and signal timing plans, the proposed model in this section formulates the following six major categories of constraints.

5.3.1.2. Network Flow Constraints

The network flow constraints define the temporal and spatial interactions among vehicle flows, including the following dynamic process:

- Vehicles are generated from and sent out of the evacuation origins;
- Vehicles travel via local streets to the side streets at critical intersections, and then to the downstream evacuation corridors or connectors; and
- Vehicles traverse connectors and evacuation corridors to target safety destinations.

Accordingly, this section applies the generalized cell transmission concept to generate the following three groups of constraints.

- The constraints to represent the evacuation flows at all possible origins are the same as Equations 5.4-5.9 proposed for signal optimization for a corridor operated individually.
- The constraints to capture the network flow evolution at side streets are similar to Equations 5.10-5.13, except that the flow conservation equation 5.13 is modified as in Equation 5.35. The binary variable $\hat{\gamma}_m^t, m \in S_m$ is removed from the equation, and its impact on side street flows will be defined separately to account for the more complex network with connectors.

$$\sum_{j \in \Gamma^{-1}(w)} y_{wj}^t \le \min\{Q_w, x_w^t\}, \qquad w \in S_w, t = 1,\ldots,T \tag{5.35}$$

- The constraints to capture the movement of vehicles along the corridor or connectors are also similar to Equations 5.14-5.16, except that the flow conservation equation 5.16 is modified as in Equation 5.36. The binary variable $\gamma_m^t, m \in S_m$ is removed from the equation, and its impact on traffic flows from the upstream arterial links will be defined separately to account for the more complex network with connectors.

$$\sum_{j \in \Gamma^{-1}(i)} y_{ij}^t \le \min\{Q_i, N_i / l_i, x_i^{t-l_i+1} - \sum_{j \in \Gamma^{-1}(i)} \sum_{k=t-l_i+1}^{t-1} y_{ij}^k\}$$

$$i \in S_I, t = 1,...,T \qquad (5.36)$$

5.3.1.3. Definition of Critical Intersections

This category of constraints defines the sufficient and necessary conditions for a critical intersection. Since the evacuation network now involves intersections between arterials and connectors, the decision of critical intersections will depend not only on the side street traffic conditions as in Equations 5.17 and 5.18, but also on traffic flows from connectors. Thus, a link usage parameter η_i is introduced to indicate if a connector link has been used by evacuation traffic or not, as shown in the following Equations 5.37-5.38.

$$x_i^t \le \infty \times \eta_i, \qquad i \in S_I \cap UT_m, m \in S_m \qquad (5.37)$$

$$\eta_i / \infty \le \sum_t x_i^t, \qquad i \in S_I \cap UT_m, m \in S_m \qquad (5.38)$$

With help of this link usage parameter, Equations 5.39-5.40 state that an intersection is operated as critical intersection if some evacuation traffic has used any minor roads upstream to the intersection, which could be either side streets or links on connectors.

$$\delta_m \geq \theta_{rw}, \qquad \forall r, w : w \in S_w \cap UT_m, m \in S_m \tag{5.39}$$

$$\delta_m \geq \eta_i, \qquad \forall i : i \in S_I \cap UT_m, m \in S_m \tag{5.40}$$

Besides, Equation 5.41 requires any critical intersection to have at least one minor road at its upstream that has been used by evacuation traffic.

$$\sum_{w \in S_w \cap UT_m} \sum_{r : w \in S_w^r} \theta_{rw} + \sum_{i \in S_I \cap UT_m} \eta_i \geq \delta_m, m \in S_m \tag{5.41}$$

5.3.1.4. Consistency between Intersection Type and Signal Timing

With enhanced formulations to address the cycle length difference on different arterials, Equations 5.42-5.45 define the following relations between signal timing and control type at each intersection: the arterial green time at a non-critical intersection ($\delta_m = 0$) will equal its cycle length, whereas a critical intersection ($\delta_m = 1$) shall give its side street(s) a green time at least equal to the preset minimal value. Besides, any offset value will lie between zero and the cycle length.

$$g_m \geq g_m^{\min}, \qquad m \in S_m \tag{5.42}$$

$$g_m \geq C_{a:m \in S_m^a} - \infty \times \delta_m, \qquad m \in S_m \tag{5.43}$$

$$g_m \leq C_{a:m \in S_m^a} - (\hat{g}_m^{\min} + 2 \times rd_m)\delta_m, \qquad m \in S_m \tag{5.44}$$

$$\Delta_m \geq 0, \quad \Delta_m < C_{a:m \in S_m^a}, \qquad m \in S_m \tag{5.45}$$

5.3.1.5. Consistency between Signal Timing and Signal Phase at Intersections

Similarly modified to address the difference in cycle length on different arterials, Equations 5.46-5.55 extend the formulations in Section 5.2.1.5 and determine the signal phase of an intersection for any time interval t based on its control type and signal timing parameters:

$$\gamma_m^t \geq 1 - \delta_m, \qquad m \in S_m \tag{5.46}$$

$$\hat{\gamma}_m^t \leq \delta_m, \qquad m \in S_m \tag{5.47}$$

$$\infty \times \gamma_m^t \geq g_m - \operatorname{mod}(t - \Delta_m - 1, C_{a:m \in S_m^a}), \qquad m \in S_m \tag{5.48}$$

$$-\infty \times (1 - \gamma_m^t) < g_m - \operatorname{mod}(t - \Delta_m - 1, C_{a:m \in S_m^a}), \qquad m \in S_m \tag{5.49}$$

$$\infty \times \beta_m^t > \operatorname{mod}(t - \Delta_m - 1, C_{a:m \in S_m^a}) - g_m - rd_m, \qquad m \in S_m \tag{5.50}$$

$$-\infty \times (1 - \beta_m^t) \leq \operatorname{mod}(t - \Delta_m - 1, C_{a:m \in S_m^a}) - g_m - rd_m, \quad m \in S_m \tag{5.51}$$

$$\infty \times \hat{\beta}_m^t \geq C_{a:m \in S_m^a} - rd_m - \operatorname{mod}(t - \Delta_m - 1, C_{a:m \in S_m^a}), m \in S_m \tag{5.52}$$

$$-\infty \times (1 - \hat{\beta}_m^t) < C_{a:m \in S_m^a} - rd_m - \operatorname{mod}(t - \Delta_m - 1, C_{a:m \in S_m^a}), m \in S_m \tag{5.53}$$

$$\hat{\gamma}_m^t > \beta_m^t + \hat{\beta}_m^t - 2, \qquad m \in S_m \tag{5.54}$$

$$-\infty \times (1 - \hat{\gamma}_m^t) \leq \beta_m^t + \hat{\beta}_m^t - 2, \qquad m \in S_m \tag{5.55}$$

5.3.1.6. Consistency between Signal Phase and Traffic Flow at Intersections

Equations 5.56-5.57 have constrained the evacuation flows traversing an intersection by the signal phase at the intersection. More specifically, vehicles can exit major roads only during the major road green phases (γ_m^t =1). Likewise, vehicles can exit minor roads only during minor road green phases ($\hat{\gamma}_m^t$ =1).

$$\sum_{k \in U_m} \sum_{j \in \Gamma^{-1}(k)} y_{kj}^t \leq \infty \times \gamma_m^t, \qquad m \in S_m \tag{5.56}$$

$$\sum_{k \in UT_m} \sum_{j \in \Gamma^{-1}(k)} y_{kj}^t \leq \infty \times \hat{\gamma}_m^t, \qquad m \in S_m \tag{5.57}$$

Except for the aforementioned six groups of operational constraints, the proposed model also includes nonnegative constraints, initial value of link state variables x_i^1, and initial value of flows between links y_{ij}^0 to provide a realistic range for the optimal solution.

5.3.2. Case Study

5.3.2.1. Study Network

This section intends to demonstrate the effectiveness of the proposed model by comparing different control plans in a real-world evacuation network as shown in Figure 5.3.

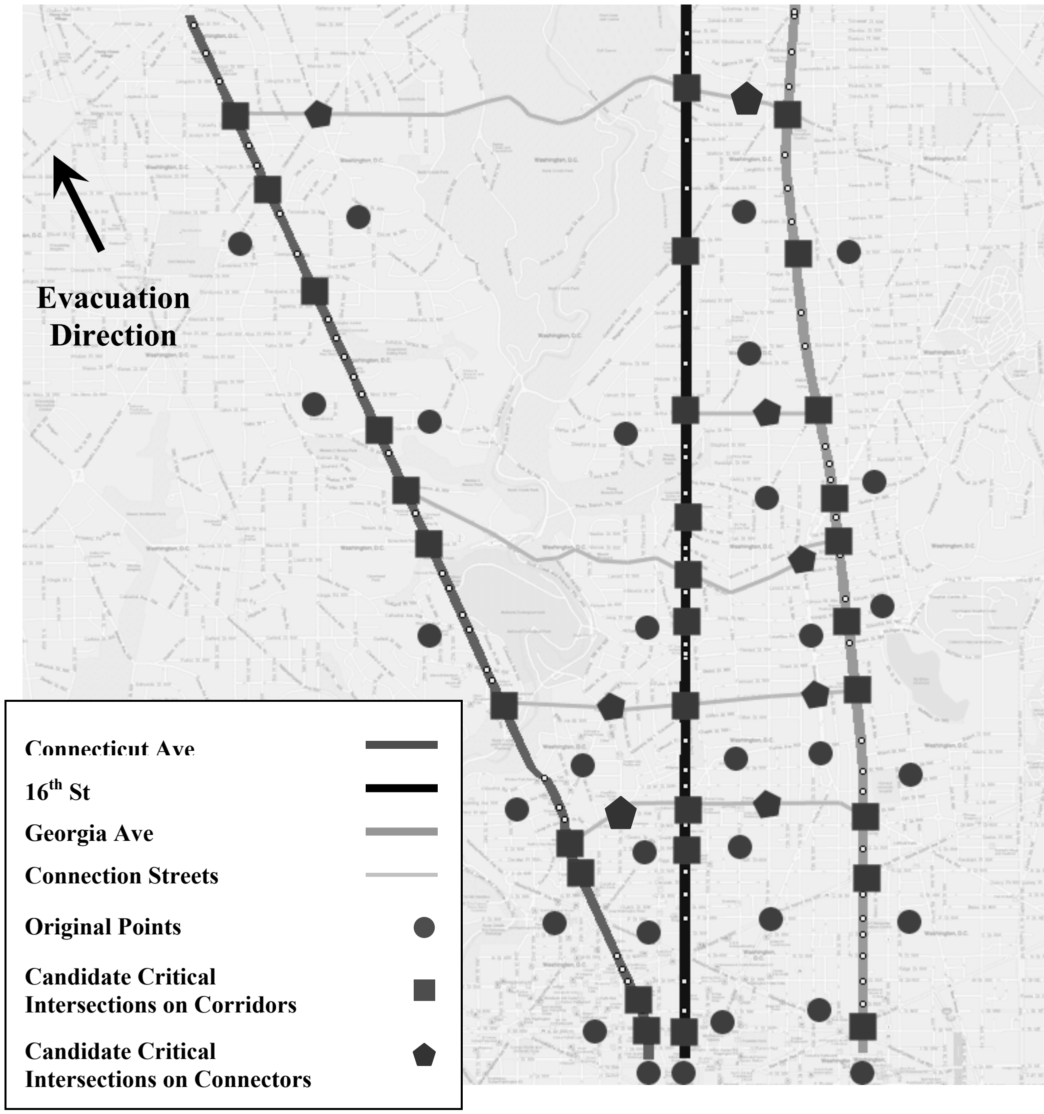

Figure 5.3 Illustration of the Study Network of Multiple Corridors

The study network includes three neighboring corridors from the Washington D.C. evacuation network:

- Connecticut Ave from K St. to Chevy Chase Circle. Its number of lanes varies from two to four in the outbound direction. Eleven of its 38 signalized intersections are selected as candidates for critical intersections.

- 16th Street from K St. to Eastern Ave. Its number of lanes varies from two to four in the outbound direction. Ten of its 43 signalized intersections are pre-selected as candidates for critical intersections.
- Georgia Ave from Mt Vernon Pl. to Eastern Ave. Most of its links have only two lanes in the outbound direction. Ten of its 48 signalized intersections are pre-selected as candidates for critical intersections.

The evacuation network also includes five major streets between these corridors as the connectors, on which there are eight intersections that can be chosen as critical intersections. The intersections connecting evacuation corridors and connectors are set as default critical intersections. Besides, the target network includes 31 predefined origins, which connect to nearby candidate critical intersections.

Based on the generalized cell transmission concept, Figure 5.4 has depicted all the origins, side streets at intersections, links in the corridors, and links on the connectors with cells. The arrows between cells represent the actual connections between all these geometric objects. Note that the cells in Figure 5.4 do not necessarily have the same size. Cells for origins and side streets always have the size of one. However, cells for links in the corridors and connectors may have different sizes, which are decided by the physical length of the corresponding link and the travel speed.

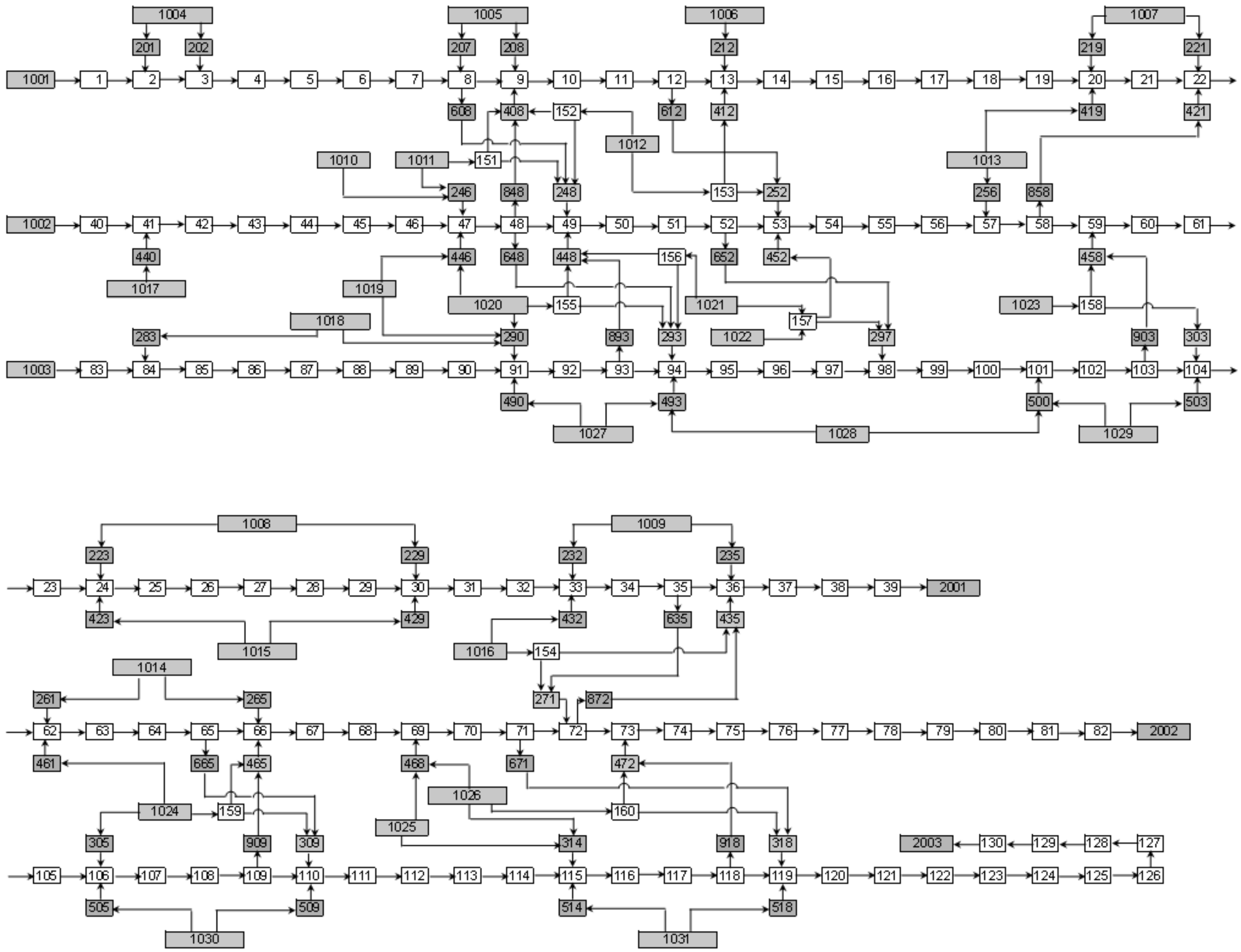

Figure 5.4 The Cell Connection Diagram for the Example Network with Multiple Corridors

5.3.2.2. Control Plans for Comparison

With the example network, this section compares the effectiveness of three plans, which combines different control strategies as shown in Table 5.8. Note that under Plan I and Plan II, each corridor is operated independently. Thus, no movement is allowed to turn from evacuation corridors to connectors, which leads to no through traffic at intersections on the connectors. Plan III offers integrated operations for the three parallel evacuation corridors, allowing traffic to travel between corridors via the connectors.

Table 5.8 Three Control Plans for Multi-Corridor Evacuation

Control Strategies		Control Plan I (Minimal Green)	Control Plan II (Individually Operated)	Control Plan III (Integrally Operated)
Selection of critical intersections and demand routing from origins		Optimized	Optimized	Optimized
Intersection on corridors	Cycle time	240s	Optimized	Optimized
	Green time for main road (corridor)	220s	Optimized	Optimized
	Green time for minor road (side/connectors)	10s	Optimized	Optimized
Intersection on connectors	Cycle time	240s	240s	Optimized
	Green time for main road (connectors)	0s	0s	Optimized
	Green time for minor road (side streets)	240s	240s	Optimized
Diverge from corridors to connectors		N/A	N/A	Optimized
Demand from side streets to connectors		Optimized	Optimized	Optimized

Those control parameters in each different plan are generated with a Genetic Algorithm based heuristic similar to the one proposed in Section 5.2.2, with the assumptions that each origin can only go to one of its connected critical intersections and the cycle time varies between 100 and 240 seconds. Note that to eliminate impact due to the random nature of the GA heuristic, this study executes the algorithm ten times and pick up the best set of parameters for design of each control plan.

5.3.2.3. Comparison Results

This section first compares the performance of those three control plans under Demand Scenarios 1-6, as shown in Table 5.9, where the total evacuation demand (17600 vehicles) shifts gradually from the three origins at the upstream of the evacuation corridors to the 28 original nodes specified over the entire network. All these demands will be loaded onto the network during the interval of 30 minutes, based on a logit function.

Table 5.9 Demand Scenarios 1-6 for Multi-Corridor Evacuation

Scenario / Total Demand from Each Origin (unit: veh)	1	2	3	4	5	6
Origin at the upstream of each evacuation corridor	5400	5120	4840	4560	4280	4000
Other minor origin	50	80	110	140	170	200

With properly designed control parameters, all three plans can help to complete the evacuation process within a three-hour time window under all six demand scenarios. Table 5.10 shows the total evacuation clearance time under different control plans.

Table 5.10 Evacuation Clearance Time under Demand Scenarios 1-6 for Multi-Corridor Evacuation (Unit: seconds)

Clearance Time	Demand scenario 1	Demand scenario 2	Demand scenario 3	Demand scenario 4	Demand scenario 5	Demand scenario 6
Plan I	7135	7085	7025	7705	9145	10585
Plan II	7135	7085	7025	7105	7105	7025
PlanIII	7090	7085	7025	7090	7070	7025

The results reported in Table 5.10 reveal the following information:

- When the evacuation demand concentrates at the upstream segment of the evacuation corridors (Demand Scenario 1-3), the Minimal Green Plan (Plan I) shows the comparable performance as under Plan II and Plan III. This is due to the fact that traffic from minor origins can be accommodated with even the minimal green time and, thus adjusting the corridor signals will not make any significant contribution to the operations.
- When evacuation demand distributes more evenly over the network (Demand Scenario 4-6), Control Plans II and III clearly outperform Plan I, the Minimal Green Plan.

- Traffic diverging between corridors in Plan III does help to reduce the evacuation clearance time, compared to Plan II. However the improvement is not significant under these six demand scenarios. This is due to the fact that the traffic demand has a relatively balanced distribution among the three evacuation corridors.

Next, this section compares the performance of the three control plans under two more demand Scenarios, as shown in Table 5.11, where more evacuation demands are generated at the upstream of Connecticut Ave and less demands at the upstream of the 16th St. All the demands will be loaded onto the network during the interval of 30 minutes based on the same distribution pattern.

Table 5.11 Demand Scenarios 7-8 for Multi-Corridor Evacuation

Demand Scenario / Total Demand from Each Origin (unit: veh)	7	8
Cell 1001: Origin at the upstream of Connecticut Ave.	7840	7280
Cell 1002: Origin at the upstream of 16th St.	1840	1280
Cell 1003: Origin at the upstream of Georgia Ave.	4840	4280
Other minor origins	110	170

With properly designed control parameters, all three plans can help to complete the evacuation process within a three-hour time window for the Demand Scenario 7 and Scenario 8. Table 5.12 shows the total evacuation clearance time. The table also compares the evacuation clearance time between Scenario 7 and Scenario 3, and between Scenario 8 and Scenario 5, since each pair of scenarios has the same demand from minor origins.

Table 5.12 Evacuation Clearance Time under the Demand Scenario 7 and Scenario 8 for Multi-Corridor Evacuation (unit: seconds)

Clearance Time	Demand scenario 3	Demand scenario 7	Demand scenario 5	Demand scenario 8
Plan I	7025	8935	9145	9145
Plan II	7025	8935	7105	8525
Plan III	7025	8470	7070	7945

Results in Table 5.12 have revealed the following information:

- When traffic from minor origins can be accommodated with the minimal green time (Scenarios 3 and 7), Control Plan II provides the same level of evacuation efficiency under Plan I, regardless of the demand distributions among the origins at the upstream of evacuation corridors. But Plan III does reduce the evacuation clearance time by around 10 minutes when the demand is more unbalanced among corridors (i.e., Demand Scenario 7).
- When the minimal green time cannot accommodate traffic from minor origins (Scenarios 5 and 8), Control Plan II has helped to reduce the evacuation clearance time under both demand scenarios. However, by allowing the traffic to redistribute among corridors using connection streets, Plan III has further improved the evacuation clearance time by 10 minutes compared to Plan II, and 20 minutes compared to Plan I, when the demand is more unbalanced among corridors (Demand Scenario 8).

In summary, the numerical results have demonstrated that demand distribution can significantly influence the effects of different control strategies on evacuation clearance time, and thus will affect the control plan selection. More specifically,

- Minimal-Green Plan or Yellow-Flash Plan is preferred when the evacuation demand mainly concentrates at the upstream of evacuation corridors and minor origins only have very light demand. Otherwise, optimizing the corridor signal timings to effectively contend with the arriving evacuation flows from the minor origins will be essential.
- When the evacuation demand distributes approximately balanced among different evacuation corridors, traffic rerouting between corridors will be unnecessary. This implies that the evacuation corridors can be operated individually. Note that whether a demand distribution is balanced or not depends on a variety of factors, such as the demand level, the number of lanes, and the roadway capacity.

5.4. Closure

In summary, Chapter 5 has presented the formulations for design of signal control strategies for designated evacuation corridors. The base model, presented in Section 5.2, is focused on an individually operated corridor typically consisting of one major safety-bound arterial connected with original nodes via side streets. As an extension, Section 5.3 has presented the generalized formulations for an integrated network of multiple corridors, which may balance evacuation traffic flows via connectors so as to improve the overall evacuation efficiency. Despite the difference in the formulations, these two models share the following two key features:

- Critical Intersection concept: i.e., only key intersections will offer protective phases for vehicles from minor roads to turn onto major roads (e.g., from side streets to arterials or from connectors to arterials). This core concept intends to reduce the disturbance of minor road traffic to the flow progression on main roads. With an effective signal control system, the evacuation arterial should be capable of progressively moving its assigned traffic flows without incurring excessive delay for those waiting on the minor roads.
- Two-phase control: to maximize the operational efficiency and to reduce the implementation complexity, the proposed model will operate all critical intersections with a two-phase signal control to account for the fact that evacuation flows travel in the same safety-bound direction along the evacuation corridors. For example, critical intersections on the evacuation

corridors allow vehicles to exit the upstream link of the arterial during the arterial green phase, and allow traffic from the side street/connectors to turn on the arterial during the side street green phase. All non-critical intersections will not provide a protective green phase for traffic from side streets.

The numerical tests in this chapter have demonstrated the potential of the proposed models for use in design of signal control strategies. Both models have proved to generate better control strategies than the Minimal Green plan, which is one widely-suggested evacuation signal control strategy. The improvement depends on the demand pattern and is more significant when demands distribute along the corridor instead of concentrating in the upstream segment. In general, a balanced demand distribution along the neighboring evacuation corridors may allow these corridors to operate independently. Otherwise, the integrated multi-corridor control will result in higher operational efficiency. Such balance is defined by a variety of factors, including the demand pattern and the roadway capacity.

Chapter 6: A Case Study with the Washington D.C. Evacuation Network

6.1. Introduction

This chapter illustrates the application of the proposed methodology for real-world applications using the Washington D.C. evacuation network. This case study intends to assist potential users in best understanding the key functions and properties of the developed integrated control system, and effectively using it for operational needs. The presentation will be focused on the following four principal aspects:

- Effective use of the proposed two-level design structure, especially on those special modeling features and the data needs in a real-world network;
- Performance comparison between the control strategies generated with the proposed system and some base plans used in practice;
- Analysis of the evacuation effectiveness based on the operational strategies produced by the proposed system, and identification of bottlenecks for potential improvements;
- Evaluation of some advanced operational strategies and development of some general guidelines.

To address key issues on the above aspects in sequence, Section 6.2 will first detail the features of the study network that covers 6 major evacuation corridors in Washington D.C., along with a description of the evacuation scenario that involves 25 traffic zones with a total of 50,510 vehicles.

Section 6.3 illustrates the two-level design structure under a concurrent evacuation operation, which starts with a presentation of the network level controls for directing the total evacuation demand to different corridors. The results from this level serve as the basis to activate the corridor-level model designed for optimizing signal controls and for refining the demand assignments within each individual corridor or clustered corridors. This section will also include the evaluation and analysis of the generated control strategies for the case study.

Section 6.4 highlights the design of staged evacuation strategies proposed to implement different types of evacuation orders for reducing network congestions. A sensitivity analysis reported in this section with respect to the expected compliance rate and response time of evacuees has yielded some imperative information for responsible planners/operators to assess the needs of executing a staged evacuation.

6.2. Study Network

The evacuation scenario used in the case study covers 25 traffic analysis zones (TAZs) and a total of 50,510 vehicles. Figure 6.1 shows the locations of these zones, and the total demand in each zone is obtained from the District Department of Transportation as listed in Table 6.1. These demands are assumed to move onto the network during a default loading time of 30 minutes.

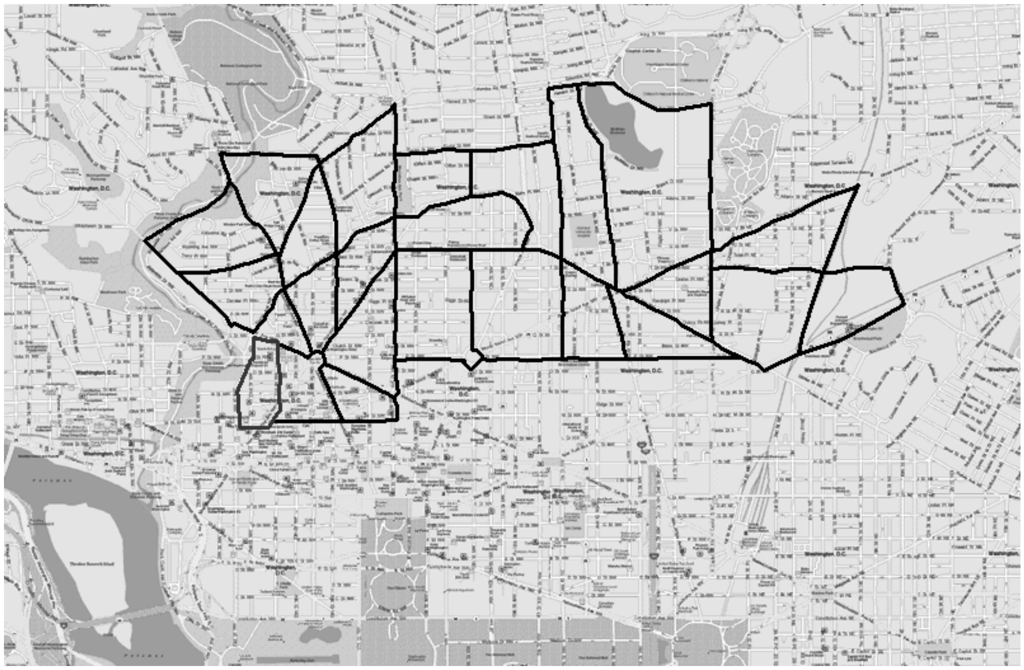

Figure 6.1 Locations of the 25 Traffic Analysis Zones

Table 6.1 Demand Distribution among the 25 TAZs

TAZ	Total Demand (veh)	TAZ	Total Demand (veh)
11	2194	106	1753
12	2340	114	3507
18	1292	115	3173
47	1988	116	4054
48	4268	123	977
49	2142	124	2157
52	3686	134	2388
53	2048	135	1690
54	3216	143	1182
56	1154	144	1129
57	1021	145	1267
104	305	147	114
105	1465	Total	50510

These 50,510 vehicles are expected to move out of the traffic zones via the pre-designated local access routes, and to use these six major evacuation corridors (from west to east in Figure 6.2) to travel to Capital Beltway.

- Wisconsin Ave.: a three-lane arterial starting from Massachusetts Ave.
- Connecticut Ave.: an arterial with the number of lanes varying from 2 to 4.
- 16th St.: an arterial with the number of lanes varying from 2 to 4.
- Georgia Ave.: an arterial with the number of lanes varying from 2 to 3.
- Rhode Island Ave.: an arterial with the number of lanes varying from 3 to 4.
- New York Ave.: an arterial with the number of lanes varying from 3 to 4.

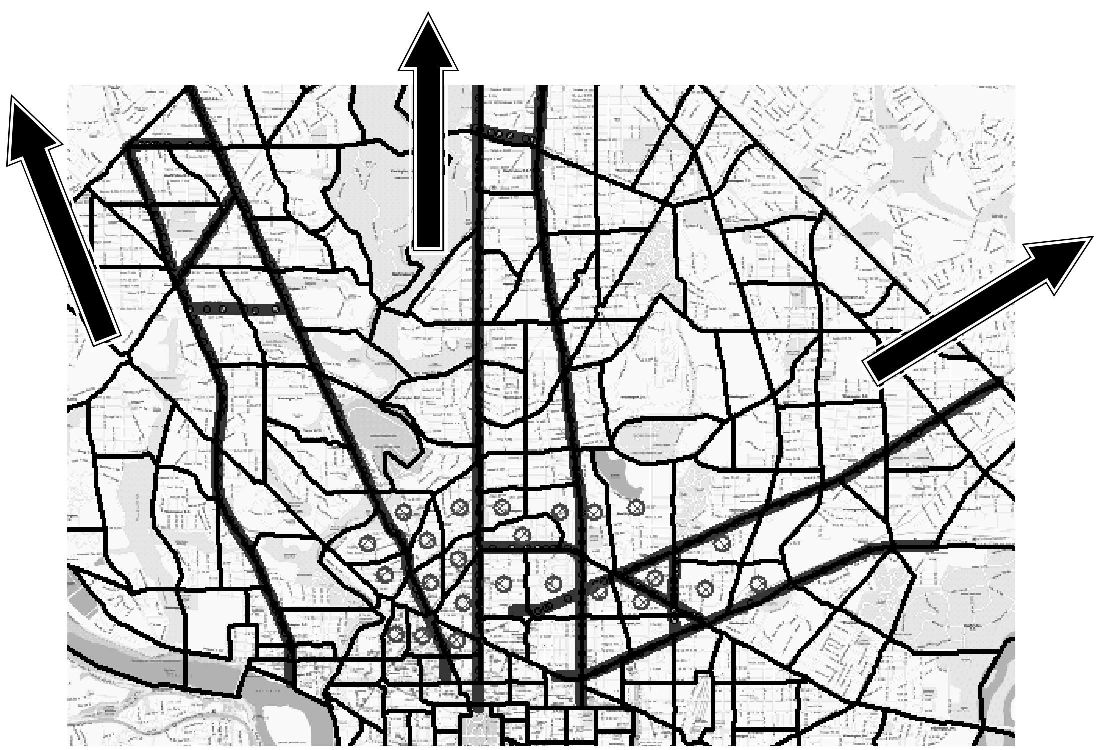

Figure 6.2 The Six Major Evacuation Corridors

Also shown in Figure 6.2 are the main arterials connecting those six corridors, which are:

- Van Ness St., Nebraska Ave., and Military Rd. between Wisconsin Ave and Connecticut Ave.;
- U St. and Military Rd. between 16th St. and Georgia Ave.; and
- N. Capital St. and Florida Ave. between Rhode Island Ave. and New York Ave.

6.3. Design Concurrent Evacuation Strategies

6.3.1. Illustration of the Two-Level Operational Structure

6.3.1.1. Network Level

To apply the revised cell transmission model presented in Chapter 4, the first step is to convert the target network into a cell connection diagram with 189 cells and 235 connectors. The update interval is selected as 30seconds, which is sufficient for such a large-size network. Thus, the evacuation time window of three hours contains a total of 360 intervals. One can then formulate the dynamic network flow constraints with Equations 4.12-4.20.

To ensure the compatibility of the results between the network-level and the corridor-level models, the numerical study employs the following Equation 6.1 to take into account the pre-designated signal phasing plans at intersections.

$$\sum_{p \in Ph_I} \{y_{ij}^t / Q_{ij}^t : \quad \forall ij \in p\} \le 1 \tag{6.1}$$

This simplified intersection capacity constraint requires that the sum of the v/c ratios on those movements in different signal phases should not exceed one for each time interval. Here, I is the index of intersections; Ph_I is the set of signal phases at intersection I; and p is the index of each signal phase at intersection I, $p \in ph_I$.

An example illustration of a two-phase control at intersections is shown in Figures 6.3-6.5:

- For the intersections between corridors and side streets/connectors (Figure 6.3), Phase-1 (p=1) will allow the movements out of the upstream arterial link 1, namely, movements 1-2, 1-3 and 1-4; Phase-2 (p=2) will permit movements from the side street/connectors to the downstream arterial link 2, i.e., movements 3-2 and 4-2.

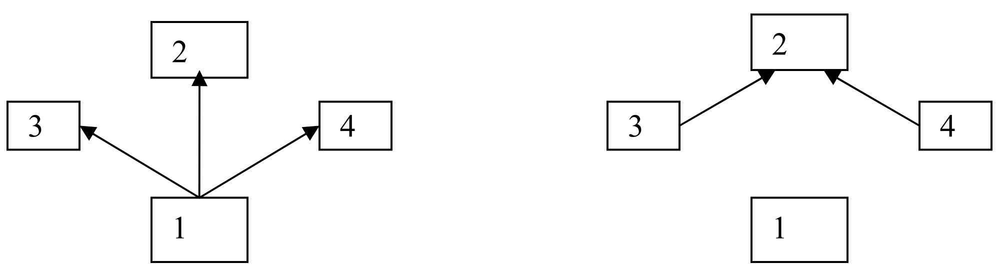

p=1: arterial green phase $\qquad$ p=2: side street green phase

Figure 6.3 The 2-Phase Control at Intersections between Corridor and Side Street/Connector

- For the intersections between side streets and connectors (Figure 6.4), Phase-1 (p=1) will allow the movements between the connector links (movements 1-2 and 3-4), and Phase-2 (p=2) will enable the movements from the side streets to connectors, i.e., movements 5-2, 5-4, 6-2 and 6-4.

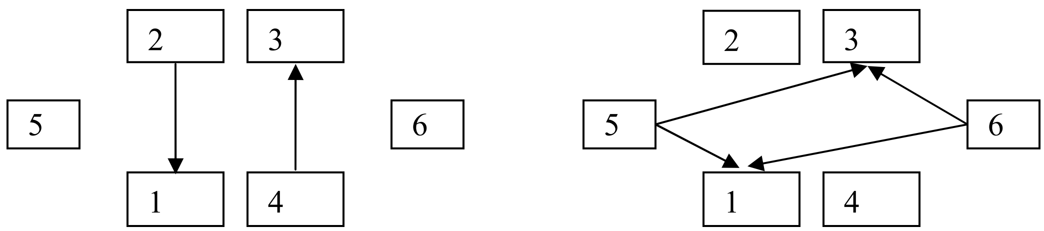

p=1: connector green phase *p*=2: side street green phase

Figure 6.4 The 2-Phase Control at Intersections between Side Streets and Connectors

- For the intersections between two connectors (Figure 6.5), Phase-1 (p=1) allows movements along one connector, i.e., movements 1-2 and 3-4, and Phase-2 (p=2) is to facilitate the movements along the other connectors (i.e., movements 5-6 and 7-8).

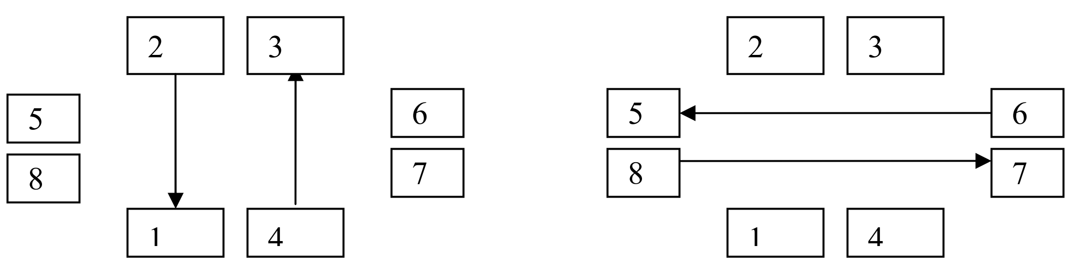

p=1: green phase for one connector *p*=2: green phase for the other connector

Figure 6.5 The 2-Phase Control at Intersections between Two Connectors

Using the commercial software LINGO 8.0, the evacuation plan starts with the maximization of the total throughput for all six destinations at the northern ends of the corridors, as defined in Equation 4.10. The results show that the maximal throughput over the 3-hour time window can reach 50,510 vehicles, which equal the total evacuation demand. This implies that the duration of three hours is sufficient to clear the evacuation area.

The system operator shall then explore the use of the objective function 4.11 for evacuation planning so as to minimize the total trip time. Note that for concurrent evacuation, to minimize the total trip time is equivalent to minimize the total time in the network that includes the total trip time as well as the response delay of evacuees. The optimal solution yields an average trip time of 3400 seconds with an evacuation clearance time of 10,350 seconds for the entire network.

The optimal plan from the network-level control will provide three types of information for executing the corridor-level control, which includes:

- The decomposition of the entire network into different groups, each with an individual corridor or connected neighboring corridors;
- The assignment of demands to different groups; and
- The initial routing plan from origins to the side streets within each group.

Based on the usage of available connectors, the optimal solution naturally divides the whole network into four groups. The demand assignment for each group of corridors is shown in Table 6.2.

- Group 1: Wisconsin Ave.;
- Group 2: Connecticut Ave.;
- Group 3:16th St. and Georgia Ave.;
- Group 4: Rhode Island Ave. and New York Ave.

Table 6.2 The Optimal Demand Assignment from the Network Level Control

TAZ	Group1	Group 2	Group 3	Group 4	Total
11	2194	0	-	-	2194
12	2340	0	-	-	2340
18	1292	0	-	-	1292
47	-	1988	-	-	1988
48	-	1650	2618	-	4268
49	-	101	2041	-	2142
52	-	-	3686	-	3686
53	-	-	2048	-	2048
54	-	-	3216	-	3216
56	-	-	-	1154	1154
57			-	1021	1021
104	0	305	-	-	305
105	1465	0	-	-	1465
106	1753	0	-	-	1753
114	-	3507	-	-	3507
115	-	3173	-	-	3173
116	-	-	4054	-	4054
123	-	-	977	-	977
124	-	-	2157	-	2157
134	-	-	0	2388	2388
135	-	-	0	1690	1690
143	-	-	-	1182	1182
144	-	-	-	1129	1129
145	-	-	-	1267	1267
147	-	-	-	114	114
Total Demand (veh)	9044	10724	20797	9945	50510
No. of TAZs Involved	5	6	8	8	25

Note: “-” indicates no access

Table 6.3 lists the traffic flows diverted to each side street based on the network level model.

Table 6.3 Flows Diverted to Each Side Street from the Network Level Control

Arterial	Side Street ID	Total Flows (vehicles)
Wisconsin Ave.	5026	5826
	5426	3218
Connecticut Ave.	1405	3738
	1412	3507
	1414	3173
	1215	305
16^{th} St.	4206	2618
	4407	1200
	4209	982
	4411	563
	4214	4054
	4414	190
Georgia Ave.	2210	1047
	2211	1060
	2215	1851
	2216	945
	2219	1923
U St.	24402	2240
	24203	44
	24204	834
	24408	1246
Rhode Island Ave.	3406	661
	3212	2388
	3412	1198
	3217	1690
	3422	103
New York Ave.	6214	11
N. Capital St.	27203	185
	27208	57
	27414	930
Florida Ave.	25409	568
	25213	2154

6.3.1.2. Corridor Level Design

With the aforementioned information, the evacuation operation will then activate the corridor level models proposed in Chapter 5 to optimize the signal controls and to refine the routing plans for each group of corridors. Prior to the analysis of the research results, there are two issues that deserve attention. The first issue is related to the update interval. The 30-second interval for the network level analysis needs to be refined at a much smaller interval of 5 seconds to yield the level of precision sufficient for local signal controls on each evacuation arterial.

The second issue is about the mechanism for refining the routing plan within each group. Note that the initial plan from the network level model gives the number of vehicles from each origin to each of its accessible side streets, which might yield some side streets with very light demand. Those intersections with such side streets will be defined as critical intersections and will operate with traffic signals. This may lead to unnecessary delays due to the lost time and minimal green time requirements associated with signal controls. To improve the overall efficiency, this study will allow the demands from each traffic zone to re-choose the target side streets at the corridor level. As shown in Figure 6.6, the network level routing plan assigns x vehicles from origin 0 to side street 1 and y vehicles from 0 to side street 2, whereas the corridor level will allow these vehicles to go to either of the side streets.

Routing plan from the network level Routing plans allowed at the corridor level

Figure 6.6 Refining the Routing Plans from the Network Level

Based on the aforementioned analysis, one can execute the corridor-level models and generate evacuation control strategies for each group of corridors. Table 6.4 presents the signal control plans generated over 10 replications with the solution algorithms in Chapter 5, which has been slightly modified to account for the following concerns:

- To be consistent with the network level formulations, the fitness function of the GA algorithm has been modified to minimize the average trip time instead of the evacuation clearance time.
- The GA algorithm uses a time window of 5 hours to ensure the evacuation operation can be completed for all four groups of corridors.
- The maximal cycle length is set as 240 seconds and the minimal green time for critical intersections is 10 seconds.
- For the first critical intersection on each corridor, the algorithm will check if there are traffic flows coming from its upstream arterial link. If not, the algorithm will assign all green time to the side street.

Table 6.4 The Signal Control Plan from the Corridor-Level Model

Arterial	Cycle Length (sec)	Intersection*	Arterial Green Time (sec)
Wisconsin Ave.	240	5026/5426	150
Connecticut Ave.	235	1010/1412	115
		1013/1414	155
		1015/1215	185
16th St.	150	4007/4407	55
		4008/4209	75
		4010/24013	90
		4011/4411	85
		4012/4214	80
Georgia Ave.	225	2011/2211	70
		2012/24009	70
		2015/2215	130
		2016/2216	185
		2018/2219	175
U St.	175	24002/24402	100
		24003/24203	175 (non-critical)
		24004/24204	110
		24005/24408	80
Rhode Island Ave.	150	3007/25023	150(non-critical)
		3011/3212	0**
		3013/27019	90
		3017/3217	85
		3022/3422	120
New York Ave.	210	6012/25014	55
		6013/6214	210(non-critical)
N. Capital St.	225	27002/27203	225(non-critical)
		27006/27208	225(non-critical)
		27013/27414	30
Florida Ave.	155	25002/25409	155(non-critical)
		25013/25213	30
		25010/27012***	80

Note: * The intersection is marked with ID of the two upstream links.

** The first critical intersection without traffic from the upstream arterial link

*** The case study only considers the arterial progression on Florida Ave.

Table 6.5 presents the demand rerouting plan based on the corridor level results. Compared with the routing plan from the network level model, the rerouting plan mainly tries to divert traffic from the side streets of a light demand and convert those intersections as non-critical intersections of no signal control during the evacuation operations. For example, the intersection between Link-27002 and Link-27203 on N. Capital St. is operated as a non-critical intersection (see Table 6.4), after the 185 vehicles from TAZ-145 to Link-27203 are rerouted to Link-25213.

Table 6.5 Demand Rerouting Plans from the Corridor-Level Model

TAZ	Original Side Street Assigned	Traffic Flows (vehicles)	Side Street Rerouted
124	24203	44	2219
56	25409	493	3406
57	25409	75	27414
144	27208	57	25213
145	27203	185	25213
147	6214	11	3422

6.3.2. Evaluation of the Generated Control Strategies

To evaluate the control plans generated from the corridor level, this section compares them with some state-of-the-practice control plans for two groups of corridors. Group 2 (Connecticut Ave.) is an independently operated corridor, for which the control generated with the proposed methodology is compared with Minimal Green Plan and the plan generated with the signal plan designed according to actual link volumes. Group 4 includes multiple arterials (Rhode Island Ave., New York Ave., N. Capital St. and Florida Ave.), and its control plan generated from the corridor level, with critical intersection selection and demand rerouting, is also compared with the control strategies derived from the actual link volumes.

6.3.2.1 Performance Evaluation with Connecticut Ave.

To test the effectiveness of the control strategies produced by the proposed model, Table 6.6 compares the following three signal timing plans under the same demand distribution from the network level results (shown in Table 6.3), where the total demand is 10,724 vehicles.

- Plan I: the signal control plan generated with the GA algorithm from the corridor-level model;
- Plan II: the Minimal Green Plan with a cycle length of 240 seconds and minimal side street green time of 10 seconds as suggested in most evacuation practices;
- Plan III: the signal timing plan with the green time for arterial links and side streets decided precisely based on their volumes.

Table 6.6 Comparison of Different Signal Control Plans for Connecticut Ave.

Control Plan	Cycle Length (sec)	Intersection	Arterial Green Time (sec)	Throughput in 3 hours (veh)	Average Trip Time in 5 hours (sec)
Plan I	235	1010/1412	115	10724	4615
		1013/1414	155		
		1015/1215	185		
Plan II	240	1010/1412	220	4931	N/A *
		1013/1414	220		
		1015/1215	220		
Plan III	120	1010/1412	55	10230	4770
		1013/1414	75		
		1015/1215	100		

Note: * Evacuation demand cannot be cleared in 5 hours for this plan.

The comparison indicates that the control strategies generated with the corridor-level model can significantly outperform the minimal green plan. Even compared with the signal plan designed precisely based on link volumes, the throughput during the period of three hours still shows an increase of 4.8% (552 vehicles) and the average trip time in 5 hours will reduce 3.2% (155 seconds)

6.3.2.2. Performance Evaluation with the Group 4 Corridors

Table 6.7 compares the following two signal timing plans for the 4th group of corridors (Rhode Island Ave., New York Ave., N. Capital St. and Florida Ave.), where the total demand is 9,945 vehicles.

- Plan I: the signal timing plan generated with the GA algorithm that exerts the critical intersection control and traffic rerouting operations;
- Plan II: the signal timing plan with the green time for arterial links and side streets decided precisely based on their volumes. The diverging rates at intersections are also extracted from the optimized network-level results.

The comparison indicates that in a complex network, the generated control strategies can significantly outperform the standard design approach, which assumes the availability of perfect information on traffic volume distributions over the evacuation period. The proposed corridor-level model has achieved a level of 22.9 percent improvement in the average trip time upon clearance.

Table 6.7 Comparison of Different Signal Control Plans for Group 4

Control Plan	Arterial	Cycle Length (sec)	Intersection	Arterial Green Time (sec)	MOEs
Plan I	Rhode Island Ave.	150	3007/25023	150(non-critical)	Throughput in three hours: 9945 vehicles
			3011/3212	0 *	
			3013/27019	90	
			3017/3217	85	
			3022/3422	120	
	New York Ave.	210	6012/25014	55	
			6013/6214	210(non-critical)	
	N. Capital St.	225	27002/27203	225(non-critical)	Average Trip Time upon Clearance: 1110 seconds
			27006/27208	225(non-critical)	
			27013/27414	30	
	Florida Ave.	155	25002/25409	155(non-critical)	
			25013/25213	30	
			25010/27012	80	
Plan II	Rhode Island Ave.	120	3007/25023	100	Throughput in three hours: 9945 vehicles
			3011/3212	10	
			3013/27019	100	
			3017/3217	75	
			3022/3422	100	
	New York Ave.	120	6012/25014	30	
			6013/6214	100	
	N. Capital St.	120	27002/27203	40	Average Trip Time upon Clearance: 1440 seconds
			27006/27208	80	
			27013/27414	20	
	Florida Ave.	120	25002/25409	60	
			25013/25213	40	
			25010/27012	95	

Note: * The first critical intersection without traffic from the upstream arterial link.

Finally, to further assess the performance of the solution algorithm, Table 6.8 has compared the average trip time generated from the corridor level with that from the optimal network-level plans. With the more relaxed intersection capacity constraints instead of the fixed-time signal control, the network-level plan certainly allows more flexibility and thus can serve as a reasonable base for performance comparison.

Table 6.8 Comparison of Average Trip Time from Network and Corridor Level Control

	Network Level (sec)	Corridor Level (sec)	Absolute Difference (sec)	Relative Difference (%)
Group 1	2286	2320	34	1.49%
Group 2	4399	4615	216	4.91%
Group 3	4520	4810	290	6.42%
Group 4	991	1110	119	12.01%
Total	3400	3594	194	5.71%

The comparison shown in Table 6.8 has indicated that the control plans generated with the GA algorithm at the corridor level can lead to quite efficient evacuation operations. The average trip time is at about the same level as that generated from the network level solution with more relaxed LP constraints.

6.3.3. Analysis of the Evacuation Plan for Further Improvements

This section will further illustrate how to best use the evacuation plans generated with the proposed methodology in real-world operations with the emphasis on the following three aspects:

- Comparison between different groups of corridors to check the distribution of evacuees on all available routes;
- Comparison between corridors within the same group to identify potential bottlenecks ; and
- Examination of the link travel time for evaluating the operational efficiency and the needs to implement additional control strategies.

The purpose is to identify the potential bottlenecks in the current evacuation network with the proposed traffic control strategies, and thus help planners to explore other complementary alternatives so as to achieve further improvements on the overall evacuation efficiency.

6.3.3.1. Performance Comparison between Different Groups of Corridors

Table 6.9 summarizes the evacuation clearance time and average trip time of the four groups of corridors produced under the optimal network level control plan.

Table 6.9 Comparison between 4 Groups of Corridors

	Total Demand (veh)	No. of TAZs Involved	Average Trip Time (sec)	Clearance Time (sec)
Group 1	9044	5	2286	6060
Group 2	10723	6	4399	10350
Group 3	20798	8	4520	10350
Group 4	9945	8	991	4890
Total	50510	25	3400	10350

Clearly, there exists significant difference in evacuation efficiency between different groups of corridors. Group 1 (Wisconsin Ave) and Group 4 (Rhode Island Ave. and New York Ave.) have much shorter evacuation clearance time and average trip time than Group 2 (Connecticut Ave.) and Group 3 (16^{th} St. and Georgia Ave.).

A detailed examination of the demand assignment to each group (see Table 6.2) shows that almost all the Traffic Zones that have access to Wisconsin Ave. and Rhode Island Ave./New York Ave. will send their demand to these two groups. This indicates that the current plan of local access routes from the District Department of Transportation cannot provide a sufficient capacity to diverge traffic between neighboring corridors under the example evacuation scenario.

6.3.3.2. Comparison between Corridors within the Same Group

Table 6.10 further presents the evacuation clearance time and total throughput for those corridors within the same group, operated under the optimal network level control plan.

Table 6.10 Comparison between Corridors within the Same Group

Group	Corridor	Total Throughput (veh)	Clearance Time (sec)
Group 3	16^{th} St.	10284	10350
	Georgia Ave	10513	10350
Group 4	Rhode Island Ave	5421	4890
	New York Ave.	4523	3090

Notably, the two corridors in Group 3 are relatively balanced with the similar throughput and the same evacuation clearance time. However, the two corridors in Group 4 have significantly different evacuation clearance times. To find the possible reasons, this study examines the network flow files for Group 4 and reveals the following information (see Figure 6.7):

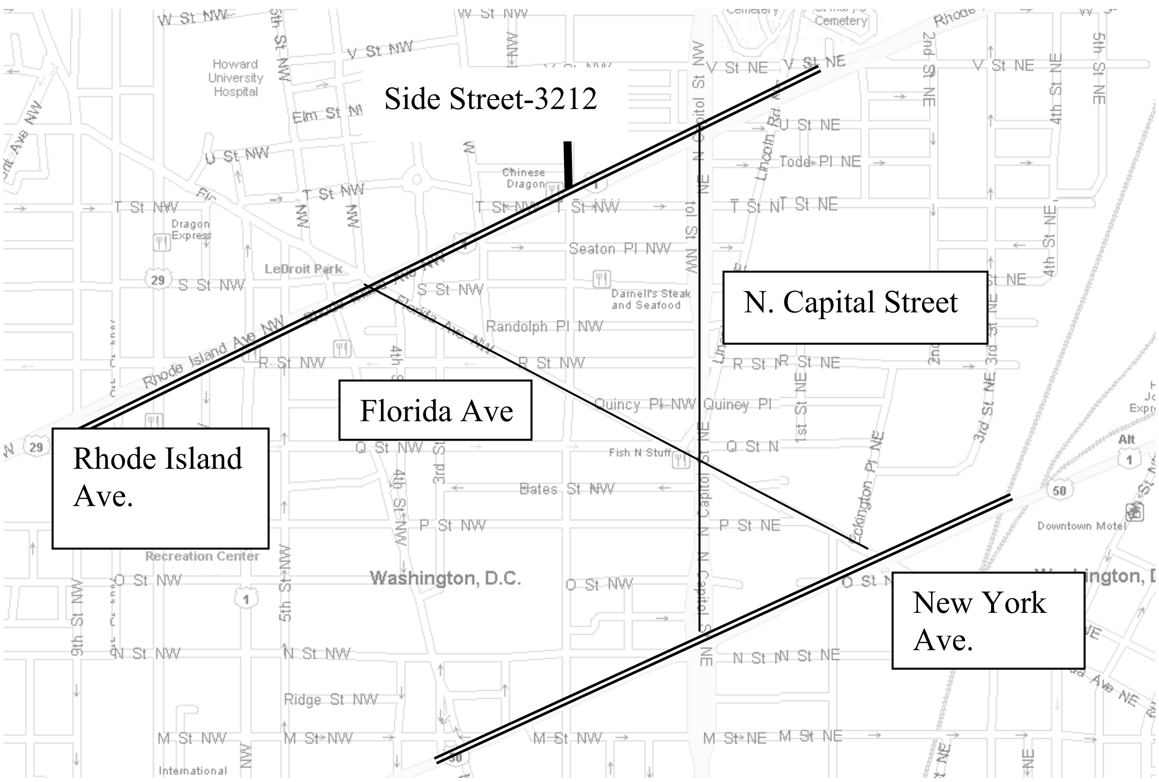

Figure 6.7 Illustration of the Network Geometry for Group 4

- All traffic volumes directed to Rhode Island Ave. before Florida Ave. have been rerouted to New York Ave. via Florida Ave.
- All traffic volumes directed to Florida Ave. have gone to New York Ave.

- Only 2.8% of the traffic volumes on Rhode Island Ave. have turned right at N. Capital Street to New York Ave.
- After 3090 seconds from the evacuation starting time, flows on Rhode Island Ave. only come from Side Street-3212 (1^{st} St. NW). Further examination of the flows out of this side street indicates that its capacity have been fully utilized to the end of the evacuation operation.

The above observations have revealed Side Street-3212 as the most critical bottleneck for Group 4. Referring back to Table 6.2 and Table 6.3, one can find that this one-lane side street is the only access route designated for Zone-134 with a total demand of 2388 vehicles. Given the flow rate at 1800 vehicles per lane per hour, it will take more than 4500 seconds to get the 2388 vehicles onto Rhode Island Ave. Thus, operators may need to add more access routes to divert traffic from Zone-134. Another option is to check the road condition on 1^{st} St. NW and, if applicable, to add additional capacity by temporarily reversing the northbound lane on Side Street-3212.

6.3.3.3. Evaluation of the Link Travel Time

Using Connecticut Ave. as an example, Table 6.11 shows the comparison of the free flow travel time and the actual average travel time on the arterial links.

Table 6.11 Comparison of Link Travel Time for Connecticut Ave

Link ID	Property	Actual (sec)	Free Flow (sec)
1006	Arterial	279	30
1007	Arterial	248	30
1008	Arterial	392	30
1010	Arterial	232	30
1013	Arterial	130	30
1015	Arterial	38	30
1016	Arterial	30	30
1019	Arterial	150	150
1032	Arterial	120	120
1046	Arterial	30	30
1050	Arterial	30	30
1053	Arterial	30	30
1405	Side St.	3121	-
1412	Side St.	3246	-
1414	Side St.	3740	-
1215	Side St.	482	-

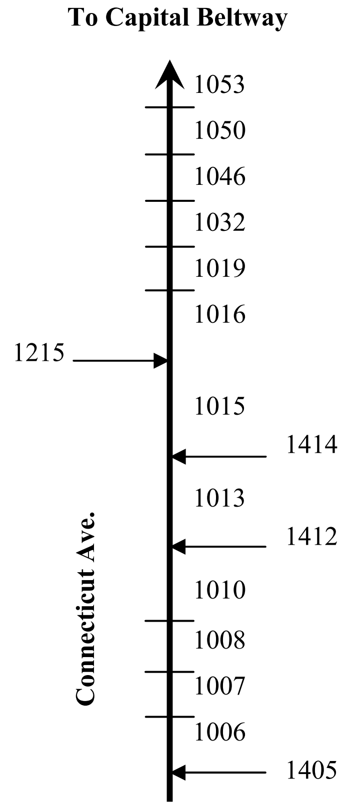

The data in Table 6.11 indicate that the congestion starts to build up at arterial Link-1013, whereas the downstream arterial Link-1015 to Link-1053 remains in the free flow traffic conditions. This is the reason why traffic is not directed from Connecticut Ave. to Wisconsin Ave by using the three connectors from Link-1019, Link-1032 and Link-1050.

Analysis in Section 6.3.3.2 reveals that Zone-104 will send its demand of 305 vehicles to Connecticut Ave. via Side Street-1215, although it can access Wisconsin Ave. that has shorter evacuation clearance time. As shown in Figure 6.8, since both Link-1013 and Link-1414 at the upstream of Intersection-1 have only two lanes, the two-phase signal control at Intersection-1 has restricted the flow to Link-1015 at a level equal to or lower than the 2-lane capacity. Thus, the demand from Zone 104 can evacuate via the Side Street-1215 to fully utilize the 3-lane links downstream of Intersection-2, without incurring excessive delay on Link-1015.

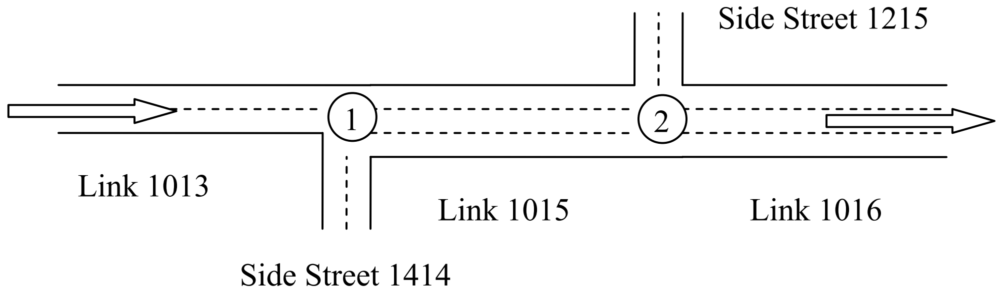

Figure 6.8 Illustration of the Network Geometry for Connecticut Ave.

Table 6.11 also indicate major delays incurred on the Side Street-1405, Side Street-1412 and Side Street-1414, which receive a large amount of demands from various origins during the first half hour, but have limited capacity to move the flows to the arterial links. This has resulted in long queues on the local streets, and thus justified the use of a staged evacuation.

6.4. Application of Staged Evacuation Strategies

6.4.1. Experimental Design

This section intends to discuss how to employ the proposed system in making the staged evacuation decision in real-world evacuation operations. Note that in the evacuation literature, staged evacuation is mostly implemented by giving evacuation orders to different zones at different times. However, this zone-based staged evacuation strategy may be inconvenient for implementation in real-world roadway networks, as all such zones are geographically adjoined and are difficult to differentiate with the descriptive instructions.

Hence, this section explores the implementation of staged evacuation by giving different types of evacuation orders (i.e., voluntary/recommended evacuation or mandatory evacuation) at different times. Generally, voluntary/recommended evacuation allow people to decide whether to follow the evacuation order or not, whereas the mandatory evacuation will enforce the entire population in the potential impact area to evacuate. Thus, operators can choose the staged evacuation operations by issuing a voluntary/recommended evacuation order at time zero, and then issuing a mandatory evacuation order at a later time. The objective is to reduce the network congestion level without deteriorating the overall evacuation efficiency.

For convenience of illustration, this section uses the same evacuation scenario as in Section 6.3, where the evacuation area covers 25 traffic zones with a total demand of 50,510 vehicles. The evacuation network also covers the 6 major evacuation corridors, the connectors between major corridors, and the local access routes from all origins to main corridors/connections. This study set the compliance rate to the voluntary/ recommended evacuation order between 10% and 50%, whereas the remaining evacuees will respond to the mandatory evacuation order. The candidate time to issue the mandatory evacuation order is set at every 10 minutes.

6.4.2. Results Analysis

6.4.2.1. Optimal Staged Evacuation Strategies

With the loading time of 30 minutes, Table 6.12 shows the optimal time to issue the mandatory evacuation order using the formulations proposed in Chapter 4. The following five types of time indices are used to define the MOEs of the optimal control plans:

- Evacuation Clearance Time: the earliest time point at which all the demands have arrived at the destinations.
- Average Travel Time: the average time of all evacuees in the corridor/connector links.
- Average Waiting Time: the average time for vehicles to get onto the corridor/connector links after evacuees have responded to the evacuation order.
- Average Trip Time: the average time for vehicles to arrive at the destinations after evacuees have responded to the evacuation order. It equals the sum of average waiting time and average travel time.
- Average Time in the Network: the average time for vehicles to arrive at the destinations. It includes the average trip time as well as the response delay.

Table 6.12 Optimal Staged Evacuation with the Loading Time of 30 Minutes

Compliance rate to the voluntary/ recommended evacuation order	10%	20%	30%	40%	50%
Optimal time to issue the mandatory evacuation order (min)	0 (concurrent evacuation)	30	50	60	80
Evacuation clearance time (sec)	10350	10440	10410	10380	10380
Average travel time (sec)	519	514	492	483	493
Average waiting time (sec)	2881	2193	1317	1222	1046
Average trip time (sec)	3400	2707	1809	1706	1540
Average time in network (sec)	4315	4582	4824	4781	4855

The comparison reported in Table 6.12 has indicated that if the compliance rate to the voluntary/recommended evacuation order is equal to or larger than 20%, the staged evacuation strategy can significantly alleviate the network congestion level. The improvement is achieved by reducing the average trip time, especially the average waiting time, at the cost of an increased evacuation clearance time and time in the network.

6.4.2.2. Impacts of the Compliance Rate to the Voluntary/Recommended Evacuation Order on the Staged Evacuation Operations

To further illustrate the impacts of the compliance rate to the voluntary/ recommended evacuation order on the staged evacuation operations, Figure 6.9 compares the relative reduction in the average trip time and Figure 6.10 shows the relative increase in the average time in network when the mandatory evacuation order is issued at different time intervals.

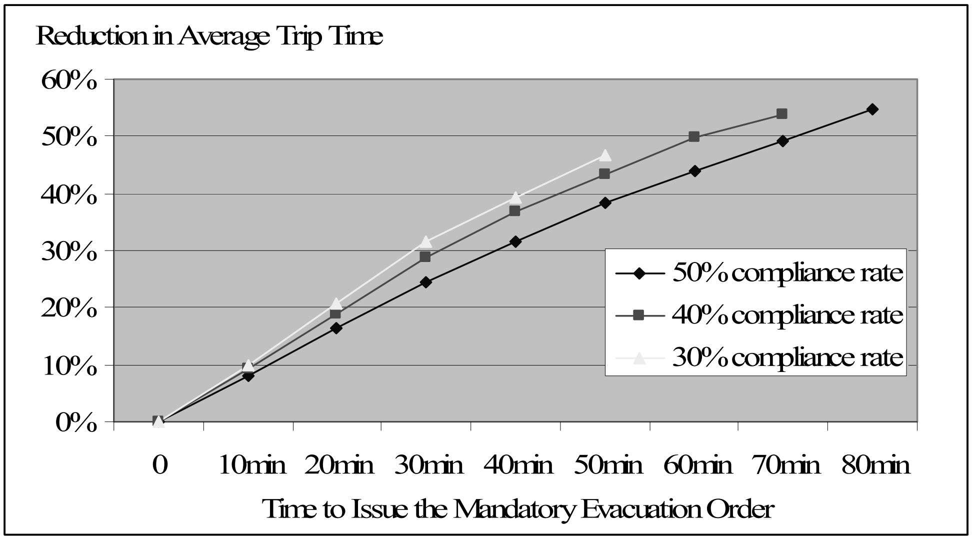

Figure 6.9 Relative Reduction in Average Trip Time with 30min Loading Time

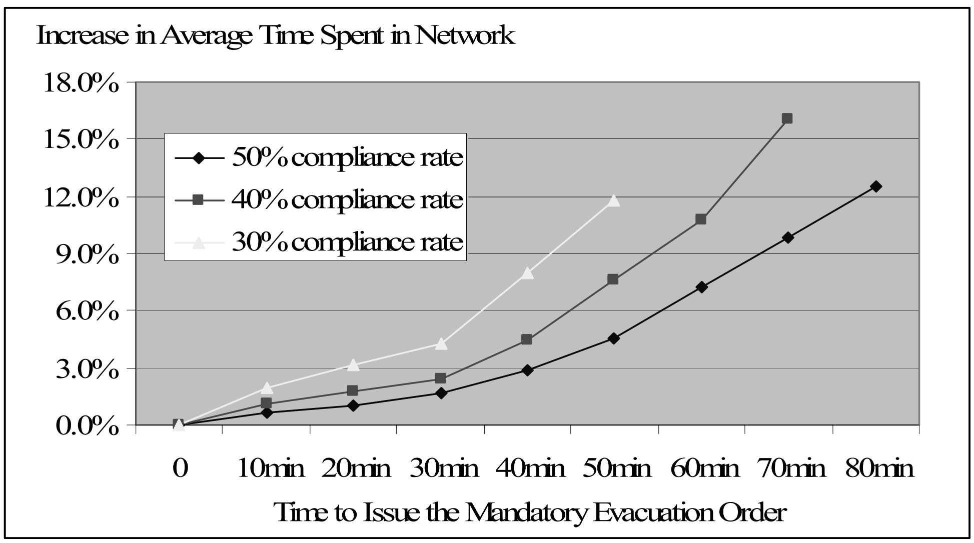

Figure 6.10 Relative Increase in Average Time in the Network with 30min Loading Time

If the mandatory evacuation order is issued at the same time (e.g., 30 minutes after the voluntary/recommended evacuation order), Figures 6.9 and 6.10 indicate that a higher compliance rate to the voluntary/recommended evacuation order will lead to less reduction in the average trip time (e.g., 24.3% reduction with 50% compliance rate versus 31.6% reduction with 30% compliance rate), but it also causes a less increase in the average time in network (e.g., 1.7% increase with 50% compliance rate compared to 4.3% increase with 30% compliance rate). Thus, for an evacuation scenario with the primary concern of the average time in the network, as in a case incurring severe potential impacts, a recommend evacuation order with a higher compliance rate would be more desirable than a voluntary evacuation order. The extreme condition is of 100% compliance rate, which is actually the concurrent evacuation that will incur the highest average trip time and the lowest average time in the network.

Given the same compliance rate, Figure 6.9 also indicates that the average trip time will be progressively decreasing as the mandatory order comes later. However, the slope of the curve becomes more flat, indicating a lower reduction rate. Besides, Figure 6.10 reflects that the average time in the network will first increase at a steady rate and then increase faster, if the mandatory order comes at a later time. As shown in the case with 50% compliance rate, if the mandatory evacuation order is issued at 20 minutes instead of 10 minutes after the voluntary/recommended evacuation, the relative reduction in the average trip time is 284 seconds and the relative increase in the average time in network is 16 seconds. If the mandatory evacuation order is postponed from 50 minutes to 60 minutes after the voluntary/recommended evacuation, the relative reduction in average trip time is 185 seconds and the relative increase in the average time in network is 116 seconds.

6.4.2.3. Impacts of Different Loading Time on the Staged Evacuation Operation

To further explore the impact of the loading time on the staged evacuation operations, this section presents the numerical analysis with two other loading times of 15 minutes and 45 minutes, respectively. Such a loading time actually reflects the response pattern of evacuees to an evacuation order. For example, the residential areas tend to have a long response time as the evacuees may take excessive time to collect their personal belongings, whereas people working/shopping at the time of the evacuation order are expected to respond quickly. The results are summarized in Table 6.13 and Table 6.14.

Table 6.13 Optimal Staged Evacuation with a 15-Minute Loading Time

Compliance rate to the voluntary/ recommended evacuation order	10%	20%	30%	40%	50%
Optimal time to issue the mandatory evacuation order (min)	10	30	50	60	80
Evacuation clearance time (sec)	10590	10380	10410	10350	10350
Average travel time (sec)	530	528	528	525	519
Average waiting time (sec)	2630	2179	1692	1342	1429
Average trip time (sec)	3160	2708	2220	1867	1947
Average time in network (sec)	4705	4613	4785	4738	4812

Table 6.14 Optimal Staged Evacuation with a 45-Minute Loading Time

Compliance rate to the voluntary/ recommended evacuation order	10%	20%	30%	40%	50%
Optimal time to issue the mandatory evacuation order (min)	0	0	50	60	80
Evacuation clearance time (sec)	10380	10380	10440	10410	10380
Average travel time (sec)	520	520	474	491	528
Average waiting time (sec)	2439	2439	995	874	654
Average trip time (sec)	2959	2959	1469	1365	1181
Average time in network (sec)	4324	4324	4934	4890	4946

Comparison between the results in Table 6.12 - 6.14 yields the following observations. If evacuees are expected to have a shorter response time to the evacuation orders, the staged evacuation can help alleviate the network congestion even with a low compliance rate to the voluntary/recommended evacuation order (as in Table 6.13). If evacuees need a long response time, the staged evacuation may not be a good choice unless evacuees have a high compliance rate to the voluntary/ recommended evacuation order, and thus the system operators shall use a recommended evacuation instead of voluntary evacuation as the first order (as in Table 6.14)

Taking the case of 50% compliance rate as an example, Figure 6.11 compares the relative reduction in the average trip time and Figure 6.12 compares the relative increase in the average time in network, if the mandatory order comes at a later time.

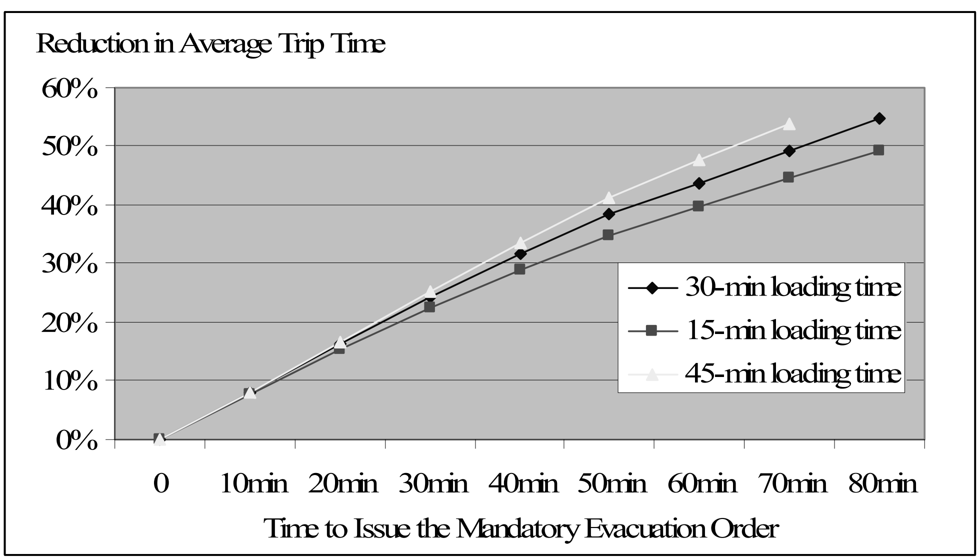

Figure 6.11 Relative Reduction in the Average Trip Time with a 50% Compliance Rate

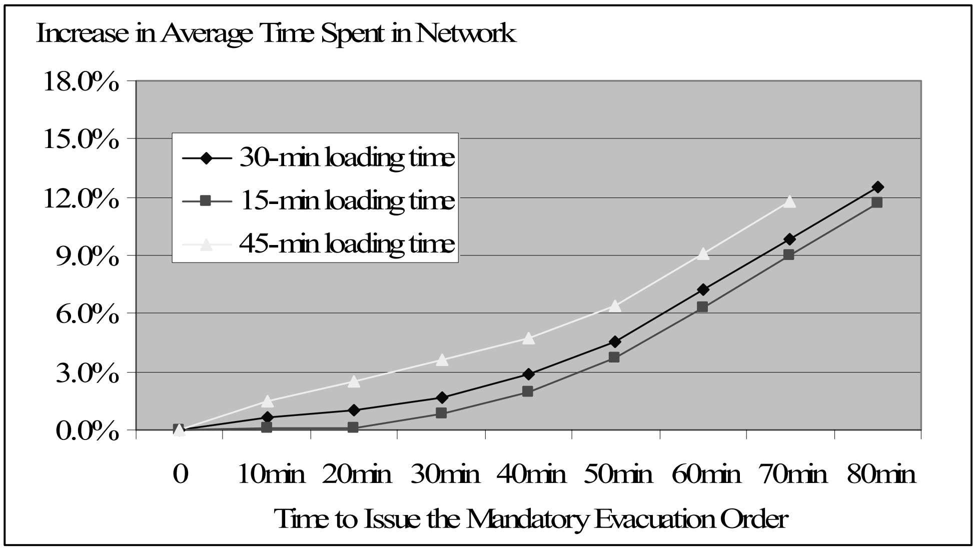

Figure 6.12 Relative Increase in the Average Time In the Network with a 50% Compliance Rate

If the mandatory evacuation order is issued at the same time, Figures 6.11 and 6.12 indicate that a shorter loading time causes less reduction in the average trip time, but also less increase in average time in the network. For example, if the mandatory evacuation order is issued at 30 minutes after the voluntary/recommended evacuation order, the reduction in the average trip time is 22.5 percent with a 15min loading time and 25.1 percent with a 45min loading time, whereas the increase in average time in the network is 0.8 percent with a 15min loading time compared to 3.6 percent with a 45min loading time. Thus, for some emergency scenarios that may result in severe impacts and thus require primary concern of the average time in the network, the system operator may justify the use of staged evacuation if the target evacuees are expected to have a short response time.

6.5. Closure

This chapter has illustrated the potential application of the proposed methodologies for real-world applications with the Washington D.C. evacuation network, which covers 6 major evacuation corridors and 25 traffic zones of 50,510 vehicles.

The numerical analysis presented in this chapter has demonstrated how to best use the proposed integrated control system for maximizing the evacuation efficiency and for revising the access plans provided to each traffic demand zone. Through the extensive information produced from the developed integrated control system, the responsible agency can efficiently evaluate the potential bottlenecks and revise the operational plans such as using the lane reversal or staged evacuation in a timely manner. The general guidelines summarized from the numerical experiment results for implementing some advanced control strategies have also been reported in this chapter.

Chapter 7: Conclusions and Future Research

7.1. Research Summary and Contributions

This dissertation is focused on design of traffic control strategies for emergency evacuation. Based on the needs and constraints in the real-world operations, this study has developed an integrated control system that enables potential users to exert different control options, including traffic routing, staged evacuation, contra-flow design, and signal optimization. The key features of such a system are presented first in Chapter 1.

Chapter 2 has provided a comprehensive review of the relevant studies on both theoretical and operational aspects of emergency evacuation operations. Not only has the review identified some critical operational constraints that have not been addressed in the literature, but it has also discovered the lack of an operational structure that can effectively integrate different control options in the evacuation practice.

In responses to the identified needs, Chapter 3 has illustrated an operational framework for the proposed integrated control system, as evacuation operations may often require concurrent implementation of different strategies. This framework for system implementation features a hierarchical structure, which allows the system users to achieve a trade-off between modeling accuracy and operational efficiency during large-scale evacuations. Its high-level component functions to approximate the traffic flows over the network under various constraints and to generate the network-wide evacuation strategies, such as assigning traffic to different corridors, selecting contra-flow segments, and identifying the sequence for staged evacuation. Grounded on the information from the high-level decisions, the low-level component is responsible for producing the optimal signal timings for each intersection at the main corridor level.

The mathematical formulations used at both levels of operations are detailed in Chapter 4 and Chapter 5, respectively. Chapter 4 has started with the development of a revised cell transmission model, which serves as the main methodology for capturing the network flow evolution. By allowing cells of a non-homogeneous size, this model can significantly reduce the number of state variables and operational constraints for modeling network traffic dynamics. The numerical results have proved its effectiveness in capturing the temporal and spatial interactions of traffic flows over the evacuation network, especially for the queue formation and dissipation. With this proposed formulation methodology for network flows, Chapter 4 has also addressed its application with the following three network level control models.

- The base model for design of traffic routing strategies with the given network geometry and demand profiles, and for capturing the potential flow interactions at intersections;
- The extended model-I for the contra-flow strategy designed to reallocate roadway capacities by reversing some travel lanes, and to address various operational differences between the normal and reversed lanes;

- The extended model-II for staged evacuation that can determine the optimal sequence for activating the evacuation order for different demand zones so as to effectively reduce network congestions during the large-scale evacuation operations.

Chapter 5 has detailed two models that take the network-level output for use in design of signal control strategies at the corridor level. The base model is for use in the scenario that each evacuation corridor is under the independent operational control, whereas its extended model takes into account the needs to concurrently optimize interdependent neighboring corridors so as to balance the congestion level and minimize the local bottlenecks on available arterials. Both models have incorporated the proposed critical intersection concept designated to reduce the disturbance of side street traffic to the arterial flow progression. Using the Genetic Algorithm based heuristics along with an embedded macroscopic simulator, this study has also developed an efficient solution method for these two optimal evacuation signal models. The results of extensive numerical experiments have showed that the control plan from the base model can increase the system throughput or reduce the evacuation clearance time, when compared with state-of-the-practice signal control plans. The extended model can further improve the evacuation efficiency if unbalanced demand distributions exist among parallel corridors.

To illustrate the application of the developed integrated control system for real-world evacuation operations, this study has presented a case study with a network from Washington D.C. that consists of 6 major evacuation corridors and actual evacuation demands from traffic zones. The results of the case study reveal that the information generated from the proposed integrated control system with respect to the routing strategies to guide evacuation populations and the optimal signal timing plan in response to the surging traffic flows can substantially improve the efficiency of the emergency evacuation operations. The case study results also reflect that the developed models and solution algorithms are sufficiently reliable for use in practice.

In summary, this research has made the following key contributions:

- Develop an operational structure to effectively integrate various essential strategies for evacuation operations, including traffic routing, staged evacuation, contra-flow operations and intersection signal controls. This critical issue of integrating all concurrently operated control strategies has not been addressed in the literature.
- Propose a revised cell transmission model for capturing complex interactions in the network traffic flows, which preserves the capability of the original cell transmission model, but significantly reduce the computing efforts by allowing cells with a non-homogeneous size.

- Formulate a new mathematical model for design of staged evacuation strategies, which can optimize the sequence of evacuation starting times for different demand zones that may suffer different levels of impact from a detected incident.
- Construct a new set of equations for design of contra-flow operations, which have taken into account some critical operational constraints existing in real-world operations but not yet been addressed in the literature.
- Design innovative arterial signal control models that employ the critical intersection concept to minimize the interference of side-street traffic on the arterial evacuation traffic flows and to maximize the operational efficiency.

7.2. Future Research

Further studies along this line of maximizing the operational efficiency during emergency evacuation and monitoring the traffic evolution are listed below.

- *Design of Efficient Solution Algorithms for Use at the Corridor Level during Real-Time Operations*

This research has employed the Genetic Algorithm-based heuristics to solve the corridor level formulations. Generally, when the problem size becomes larger, the chromosome length will increase and the GA-based heuristic will need a larger size of population and/or more generations of evolution due to its random search nature. Thus, it is desirable that an efficient solution algorithm that is less sensitive to the network size can be developed. One potential direction is to incorporate some tools to narrow down the search directions. The other way may be to utilize the inherent hierarchical structures involved in the corridor-level control decisions. For example, traffic routing will affect the selection of critical intersections, and consequently the signal timings at intersections. This research has used the gene activation mechanism in the decoding procedure to take advantage of this special hierarchical structure. This can certainly reduce the computation efforts, but may not contribute to the searching efficiency since all those inactive controls will remain in the chromosome structure and are carried throughout all generations.

- *Development of Efficient Solution Algorithms at the Network Level for Real-Time Operations and Traffic Monitoring*

This research has used the commercial software LINGO to solve the proposed network level formulations. For a large-scale network, LINGO may encounter problems in reading the input files, providing optimal solutions, or saving the optimal output files. Even for a small to medium network, it may take a long computation time to reach an optimal solution when the contra-flow and staged evacuation operations are implemented. This may be sufficient for planning needs, but not for real-time operations of emergency evacuation. The current design practice addresses this problem by defining and preparing for multiple evacuation scenarios. System operators can pick the most similar scenarios and execute the corresponding control plans. Such practice can certainly be improved by efficient heuristic algorithms for real-time operations and monitoring of traffic flow evolutions.

- *Coordinating Different Transportation Modes in Evacuation Operations*:

This research has addressed the evacuation operations with only the roadway networks and passenger cars. However, it is likely that some evacuees in urban areas may not have any access to vehicles. Hence, they need to reach metro stations or emergency bus pickup sites to get out of the evacuation zone. This type of multi-mode evacuation operations contains several critical issues to be studied, including pickup locations, emergency bus dispatching, pedestrian routings, interactions between bus and passenger-car flows, and revising the signal system to accommodate the large volume of pedestrian flows. Efficient models and solution algorithms for tackling such complex multi-mode evacuation scenarios remain to be developed.

Appendix A

Mathematical Proof of Flow Propagation Equation 4.7

Proof: First, one can divide the long cell i into l_i homogenous sub-cells of size 1, which can be traversed in a unit time interval at free flow speed. Define sx_k^t = the number of vehicles on sub-cell k at the beginning of interval t; Ω_k^t = the flow that can be sent from sub-cell k to sub-cell $k+1$ during t; Ψ_k^t = the surplus flow on sub-cell k after sending Ω_k^t to sub-cell $k+1$.

If $Q_i^t \geq N_i^t / l_i$, one can find the following iteration relations:

$$\Omega_{li-1}^t = \min\{N_i^t / l_i - sx_{li}^t, sx_{li-1}^t\} \Rightarrow \Psi_{li-1}^t = \max\{sx_{li-1}^t + sx_{li}^t - N_i^t / l_i,\ \ 0\}$$

$$\Omega_k^t = \min\{N_i^t / l_i - \Psi_{k+1}^t, sx_k^t\} \Rightarrow \Psi_k^t = \max\{sx_k^t + \Psi_{k+1}^t - N_i^t / l_i,\ \ 0\},$$

$$k=1, \dots,\ l_i - 2$$

Substituting Ψ_2^t into the equation of Ψ_1^t and considering $\sum_{k=1}^{i} sx_k^t \leq iN_i^t / l_i$, one can have

$$\begin{aligned}\Psi_1^t &= \max\{sx_1^t + sx_2^t + \Psi_3^t - 2N_i^t / l_i,\ \ 0,\ \ sx_1^t - N_i^t / l_i\} \\ &= \max\{sx_1^t + sx_2^t + \Psi_3^t - 2N_i^t / l_i,\ \ 0\}\end{aligned}$$

Then by substituting $\Psi_3^t,\ldots,\Psi_{li-1}^t$ one by one, one can finally have

$$\Psi_1^t = \max\{\sum_k sx_k^t - (l_i - 1)N_i^t / l_i,\ \ 0\} = \max\{x_i^t - (l_i - 1)N_i^t / l_i,\ \ 0\}$$

Thus the vacant in sub-cell 1, namely the receiving capacity of cell i is given by

$$R_i^t = N_i^t / l_i - \Psi_1^t = \min\{N_i^t - x_i^t,\ \ N_i^t / l_i\} = \min\{N_i^t - x_i^t,\ \ N_i^t / l_i,\ \ Q_i^t\}$$

If $Q_i^t < N_i^t / l_i$, one can find a more complex iteration relations:

$$\Omega_{li-1}^t = \min\{N_i^t / l_i - sx_{li}^t, sx_{li-1}^t, Q_i^t\}$$
$$\Rightarrow \Psi_{li-1}^t = \max\{0, sx_{li-1}^t - Q_i^t, sx_{li}^t + sx_{li-1}^t - N_i^t / l_i\}$$

$$\Omega_k^t = \min\{N_i^t / l_i - \Psi_{k+1}^t, sx_k^t, Q_i^t\}$$

$$\Rightarrow \Psi_k^t = \max\{0, sx_k^t - Q_i^t, \Psi_{k+1}^t + sx_k^t - N_i^t / l_i\},\ k=1,\ \ldots,\ l_i - 2$$

By following the same substitution procedure and using $\sum_{k=1}^{i} sx_k^t \le iN_i^t / l_i$, one can find $\Psi_1^t = \max\{0, sx_1^t - Q_i^t, x_i^t - (l_i - 1)N_i^t / l_i\}$. Thus the receiving capacity of cell i is given by

$$R_i^t = \min\{Q_i^t, N_i^t / l_i - \Psi_1^t\} = \min\{Q_i^t, N_i^t / l_i, N_i^t / l_i - x_1^t + Q_i^t, N_i^t - x_i^t\}$$
$$= \min\{Q_i^t,\ \ N_i^t / l_i,\ \ N_i^t - x_i^t\}$$

□

Appendix B:

Numerical Test for Effectiveness of the Revised Cell Transmission Formulations

This test intends to compare the performance of the following three network flow formulations:

- Model 1: original cell transmission model with homogenous cells (Daganzo 1994, 1995);
- Model 2: Ziliaskopoulos' model with averaging technique for longer cells (Ziliaskopoulos and Lee 1996);
- Model 3: the revised cell transmission formulation proposed in this study.

A 10 km link of two lanes is built in this test, and its key characteristics are given as: free-flow speed = 60 km per hour, jam density = 106 vehicles per km per lane, and saturation flow rate = 2160 vehicles per hour per lane. The travel demand is randomly generated between 0 ~ 1.5 times of link flow capacity.

Figure B.1 shows two different cell connection diagrams for a unit interval of one minute. The first one using equal-sized cells is for Model 1 with $Q_i^t = 36veh$ and $N_i^t = 106veh$, i=1, …, 10. The second diagram is for Models 2 and 3, which combines cells between Cell 2 and Cell 9 in the first diagram to form a long cell. The cell marked with *r* indicates the origin, whereas the cell marked with *s* denotes the destination.

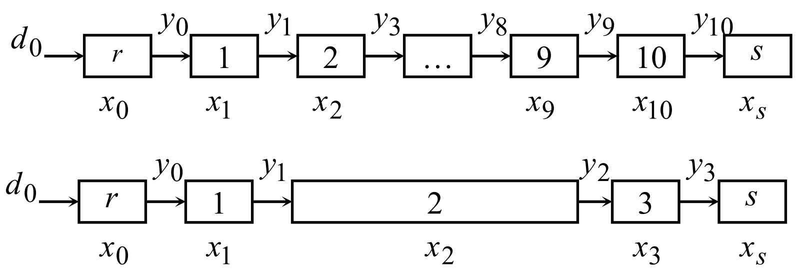

Figure B.1 Cell Connection Diagrams for the Segment

Two scenarios are tested here. The first scenario is the normal traffic condition without queues. The second scenario presents an accident in the cell ahead of the destination. The capacity of this cell decreases to $Q_i^t = 10veh$ during the time interval *t*=20, …, 40min due to the accident. Figure B.2 illustrates the cumulative arriving curves at the destination for all three models.

As shown in the graphical results, the proposed Model 3 has nearly the same performance as Model 1 (the original cell transmission formulation), regardless of traffic conditions. However, Model 2 tends to deviate from Model 1 in each scenario. Regarding the computational efficiency, the total number of variables with Model 3, although slightly exceeding that of Model 2, is significantly less than the number of variables with Model 1. The number of cell state variables per time interval decreases from 12 in Model 1 to 5 in Model 3, while the number of connector flows per time interval decreases from 11 in Model 1 to 4 in Model 3. The reduction with respect to the number of variables exceeds 60%. This implies that the proposed revised cell transmission formulations can substantially reduce the size of the entire optimization formulations and the computation time for the solution.

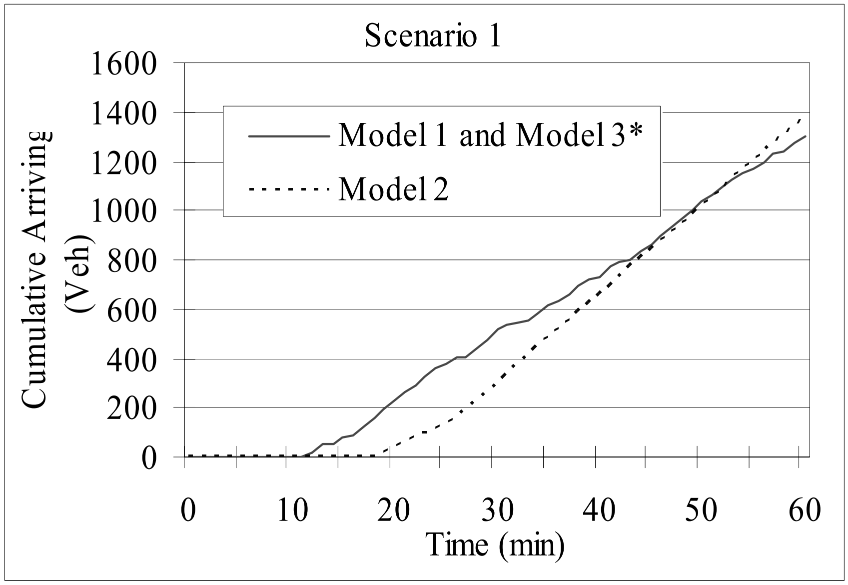

* Models 1 and 3 produce the identical results

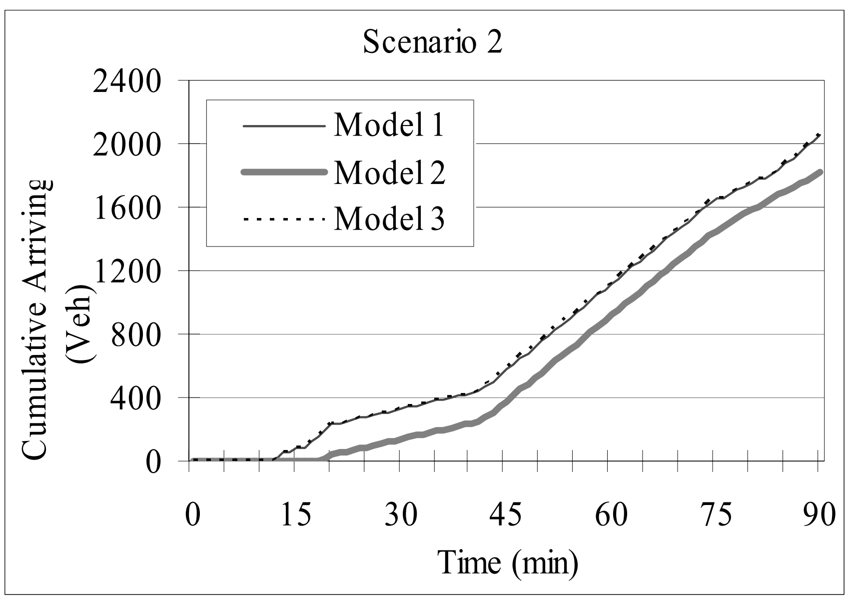

Figure B.2 Cumulative Arriving Curves for Testing Scenarios

Bibliography

Alam, S.B., Goulias, K.G., "Dynamic emergency evacuation management system using geographic information system and Spatiotemporal models of behavior," Transportation Research Record, n. 1660, pp. 92-99, 1999

Alsnih, R., and Stopher, P.R. (2003). "Review of the Procedures Associated with Devising Emergency Evacuation Plans." Transportation Research Record 1865, Transportation Research Board, Washington D.C., 89-97.

Ballard, A.J., and Borchardt, D.W., "Recommended Practices For Hurricane Evacuation Traffic Operations," Technical report, FHWA/TX-06/0-4962-P2, 2005

Bullock D., Morales J. and Sanderson B., "Evaluation of Emergency Vehicle Signal Preemption on the Route 7, Virginia, Corridor," Technical Report, FHWA-RD-99-070, 1999

Campos, V.B.G., de Silva, P.A.L., and Netto, P.O.B., "Evacuation transportation planning: A method of identify optimal independent routes," Urban Transport and the Environment for the 21st Century, pp.555-564, 2000

Chalmet, L., Francis, R., Saunders, P., "Network Models for Building Evacuation," Management Science, vol.28, 1982, pp.86-105.

Chen, M., "Traffic Signal Timing For Urban Evacuation," Thesis for the University of Maryland, 2005

Chen, X., Zhan, F.B., “Agent-Based Modeling and Simulation of Urban Evacuation: Relative Effectiveness of Simultaneous and Staged Evacuation Strategies,” Presented at the 83rd annual conference of Transportation Research Board, 2004

Chiu, Y.C., “Traffic Scheduling Simulation and Assignment for Area-Wide Evacuation,” 2004 IEEE Intelligent Transportation Systems Conference, Washington, D.C., October, 2004

Chiu, Y.C., Villalobos, J., Gautam, B., and Zheng, H., “Optimal Scheduling of Evacuation Operations,” presented at the 85th annual meeting of transportation research board, 2006

Choi, W., Hamacher, H. W., and Tufekci, S., “Modeling of Building Evacuation Problems by Network Flows with Side Constraints,” European Journal of Operational Research, vol.35, 1988, pp.98-110.

Cova, T.J., Johnson, J.P., “Microsimulation of neighborhood evacuations in the urban-wildland interface,” Environment and Planning A, vol.34, pp. 2211-2229, 2002

Cova, T.J., Johnson, J.P., “A network flow model for lane-based evacuation routing,” Transportation Research A, vol.37, pp.579-604, 2003

Daganzo, F.C., “The Cell Transmission Model: A Dynamic Representation of Highway Traffic Consistent with the Hydrodynamic Theory,” Transportation Research. Part B, Vol. 28B, No. 4, pp. 269-287, 1994.

Daganzo, F.C., “The Cell Transmission Model. II. Network Traffic,” Transportation Research. Part B, Vol. 29B, pp. 79-93, 1995.

de Silva, F., Eglese, R, “Integrating simulation modeling and GIS: spatial decision support systems for evacuation planning,” Journal of the Operational Research Society, vol. 51, pp. 423-430, 2000

Dotson, L.J., Jones, J., Schneck, D., and Sullivan, R., “Development of evacuation time estimate studies for nuclear power plants,” Technical Report, NUREG/CR-6863 (SAND2004-5900), 2005

Dunn C.E., Newton, D., “Optimal routes in GIS and emergency planning applications,” Area, vol.24, n.3, pp.259-267, 1992

Eschenauer, H.A., Koski, J., and Osyczka, A., “Multicriteria Design Optimization : Procedures and Applications,” Springer-Verlag, New York, 1986

Farrell, J., “Alternatives to Road Building to Improve Hurricane Evacuation in Coastal South Carolina,” Presented at Environmental Advocacy Seminar, April, 2005

FEMA, “Southeast United States Hurricane Evacuation Traffic Study-Executive Summary,” Final Report for Southeast United States Hurricane Evacuation Traffic Study, 2000

Goldberg D., “Genetic Algorithms,” Addison Wesley, Reading, MA, 1988

Hamacher, H.W., Tufekci, S., “On the Use of Lexicographic Min Cost Flows in Evacuation Modeling,” Naval Research Logistics, vol. 34, 1987, pp.487-503.

Harrington, G., “Emergency preparedness: path to safety,” Building Operating Management, Apr. 2005

Hobeika, A.G., Kim, S., and Beckwith, R.E., “A decision support system for developing evacuation plans around nuclear power stations,” Interfaces, vol.24, n.5, pp.22-35,1994

Hobeika, A., Kim C., “Comparison of traffic assignments in evacuation modeling,” IEEE transactions on engineering management, vol.45, n.2, pp.192-198, 1998

Homburg, C., “ Hierarchical multi-objective decision making,” European Journal of Operational Research, vol.105, n.1, pp. 155-161, 1998

ITE, “Emergency Planning and Preparedness: Guidelines For Transportation Professionals,” 2004

Kwon, E., Pitt, S., “Evaluation of emergency evacuation strategies for downtown event traffic using a dynamic network model”, Presented at the 84th Annual Meeting of the Transportation Research Board, Washington, D.C., 2005

Ladd, S.R., “Genetic Algorithms in C++,” M&T Books, New York, 1996

Li, Y, A.K. Ziliaskopoulos and S. T. Waller, “Linear Programming Formulations for System Optimum Dynamic Traffic Assignment with Arrival Time-based and Departure time-based Demands,” Transportation Research Record 1667, TRB, National Research Council, Washington, D.C., pp. 52-59, 1999.

Lim, E., Wolshon, B., “Modeling and performance assessment of contraflow evacuation termination points,” Presented at the 84th Annual Meeting of the Transportation Research Board, Washington, D.C., 2005

Liu, H.X., Ban, J.X., Ma, W., Mirchandani, P.B., "Model Reference Adaptive Control Framework for Real Time Traffic Management under Emergency Evacuation," Presented at the 85th Annual Meeting of the Transportation Research Board, Washington, D.C., 2006

Louisell, C., Collura, J. and Tignor, S, "A Proposed Method to Evaluate Emergency Vehicle Preemption and the Impacts on Safety." Presented at the 82nd Annual Meeting of Transportation Research Board, Washington, D.C., 2003

Louisell, C., Collura, J., Teodorovic, D. and Tignor, S., "A Simple Work Sheet Method to Evaluate Emergency Vehicle Preemption and the Impacts on Safety." Presented at the 83rd Annual Meeting of Transportation Research Board, 2004

Louisell, C., Collura J., "A Simple Algorithm to Estimate Emergency Vehicle Travel Time Savings on Preemption Equipped Corridors: A Method Based on a Field Operational Test." Presented at the 84th Annual Meeting of Transportation Research Board, 2005

Mahmassani, H., Sbayti, H., "Optimal Scheduling of Contraflow Operations for Network Evacuation Planning", Presented at the 2005 INFORMS Annual Meeting, San Francisco, 2005

McHale G.M., Collura J., "Improving Emergency Vehicle Traffic Signal Priority System Assessment Methodologies," presented at the 82nd Annual Meeting of Transportation Research Board, Washington, D.C., 2003

McLoughlin, D., "A Framework for Integrated Emergency Management," Public Administration Review, vol.45, 1985, pp.165-172

Mei, B., “Development Of Trip Generation Models Of Hurricane Evacuation,” Thesis of Louisiana State University, 2002

Miller-Hooks, E., Patterson, S. S., “On Solving Quickest Time Problems in Time-Dependent, Dynamic Networks,” Journal of Mathematical Modeling and Algorithms, vol.3(1), 2004, pp.39-71.

Mitchell, S.W., Radwan, E., “Heuristic Prioritization of Emergency Evacuation Staging to Reduce Clearance Time,” presented at the 85th annual meeting of transportation research board, 2006

Opasanon, S., “On Finding Paths and Flows in Multicriteria, Stochastic and Time-Varying Networks,” Ph.D. dissertation, University of Maryland, 2004

Pauls, J.L, Jones, B.K, “Building Evacuation: Research Methods and Case Studies,” Fires and Human Behaviour, pp.227-250, John Wiley and Sons, New York, 1980

PBS&J, “Southeast United States Hurricane Evacuation Traffic Study-Technical Memorandum Number 3: Reverse Lane Standards And ITS Strategies,” Final Report for Southeast United States Hurricane Evacuation Traffic Study, 2000

PBS&J, “Florida Department of Transportation Hurricane Response Evaluation and Recommendations,” Technical Memorandum, 2005

Pidd, M., de Silva, F., Eglese, R, “A simulation model for emergency evacuation,” European Journal of Operational Research, vol. 90, n. 3, pp. 413-419, 1996

Rontiris, K., Crous, W., “Emergency evacuation modeling for the Koeberg nuclear power station,” 2nd Asian EMME/2 Users' Meeting, 2000

Sadek, A.W., Chowdhury, M.A., “Fundamentals of Intelligent Transportation Systems Planning,” Artech House, 2003

Sattayhatewa, P., Ran, B., “Developing a dynamic traffic management model for nuclear power plant evacuation,” Presented at the 79th Annual Meeting of the Transportation Research Board, Washington, D.C., 2000

Sbayti, H., Mahmassani, H., “Optimal Scheduling of Evacuation Operations,” presented at the 85th annual meeting of transportation research board, 2006

Sheffi, Y., Mahmassani, H., and Powell, W., “A transportation network evacuation model,” Transportation Research A, vol.16, n.3, pp.209-218, 1982

Sheffi, Y., “Urban Transportation Networks,” Englewood Cliffs, NJ: Prentice-Hall, 1985.

Sisiopiku, V.P., Jones, S.L., Sullivan, A.J., Patharkar, S.S., Tang, X., “Regional Traffic Simulation for Emergency Preparedness,” Technical report, Department of Civil and Environmental Engineering, The University of Alabama, 2004

Smith, J.M., “State-dependent queuing models in emergency evacuation networks,” Transportation Research B, vol. 25, pp. 373-389, 1991

Snyder D., “Regional Emergency Evacuation Transportation Coordination Annex of the Regional Emergency Coordination Plan,” Presentation to the Metropolitan Washington Council of Governments, 2004

Sorensen, J., Vogt, B.M., Mileti, D.S., “Evacuation: an assessment of planning and research,” Technical Report for Oak Ridge National Laboratory, ORNL-6373, 1987

Southworth, F., “Regional evacuation modeling: a state-of-the-art review,” Technical Report for Oak Ridge National Laboratory, ORNL/TM-11740, 1991

Talebi, K., Smith, J.M., “Stochastic Network Evacuation Models,” Computers & Operations Research, vol.12 (6), 1985, pp.559-577.

Teo, A.P.Y., “Validation of An Evacuation Model Currently under Development,” Thesis, University of Canterbury, New Zealand, 2001

Theodoulou, G., Wlshon, B., “Modeling and Analyses of Freeway Contraflow to Improve Future Evacuations,” Presented at the 83rd Annual Meeting of the Transportation Research Board, Washington, D.C., 2004

Tuydes, H., Ziliaskopoulos, A., “Network Re-design to Optimize Evacuation Contraflow,” presented at the 83rd annual meeting of transportation research board, 2004

Tuydes, H., “Network Traffic Management under Disaster Conditions,” Ph.D. Thesis, Northwestern University, 2005.

Tuydes, H., Ziliaskopoulos, A., “The Network Evacuation Problem and Solution Algorithms,” Presented at the 2005 INFORMS Annual Meeting, San Francisco, 2005

Tuydes, H., Ziliaskopoulos, A., “A Tabu-based Heuristic Approach for the Optimization of Network Evacuation Contraflow,” presented at the 85th annual meeting of transportation research board, 2006

Tweedie, S., Rowland, J., Walsh, S., Rhoten, R., and Hagle, P., “A methodology for estimating emergency evacuation times,” The Social Science Journal, vol. 23, pp. 189-204, 1986

Urbanik T. II., “Evacuation time estimates for nuclear power plants,” Journal of Hazardous Materials, vol.5, pp.165-180, 2000

Urbina, E.A., “A state-of-the-practice review of hurricane evacuation plans and policies,” Thesis of the Louisiana State University, 2002

Urbina, E., Wolshon, B., “National review of hurricane evacuation plans and policies: a comparison and contrast of state practices,” Transportation Research A, vol.37 (3), pp.257-275, 2003

US Army Corps of Engineers, “South Carolina Hurricane Evacuation Study,” Technical Data Report, Charleston District, December 1986.

US Army Corps of Engineers, “Treasure Coast Region Hurricane Evacuation Study,” Technical Data Report, 1994.

US Army Corps of Engineers, “Rhode Island Hurricane Evacuation Study,” Technical Data Report, May 1995

US Army Corps of Engineers, “Alabama Hurricane Evacuation Study Technical Data Report: Behavioral Analysis”, Final Report, 2000.

Wilmot, C.G., Meduri, N., “A methodology to establish hurricane evacuation zones,” Presented at the 84th Annual Meeting of the Transportation Research Board, Washington, D.C., 2004

Wolshon, B., ““One-way-out”: contraflow freeway operation for hurricane evacuation”, Natural hazards review, August, pp.105-112, 2001

Wolshon, B., “Planning for the evacuation of New Orleans,” ITE Journal, vol.72 (2), pp.44-49, 2002

Yuan, F., Han, L.D., Chin, S.M., Hwang, H., "A Proposed Framework for Simultaneous Optimization of Evacuation Traffic Destination and Route Assignment," Presented at the 85th Annual Meeting of the Transportation Research Board, Washington, D.C., 2006

Ziliaskopoulos, A., and S. Lee, "A Cell Transmission Based Assignment-Simulation Model for Integrated Freeway/Surface Street Systems," Presented at the 76th Annual Meeting of the Transportation Research Board, Washington, D.C., 1997

Ziliaskopoulos, A.K., "A Linear Programming Model for the Single Destination System Optimum Dynamic Traffic Assignment Problem," Transportation Science, Vol. 34, No. 1, pp. 37-49, 2000.

Zou, N., Yeh, S.T., and Chang, G.L., "A simulation-based emergency evacuation system for Ocean City, Maryland under hurricane attacks," Transportation Research Record 1922, Transportation Research Board, Washington D.C., 138-148, 2005